



TECHNISCHE UNIVERSITÄT MÜNCHEN
Fakultät für Elektrotechnik und Informationstechnik
Lehrstuhl für Streuerungs- und Regelungstechnik

Dynamical Processes on Social Networks: Modeling, Analysis, and Control

Fangzhou Liu

Vollständiger Abdruck der von der Fakultät für Elektrotechnik und Informationstechnik der Technischen Universität München zur Erlangung des akademischen Grades eines

Doktor-Ingenieurs (Dr.-Ing.)

genehmigten Dissertation.

Vorsitzende/-r: Prof. Dr.-Ing. Wolfgang Kellerer

Prüfende/-r der Dissertation:

1. Prof. Dr.-Ing. Martin Buss

2. Prof. dr. ir. Ming Cao

University of Groningen, the Netherlands

Die Dissertation wurde am 18.01.2019 bei der Technischen Universität München eingereicht und durch die Fakultät für Elektrotechnik und Informationstechnik am 31.05.2019 angenommen.

Preamble

This dissertation summarizes my research conducted over the last years at the Chair of Automatic Control Engineering, LSR, at the Technical University of Munich, Germany. In this chair, I have experienced an excellent and inspiring atmosphere. Here I would like to take this opportunity to acknowledge the people who supported me in achieving my goals.

Foremost, I would like to sincerely thank my advisor and head of the chair Prof. Martin Buss for his strong support during my years in LSR. His trust and confidence in me were great encouragement for my research. I benefit a lot from the freedom he granted in this lab, as well as his insightful comments and suggestions, so that I can concentrate on the topics I am interested in. I appreciate all his valuable contributions to my work. Furthermore I want to thank my mentor and head of the Chair of Information-oriented Control (ITR) Prof. Sandra Hirche for her constructive suggestions on this my research on opinion dynamics and other related works.

Furthermore, I want to thank Prof. Wolfgang Kellerer and Prof. Ming Cao for their valuable feedback on this work.

I also want to express my gratitude to Dr. Marion Leibold for the detailed discussion on the optimization problems and control theory.

I thank the whole team at LSR and ITR for both the productive and the fun times we shared. A special thanks goes to my friends and colleagues in LSR: Sotiris Apostolopoulos, Tim Bruedigung, Philine Donner, Yingwei Du, Stefan Friedrich, Volker Gabler, Rameez Hayat, Gerold Huber, Stefan Kersting, Tong Liu, Özgür Ögüz, Alexander Pekarovskiy, Markus Schill, Michaela Semmler, Zengjie Zhang, and Zhehua Zhou. Without our extensive discussions, your constructive feedback, and our weekly SHRINE meeting, this work would not have been possible. I would also like to thank Dr. Dong Xue and Dr. Xianwei Li in the ITR team for their valuable collaboration.

Most importantly, no words can fully express my gratefulness to my family. I would like to thank my parents and my grandma for their love, continuous support and valuable advice in all these years. Last but not least, I am forever grateful to my girlfriend Qiuyue Ma for her love, support, and encouragement during my doctor career.

Abstract

Dynamical processes on social networks, e.g., information diffusion and opinion dynamics, draw enormous attention for researchers from multitudes of fields. This growing trend motivates our works in this dissertation. Our focus is to build a bridge filling the gap between control theory and dynamical processes on social networks by providing mathematical tools for modeling, analysis, and control.

By analogy, the information diffusion process is modeled as epidemic spreading, which is then termed as information epidemics. In particular, the susceptible-infected-susceptible (SIS) model and the susceptible-infected-recovered/removed-susceptible (SIRS) model are adopted. Hence, by using the mean-field approximation, the node-based SIS and SIRS models are introduced, which characterize both the heterogeneities in the communication topology and individual transition rates. Additionally, the node-based SIS model is extended to multi-layer networks in light of diverse information diffusion paths. Apart from the modeling, the existence, uniqueness and stability of the disease-free and endemic equilibria are analyzed by using the properties of Metzler matrices. The attained conditions emphasize the significance of the social connections and the diffusion process itself.

In addition to the analysis and modeling, the control problems of the information epidemics are inspected, especially the optimal control design such that the information spreads in a desired manner. By interacting with the spreading rate, two optimal control problems are proposed with respect to two typical scenarios, i.e., to impede the spread of rumors and to enhance the spread of marketing or campaign information. This framework is then utilized to the SIS model with noisy transition rates. By using the distribution analysis techniques, we address the robust optimal control problem: maximizing the spreading performance at the finite time instant given a fixed budget. A novel approach combining the forward backward sweep method and the secant method is proposed to efficiently reduce the computation burden.

Following the diffusion process, the opinion dynamics are studied in light of the social influence. Opinion dynamics on social networks with cooperative (cooperative-competitive) interactions may result in polarity, consensus or neutrality under different opinion protocols. The antecedent of protocol design is to study the accessibility problem: whether or not there exist admissible control rules to polarize, consensus, or neutralize individual opinions in a large population. From an operational perspective, we investigate the polarizability, consensusability, and neutralizability of opinion dynamics in question. Particular emphasis is on the joint impact of individual dynamical properties and their social ties. Sufficient and/or necessary conditions for these accessibility problems are provided by using powerful tools from spectral analysis and algebraic graph theory. To characterize the individual diversity in real life, we further investigate the solvability of opinion formation problems in heterogeneous systems with non-identical dynamics. Accordingly, sufficient and/or necessary criteria for heterogeneous network polarizability, consensusability, and neutralizability are derived.

Zusammenfassung

Dynamische Prozesse in sozialen Netzwerken, wie beispielsweise die Informationsdiffusion und Meinungsdynamik, ziehen enorme Aufmerksamkeit von Forschern verschiedenster Disziplinen auf sich. Dieser weiterhin wachsende Trend motiviert die Arbeiten dieser Dissertation. Der Fokus dieser Arbeit ist es, die Lücke zwischen Regelungstheorie und dynamischen Prozessen in sozialen Netzwerken durch die Bereitstellung der dazu benötigten mathematischen Werkzeuge für die Modellierung, Analyse und Regelung zu schließen.

Analog dazu wird der Prozess der Informationsverbreitung als Epidemiologie modelliert, die im Folgenden als Informationsepidemie bezeichnet wird. Dabei werden insbesondere das Suszeptible-Infected-Susceptible-Modell (SIS), sowie das Suszeptible-Infected-Recovery / Removal-Susceptible-Modell (SIRS) angenommen. Daher werden unter Verwendung der Mittelfeldnäherung die knotenbasierten SIS- und SIRS-Modelle eingeführt, die sowohl die Heterogenität in der Kommunikationstopologie, als auch die individuellen Übergangsraten charakterisieren. Außerdem wird das knotenbasierte SIS-Modell im Hinblick auf verschiedene Informationsdiffusionspfade auf mehrschichtige Netzwerke erweitert. Außerdem werden Existenz, Einzigartigkeit und Stabilität der krankheitsfreien und endemischen Gleichgewichte anhand der Eigenschaften der Metzler-Matrizen analysiert. Die erreichten Bedingungen unterstreichen die Bedeutung der sozialen Verbindungen und des Diffusionsprozesses selbst.

Neben der Analyse und Modellierung werden die regelungstheoretischen Probleme der Informationsepidemie überprüft. Dabei wird insbesondere der Entwurf einer optimalen Steuerung betrachtet, um so die Informationsausbreitung einem gewünschten Verhalten folgen zu lassen. Durch die Interaktion mit der Ausbreitungsrate werden zwei optimale Steuerungsprobleme in Bezug auf zwei typische Szenarien dargelegt, zum einen die Verhinderung der Verbreitung von Gerüchten, zum anderen die Verbesserung der Verbreitung von Marketing- oder Kampagneninformationen. Dieses Framework wird dann für das SIS-Modell mit verrauschten Übergangsraten verwendet. Durch die Verwendung der Verteilungsanalyseverfahren behandeln wir das robuste optimale Steuerungsproblem: Die Maximierung der Ausbreitungsleistung bei endlicher Zeit und fixem Budget. Es wird ein neuartiger Ansatz eingeführt, der das Vorwärts-Rückwärts-Sweep-Verfahren und das Sekanten-Verfahren kombiniert, um den Rechenaufwand effizient zu reduzieren.

Im Anschluss an den Diffusionsprozess wird die Meinungsdynamik unter Berücksichtigung des sozialen Einflusses untersucht. Die Meinungsdynamik in sozialen Netzwerken mit kooperativ-kompetitiven Interaktionen kann unter verschiedenen Meinungsprotokollen zu Polarität, Konsens oder Neutralität führen. Die Vorstufe des Protokolldesigns besteht darin, das Problem der Zugänglichkeit zu untersuchen: Gibt es zulässige Regelegesetze, um einzelne Meinungen zu polarisieren, vereinbaren oder zu neutralisieren? Aus methodischer Sicht untersuchen wir die Polarisierbarkeit, Konsensfähigkeit und Neutralisierbarkeit der jeweiligen Meinungsdynamik. Ein besonderer Schwerpunkt liegt dabei auf der gemeinsamen Wirkung einzelner dynamischer Eigenschaften, sowie deren sozialen Bindungen. Ausreichende und/oder notwendige Bedingungen für diese Zugänglichkeitsprobleme werden unter Verwendung leistungsfähiger Werkzeuge aus der Spektralanalyse und der algebraischen Graphentheorie bereitgestellt. Um die Vielfalt der Realität zu charakterisieren, untersuchen wir überdies die Lösbarkeit von Meinungsbildungsproblemen in heterogenen Systemdynamiken. Basierend darauf, werden ausreichende und/oder notwendige Kriterien für heterogene Netzwerkpolarisierbarkeit, Konsensfähigkeit und Neutralisierbarkeit abgeleitet.

Contents

Notation	vii
List of Figures	xi
List of Tables	xiii
1 Introduction	1
1.1 Challenges	2
1.1.1 Information Diffusion Dynamics	2
1.1.2 Opinion Dynamics	5
1.2 Contribution and Framework	7
2 Modeling and Analysis of Information Epidemics	9
2.1 Information Epidemics Models	9
2.1.1 Single-Layer Models	10
2.1.2 Multi-Layer Model	14
2.2 Equilibria and Stability Analysis of Single-Layer Information Epidemics . . .	16
2.2.1 Preliminaries	18
2.2.2 The Disease-Free Equilibrium	19
2.2.3 The Endemic Equilibrium	20
2.3 Equilibria and Stability Analysis of Multi-Layer Information Epidemics . . .	27
2.3.1 The Disease-Free Equilibrium	29
2.3.2 The Endemic Equilibrium	32
2.4 Discussion	35
3 Control Design for Information Epidemics	39
3.1 Optimal Control for the SIRS Information Epidemics	39
3.1.1 Existence of the Solutions	41
3.1.2 Solutions to the Optimal Control Problems	43
3.1.3 Numerical Experiments	45
3.1.4 Discussions on Influence of the Parameters	47
3.2 Robust Optimal Control for Information Epidemics with Noisy Infection Rates	49
3.2.1 The Node-Based SIS Model with Noisy Transition Rates	51
3.2.2 Problem formulation	53
3.2.3 Solution to the Robust Control Problem	53

3.2.4	Solution Techniques for Robust Optimal Control of Information Epi- demics	57
3.2.5	Numerical Experiments	58
3.3	Discussion	61
4	Opinion Dynamics on Coopetitive Social Networks	65
4.1	Modulus Consensusability	66
4.2	Modulus Consensusability of Homogeneous Opinion Dynamics on Coopetive Networks	68
4.2.1	Bipartite Consensusability of Opinion Dynamics	68
4.2.2	Neutralizability of Opinion Dynamics	74
4.2.3	Numerical Experiments	75
4.3	Modulus Consensusability of Heterogeneous Opinion Dynamics on Coopetive Networks	79
4.3.1	Problem Formulation	79
4.3.2	Bipartite Consensusability of Opinion Dynamics	82
4.3.3	Neutralizability of Opinion Dynamics	85
4.3.4	Numerical Experiments	85
4.4	Discussion	87
5	Conclusions and Outlook	89
5.1	Conclusions	89
5.2	Outlook	90
A	Graph Theory	93
A.1	Unsigned Graphs	93
A.2	Signed Graphs	94
B	Consensus Theory	99
	Bibliography	107

Notation

Acronyms and Abbreviations

B-A	Barabási-Albert
DFE	disease-free equilibrium
E-R	Erdős-Rényi
FBSM	forward-backward sweep method
HJB	Hamilton-Jacobi-Bellman
HK	Hegselmann-Krause
ICM	independent cascade model
LrGep	local rule-global emergent properties
MFA	mean field approximation
PMP	Pontryagin Maximum Principle
QSC	quasi-strongly connected
SB	structural balanced
SC	strongly connected
SDIE	single dominant information equilibrium
SI	susceptible-infected
SIS	susceptible-infected-susceptible
SIRS	susceptible-infected-recovered/removed-susceptible
G-SEIV	generalized susceptible-exposed-infected-vigilant
SNA	social network analysis

Conventions

Number Sets

\mathbb{R}^n	n -dimension Euclidean space, n is omitted if $n = 1$
\mathbb{C}	set of complex numbers
$\mathbb{C}_{>0}$ ($\mathbb{C}_{\geq 0}$, resp.)	set of complex numbers with positive (nonnegative resp.) real part
$\mathbb{C}_{<0}$ ($\mathbb{C}_{\leq 0}$, resp.)	set of complex numbers with negative (nonpositive resp.) real part
\mathbb{N}	set of all natural numbers, i.e., $0, 1, 2, \dots$
$\mathbb{N}_{[m:n]}$	set of natural numbers from m to n , i.e., $\{m, m + 1, \dots, n\}$

Sets and Their Operations

\mathcal{G}	a graph \mathcal{G}
\mathcal{V}	set of labeled vertices in a graph
\mathcal{E}	set of all edges in a graph
$ \mathcal{S} $	cardinality of a set \mathcal{S}
\mathcal{M}	set of all marginally stable matrices
$\mathcal{B} \setminus \mathcal{A}$	the set of elements in set \mathcal{B} but not in set \mathcal{A} .

Matrices Operations

A^T	transpose of a matrix A
A^{-1}	inverse of a matrix A
$\text{sp}\{A\}$	the spectrum of a square matrix A
$\rho(A)$	the spectral radius of matrix A , i.e., $\rho(A) = \max\{ \lambda : \lambda \in \text{sp}\{A\}\}$
$s(A)$	the largest real part of the eigenvalues of matrix A
$\ker A$	kernel of a matrix A
$\dim A$	dimension of a space spanned by the columns of matrix A
$\det A$	the determinant of a square matrix A
$\text{rank} A$	the rank of a matrix A

$\text{diag}(a)$	the diagonal matrix whose i th diagonal entry equals to the i th element of vector a
$\text{diag}(A_1, A_2, \dots, A_n)$	the (block) diagonal matrix in which the i -th ($i = 1, 2, \dots, n$) element on the diagonal is the matrix A_i
$A \leq (\geq, \text{resp.})B$	$a_{ij} \leq (\geq, \text{resp.})b_{ij}$ where a_{ij} and b_{ij} are the i th row and j th column entry of the identical dimensional matrices A and B
$A < (>, \text{resp.})B$	$A \leq (\geq, \text{resp.})B$ and $A \neq B$
$A \ll (\gg, \text{resp.})B$	$a_{ij} < (>, \text{resp.})b_{ij}$ where a_{ij} and b_{ij} are the i th row and j th column entry of the identical dimensional matrices A and B
$A \prec (\preceq, \text{resp.})0$	matrix A is (semi-, resp.)negative definite
$A \succ (\succeq, \text{resp.})0$	matrix A is (semi-, resp.)positive definite
$A \otimes B$	the kronecker product of matrices A and B

Symbols and Operations

$\text{Prob}(\cdot)$	the probability of certain event
$E(\cdot)$	the expectation of random variable
$\text{cov}(X, Y)$	the covariance of random variables X and Y
$\delta_{m,n}$	Kronecker delta function
$\text{sgn}(\cdot)$	sign of a scalar, outputs are 1, 0, and -1
$\text{Re}\lambda$ ($\text{Im}\lambda$, resp.)	the real (imaginary, resp.) part of a complex number λ
i	imaginary unit, $i^2 = -1$
$\mathbb{1}_n$ ($\mathbb{0}_n$, resp.)	n -dimension column vector with each entry equals to 1 (0, resp.)
I_n	n -dimension identity matrix
O_n ($O_{n \times m}$, resp.)	$n(n \times m$, resp.)-dimension zero matrix
∇f	gradient of function f

List of Figures

2.1	Transitions between different states (S and I) of node i with rates $\bar{\alpha}_i = \sum_{j=1}^N \alpha_j w_{ij} p_j$ and β_i in the node-based SIS model	11
2.2	Node-based SIRS model of node i with transition rates $\bar{\alpha}_i = \sum_{j=1}^N \alpha_j w_{ij} p_j^I$, β_i and γ_i between different states	13
2.4	State transitions of the SIS model for M -competitive information	16
2.5	Multi-layer networks and its equivalent graph on which the information spreads	17
2.6	The infection and recovery probabilities reach the DFE	21
2.7	The infection and recovery probabilities reach the endemic equilibrium	28
2.8	The infection probabilities in the model (2.59) reaches the DFE	31
2.9	The infection probabilities in the model (2.59) reaches the endemic equilibrium	32
2.10	The multi-layer SIS model reaches the DFE	33
2.11	The multi-layer SIS model reaches the SDIE	36
3.1	Control frame for node-based SIRS model	40
3.2	Performance of information epidemics with optimal control in (3.4) and without control along with the cost overtime	47
3.3	Selected p_i^I for nodes labeled 26 and 61	48
3.4	Performance of information epidemics with optimal control in (3.5) and without control along with the consumption overtime	49
3.5	Selected $-J_2(t)$ for nodes labeled 26 and 61	50
3.6	Influence of u_{\min} and t_f in (3.4)	51
3.7	Influence of u_{\max} and t_f in (3.5)	52
3.8	Comparison of $ J(t) $ with no control, with heuristic control, and with robust optimal control on a network of 67 nodes	60
3.9	Comparison of $ J(t) $ with no control, with heuristic control, and with robust optimal control on a network of 214 nodes	61
3.10	Comparison between robust optimal control and nominal control in the form of $ J _{rob} - J _{nom}$	62
3.11	$ J(t_f) $ under different configuration of r and \mathcal{B}	63
4.1	Venn diagram on the relations between the concepts in Definition 3.	68
4.2	An example of SB and QSC graph	75
4.3	Polarization of homogeneous opinion dynamics	77
4.4	A network topology on which the opinion dynamics can achieve inconsistent polarization	78

4.5	Polarization can be inconsistent with structural bipartition in homogeneous opinion dynamics	78
4.6	A structurally unbalanced graph on which the opinion dynamics is polarizable	80
4.7	Polarization of homogeneous opinion dynamics on a structurally unbalanced graph	80
4.8	Neutralization of homogeneous opinion dynamics	81
4.9	Polarization of heterogeneous opinion dynamics	86
4.10	Neutralization of heterogeneous opinion dynamics	87
A.1	A graph with in-isolated subgraphs	94
A.2	Examples of SC and QSC graphs	95
A.3	Structural balance and unbalance of coopetitive networks	96
B.1	Opinion dynamics described as the French-DeGroot model reaches consensus	101
B.2	Opinion dynamics described as the Abelson's model reaches neutralization . .	103
B.3	Opinion dynamics described as the Abelson's model reaches consensus	104
B.4	Opinion dynamics described as the Altafini's model reaches neutralization on structural unbalanced graphs	105
B.5	Opinion dynamics described as the Altafini's model reaches polarization on SB graphs.	106

List of Tables

2.1	$(\ \Delta p^I(t_f)\ _2, \ \Delta p^R(t_f)\ _2)$ in 5-node graphs	15
2.2	Transition rates of three kinds of information reaching the DFE in a two-layer network.	32
2.3	Transition rates of three kinds of information reaching the SDIE in a two-layer network.	35

Introduction

Social networks are constituted by social agents, e.g., individuals and communities, and social relations, e.g., friendship or competition, among them. Recent decades witnessed the explosive development of the online social media thanks to the advancement of information technology, apart from which the study of social network becomes attractive in multitudes of research fields recently including sociology, psychology, economics, computer science, and control engineering [1], [2]. Nonetheless, the history of the research of social networks dates back to a century ago.

The concept of social network is gradually formed by the early researchers around the early 20th century. Among the first researches of social networks, Georg Simmel pointed out that it is the network but not the individual themselves plays the key role in social interactions [3]. This idea is finally formed as an axiom of the social network approach to understanding social interaction, i.e., social phenomena should be primarily conceived and investigated through the properties of relations between and within units, instead of the properties of these units themselves [4]. The 1930s experienced the breakthrough in the analysis of social networks in the fields of psychology, anthropology, and mathematics. As a pioneering work among the major developments, the systematic and quantitative method for measuring social relationships, named *sociometry* is introduced by Jacob Moreno [5], [6] as well as the graphically representation, *sociogram*. Concomitantly, the term “network” is widely used and finally the term *social network* arises. It is well known now that sociometry has given birth to the science of Social Network Analysis (SNA) which focuses on the analyzing the topological properties of social networks and movements [7], [8].

Apart from the structural properties of social networks, the dynamic processes related to social networks are more attractive from the control theoretical point of view. On social networks, one of the typical dynamic processes is the information diffusion process [9]. As the media through which the information spreads, social networks plays dominant role in the form of conventional face-face communication, email networks within companies, the online social media, etc. Nowadays, all major brands, as well as many small businesses, run their own websites online and advertise their products and services using social media. The warming up promotion of movies has become a must in order to be box office smashes. In combination with the social media, movie distributors can create strong buss before the release [10]. More instances can be found for scientific conferences, sport teams and charity campaigns. It is undeniable that the social media have become indispensable for information diffusion and have the trend to eliminate the traditional way. From another perspective,

individuals may also be strongly influenced by the information obtained from networks, especially their opinions and beliefs towards certain topics and events. It is reported in [11] that the fluctuations of U.S. population's certainties of belief on the decision to invade Iraq is highly guided by several political statements. From scientific point of view, to understand the mechanisms of opinion evolution and even to guide the public opinion becomes interesting topics in the fields of sociology, psychology, and politics.

However, few works have been done in the field of social systems by modern control theory [12]. To model, analyze, and control these processes is of great significance for both theory and applications. Very recently, the coordination and control of social systems is regarded as the fundamental problem of sociology [13]. Thus in this dissertation, the focus is to build a bridge filling the gap between control theory and dynamical processes on social networks by providing mathematical tools for modeling, analysis, and control.

1.1 Challenges

In this thesis, we concern the following three challenges revolving around dynamical systems on social networks from control theoretical perspective.

- i) **How to model dynamical systems on social networks.**
- ii) **What are the mathematical properties of the models.**
- iii) **How to control the dynamical systems on social networks.**

Among multitudes of dynamical systems on social networks, the representative ones are the information diffusion processes and the opinion dynamics. Information diffusion can be macroscopically regarded as the information cascade from sources to targets. The specific concerns are: How can we model the diffusion process? What is the steady state? Can we efficiently influence the diffusion to achieve desired performance? Thus the study of this dynamical process is naturally associated to the aforementioned challenges. Besides, opinion dynamics describes the evolution of individual states on social networks. To model the opinion update mechanisms is the fundamental step to understand opinion dynamics. Following the models, the limit behavior of public opinion may become consensus, polarized, and neutral under different conditions. Hence, in order to influence and to guide the individual opinions, the control design is required. Thus in this dissertation, we inspect these two specific dynamical systems, which, in turn, can provide valuable insights on the general topic of dynamical processes on social networks.

A brief introduction of these two categories of systems is provided in the following subsections. In the end of this chapter, we highlight the contribution and illustrate the structure of this dissertation.

1.1.1 Information Diffusion Dynamics

Nowadays, social networks, no matter offline or online, are important media for information diffusion. Multitudes of research has been conducted to shed light on the dynamics of information diffusion on social networks. Mathematical modeling and analysis of information diffusion processes plays the fundamental role in this field and still is the main trend [9].

Numerous models have been reported from different points of view, to name a few, the self-excited Hawkes process model [14], the SPIKEM model [15], and the linear influence model [16]. Since all the models mentioned above mainly concentrate on the population performance, we name them the *macroscopic* or *population-based* models. Apart from these models, the epidemic models plays an important role. For certain kind of information, e.g., a rumor, a commercial advertisement of a product or the political views, its dissemination can be described as the disease-like dissemination over networks and is consequently named as *information epidemics*. Thus it is not surprising that epidemic models are deployed [17]. The shared feature of the epidemic models is that individuals in networks are distinguished into different *compartments*. The elementary compartments are susceptible (S) and infected (I). By considering the transition between different compartments and introducing other classes, e.g. recovered/removed (R) and exposed (E), diverse models are obtained, e.g. the SIR, SIRS and SEIR models [18]. Since information epidemics is one of the main models considered in this dissertation, the macroscopic epidemic models are reviewed as follows.

The SI Model The elemental epidemic model is the SI model [19], where only two compartments and no impact of birth and death rates are considered. For a network of N people, denote $s(t)$ and $i(t)$ the proportion of the susceptible and infected at time t , respectively. The infection rate or daily contact rate λ is assumed to be constant. It follows that given the initial proportion of the infected, the SI model reads

$$\dot{i}(t) = \lambda i(t)(1 - i(t)). \quad (1.1)$$

The dynamics (1.1) implies that the expectation of the susceptible individuals becoming infected within time dt is $\lambda i(t)s(t)N$. Meanwhile, the differential equation regarding $s(t)$ can be omitted because there always holds $s(t) + i(t) = 1$.

The SIS Model Apparently, the SI model only allows the one-way transition from S to I, which is not practical in real situations. By introducing the backward transition from I to S and the corresponding curing rate μ , the SIS model [20] can be derived as follows

$$\dot{i}(t) = \lambda i(t)(1 - i(t)) - \mu i(t). \quad (1.2)$$

Compared with the SI model in (1.1), the SIS model also takes into account the curing process, i.e., there will be $\mu i(t)N$ people become susceptible in time dt .

The SIRS Model Distinct from the SIS model, the SIRS model [21] introduces the recovered or removed state bearing in mind the fact there could exist the temporary immunity phenomenon. In addition to the aforementioned efficient and variables, we denote $r(t)$, σ as the proportion of the recovered at time t and the recovering rate, respectively. Akin to the idea to obtain the SIS model, the SIRS model can be achieved as

$$\begin{aligned} \dot{i}(t) &= \lambda i(t)(1 - i(t)) - \mu i(t) \\ \dot{r}(t) &= \mu i(t) - \sigma r(t). \end{aligned} \quad (1.3)$$

The dynamics of $s(t)$ is omitted due to the fact that there always holds $s(t) + i(t) + r(t) = 1$.

Apart from the three epidemic models, there exist many other extended versions which are detailed gathered in [22].

Although the population-based models capture the feature of information diffusion macroscopically, the reason and mechanism underneath, which may be more important, are ignored. To this end, the *microscopic* models are introduced. The microscopic models, in contrast, concentrate on individuals. Thus they are also called the *node-based* models. Since every character is the investigated subject and his/her activities may be influenced by others, the related networks, e.g. (online) social networks, need to be taken into consideration. Thus the microscopic models are able to characterize the feature of information diffusion dynamics on social networks in nature. To this end, the microscopic models are our main focus in this dissertation. Typical examples of the microscopic models are briefly introduced as follows.

Independent Cascade Model In order to characterize the adoption probability, the independent cascade model (ICM) is proposed. The fundamental assumptions in the ICM are i) the diffusion probability, p_{wv} (from node w to node v) are given and ii) the diffusion processes from distinct active nodes to the target node are independent.

Firstly, the nodes in the social group to be studied are set to be in one of the following two states, a) inactive, i.e. the agent is still not be aware of the information or be influenced and b) active, i.e. the agent has known the information and is willing to spread it to her neighbors. The initial active agents in the network are called *seeds*. Note that the active nodes will never be inactive again.

At each sampling instant, an active node will choose one of the inactive neighbors to spread the information according to the given diffusion probability, p_{wv} , which can be chosen randomly or selected proportional to the tightness of the connection between these two agents. The propagation runs in discrete time and node v becomes active if the diffusion succeeds. Specially, if multiple neighbors of node v are active, the overall diffusion probability are calculated as $1 - \prod_w (1 - p_{wv})$ where w is the active neighbor of node v .

Threshold Model Taking into consideration whether to spread the information or not, an agent should make a decision according to some given rules. An intuitive way, e.g. in the threshold model, is to assign a threshold of each agent to judge whether she is active or not.

Threshold model is first described in 1970s and among the earliest articles and papers, [23] and [24] propose the node-based threshold, i.e. the number or proportion of others who must make one decision before a given actor does so. The threshold for different agent is different according to the preference, goal, perception of the situation, etc..

The early threshold model is developed to linear threshold (LT) model [25] where the influence on a vertex v are assumed to come from the active vertices at time instant t in the set $Y(v, t)$. The specific influence of vertex w to v is normalized as

$$\lambda_{wv} = \frac{1}{1 + |Y(v, t)|} \quad (1.4)$$

such that the total influence for each node is bounded by 1.

To start the diffusion process, an initial active set \mathcal{S} is given usually randomly. Hence, for any node v , a threshold $\theta_v \in [0, 1]$ is assigned randomly. At time-step t , an inactive node v is influenced by each of its active parent nodes w according to weight λ_{wv} . If the sum of the influence of its activated neighbors reaches its threshold, i.e.

$$\sum_{w \in \mathcal{S}} \lambda_{wv} \geq \theta_v, \quad (1.5)$$

node v turns to be active at time $t + 1$. The process terminates if no more activations are possible.

Microscopic Epidemic Models Distinct from the macroscopic epidemic models, the microscopic epidemic models focus on the states of individuals in the social networks. One of the thoroughly studied node-based epidemic models is the N -intertwined SIS model, which is first reported in [26]. By introducing Markov chain into the transmission between the susceptible and infected compartments, the N -intertwined SIS model can be obtained by using the mean-field approximation. Impressive results on the equilibria analysis and the condition for disease free case have been reported in [27] and [28]. In this dissertation, the node-based SIS and SIRS model are inspected as important examples of information diffusion models. Detailed derivations of these models are presented in Section 2.1.

1.1.2 Opinion Dynamics

Individuals' opinions reveal their cognitive orientations towards some objects in terms of displayed attitudes [29] or subjective certainties of belief [30]. These orientations is able to be influenced by the environment and other individuals, especially the ones in the same social group. By taking the social influences into consideration, the opinion dynamics models are introduced where the opinions are scalars or vectors associated with social actors from mathematical point of view.

The original idea of the research in sociology focuses on social influence, which is a pervasive force in human social interaction [31]. Meanwhile, individuals' opinions can be changed according to the social influence in the forms of persuasion by convincing arguments, leadership, and social pressures [32]–[34]. Thus the opinion dynamics, as a result, also reveals the process and the effect of social influence. In this dissertation, we generally name the related models as opinion dynamics since the dynamic system is the main focus in the context of control theory.

In the recent survey [31], The models regarding opinion dynamics can be classified into three categories based on the assimilative social influence, the similarity biased influence and the repulsive influence, respectively.

The research on assimilative influence dates back to the early pioneering works of Festinger and Heider. As one of the fundamental theories of the assimilative influence, the *cognitive consistency* theory and social balance theory point out that individuals seek to be similar to people they like or respect [35], [36]. Representatives of this kind of opinion dynamic models are the averaging models developed in the 1950s and 60s, among which the French-DeGroot model [37], [38] and the Abelson's model [39] are prominent. Although the opinion evolution process is respectively illustrated in continuous and discrete time in these two models, the idea underneath is identical. By taking into consideration a group of individuals in a network sharing opinions, the opinion update law of each agent is set as averaging the neighbors' opinions with weights representing the social influence. In these kind of models, the limit performance of the public opinion may converge and even reach consensus under certain condition on the communication topology. It is interesting that the consensus problem which plays an important role in multi-agent systems occurs much earlier in the study of opinion dynamics. In Section B, the properties of the aforementioned models and the conditions for them to establish consensus are discussed in detail.

One may notice that in the assimilative-influence-based models, the structural connection is usually fixed and the influence is always available through the connection. However, this is not always true since individuals, who are similar to each other, may be more influential. Conversely, the connected individuals with large opinion difference even have no mutual influence. This assumption is adopted by the models with similarity bias, which emphasizes that the similarity of individuals plays a determinant role on the influence through the social tie. Prominent examples are the Hegselmann-Krause (HK) model [40] and the Deffuant model [41]. A general description for these models is as follows

$$x_i(t+1) = x_i(t) + f(x_i(t), x_j(t))(x_j(t) - x_i(t)), \quad (1.6)$$

with

$$f(x_i(t), x_j(t)) = \begin{cases} \mu, & \text{if } |x_j(t) - x_i(t)| < \epsilon \\ 0, & \text{otherwise,} \end{cases} \quad (1.7)$$

where $x_i(t) \in \mathbb{R}$ is the opinion of agent i at time instant t , $f: \mathbb{R} \times \mathbb{R} \rightarrow \mathbb{R}$ is the influence weight function, and μ is the convergence rate. At each time step, a random agent i is selected to update her opinion based on the opinion of a randomly chosen agent j . Since the opinion evolution is active only when the confidence level (the upper bound of the opinion difference) $\epsilon > 0$ is not exceeded, the models similar to the form (1.6) are also named the *bounded confidence* models. Unlike the models based on assimilative influence, there exists no prior fixed communication network in (1.6). Furthermore, due to the truncate function in (1.7), this model is essentially nonlinear.

In both kinds of models mentioned above, assimilation comes into being once the influence occurs between individuals. This assumption is relaxed by the models with repulsive influence by allowing differentiation (to become more dissimilar to others) [42], [43]. This opposite effect is also named as *boomerang* in [29]. The implementation of this assumption can be illustrated with the same dynamics in (1.6) but with discrepant influence weight as follows

$$f(x_i(t), x_j(t)) = \mu(1 - 2|x_j(t) - x_i(t)|). \quad (1.8)$$

In the expression (1.8), the opinion value is bounded in $[0, 1]$ for each agent. It implies that the critical value which determines the pulling towards or pushing away effect of the j th agent's opinion is set to 0.5. These requirements are relaxed by smoothening or truncating function in [44] and [45], respectively.

From control theoretical point of view, the averaging behavior of the public opinion is of great significance. This is highly related to the consensus problem in multi-agent systems. Apart from that, the scholars in control science start to pay more attention to the original model analysis problem regarding diverse opinion dynamic models, especially for the models based on assimilative influence and bounded confidence. In detail, the popular Altafini's model [46] is proposed based on the Abelson's model while on signed graphs. Further extensions to nonlinear opinion protocols [47] and time-varying network structures [48] have been thoroughly studied. Our work [49] extends the original model analysis problem into the accessibility problem based on the protocol similar to the one in Altafini's model. As for the bounded confidence model, detailed analysis has been reported in [50]. While introducing noise into the HK model, the robust consensus problem is addressed recently in [51]. The main trend of the research on opinion dynamics in theoretical control field is to provide rigorous mathematical proof to guarantee certain performance of the systems, which is also

one of the major concern of this dissertation. Future work may include the study of opinion dynamics in general cases and optimal guiding strategy for the public opinion.

1.2 Contribution and Framework

This dissertation provides solutions to the motivated challenges arising for dynamical systems on social networks. Before going into details, the reader may refer to Appendix A for the preliminary information on graph theory and Appendix B for the helpful background on consensus theory. Chapter 2 and 3 are on our first focus, the information epidemic processes. The modeling and analysis parts are provided in Chapter 2. In the modeling section, the detailed derivation of the node-based information epidemic model is provided. Furthermore, we extend the single-layer model into the multi-layer model. Following the modeling, the rigorous mathematical proof for the existence, uniqueness, and stability of the equilibria of the SIRS model is given. In Chapter 3, we address the control design of the information epidemics in the form of optimal control for both noise-free and noisy models. Numerical experiments on real social networks are conducted to demonstrate the effectiveness of the proposed approaches. As another focus of this dissertation, the opinion dynamics on cooperative-competitive social networks are considered in Chapter 4. Specifically, we address the fundamental question: Under what conditions, there exists certain kind of distributed protocols such that the opinion dynamics over cooperative (cooperative-competitive) networks are polarized, consensus and neutralized, respectively. Sufficient and/or necessary conditions are provided for these accessibilities of both homogeneous and heterogeneous opinion dynamic models. We conclude this dissertation in Chapter 5 as well as providing future work on the related topics.

The contribution of this dissertation is to build a bridge between control theory and the study of dynamical processes on social networks by providing mathematical tools for modeling, analysis, and control. Specifically, the contribution are as follows:

i) Modeling and analysis of information epidemics (Chapter 2)

For the modeling and analysis of information epidemics, we introduce the node-based epidemic models by taking into consideration the similarity between the epidemic spread and information dissemination processes. By using the mean-field approximation approach, we extend the thoroughly studied SIS model into the node-based SIS and SIRS models. It is worthy to point out that both the heterogeneities on the network structure and the diffusion processes are considered. Bearing in mind the diverse information spreading media in our daily lives, the multi-layer SIS model is proposed in which each layer stands for certain diffusion channel. Apart from the modeling, mathematical analysis of the properties of the information epidemic models are discussed, especially for the existence, uniqueness, stability of both the trivial and non-trivial equilibria. These results shed light on the interesting behavior of the information epidemics which is essentially nonlinear.

These results on the modeling and analysis of the SIRS model were partially published in [52].

ii) Control design for information epidemics (Chapter 3)

For the control of information epidemics, we aim at offering a framework to design control strategy to guide the information spreading such that the desired performance can be achieved. For the SIRS mode, two practical situations of information diffusion are considered, i.e., to impede the rumor propagation and to enhance the positive information spreading. Furthermore, for the first time, a robust optimal control strategy enhancing the information diffusion with perturbed parameters is designed for information epidemics over heterogeneous communication networks. In light of the real life scenarios, the fixed budget constraint is taken into account. Recalling the distribution analysis approach, the inspected problem is transformed into an optimal control problem with a cost function combining the nominal control performance and the influence of the noise. The solution to the proposed problem is achieved taking advantage of the Pontryagin Maximum Principle (PMP). To attain a practically efficient solution, a computationally cheap algorithm combining the forward backward sweep method (FBSM) and the secant method is provided. This result is especially significant for large scale social networks.

The contribution in the directions of optimal control is partially based on the publication [53]. Furthermore, the results on the robust optimal control for information epidemics has been published in Physica A: Statistical Mechanics and its Applications [54].

iii) **Polarizability, consensusability, and neutralizability of opinion dynamics (Chapter 4)**

For the opinion dynamics on cooperative (cooperative-competitive) networks, we address the fundamental question: Under what conditions, there exists certain kind of distributed protocols such that the opinion dynamics over cooperative networks are polarized, consensus and neutralized, respectively. In specific, the formal definitions of these novel concepts, under the umbrella of “modulus consensusability”, are introduced as an appetizer. In view of the bipartite consensus at the heart of modulus consensus, we set out to study the bipartite consensusability that examines whether or not there exist admissible protocols such that the individual opinions asymptotically reach the same value but may differ in signs. Specifically, sufficient and/or necessary conditions for bipartite consensusability of opinion systems with identical dynamics are provided. The developed criterion emphasizes the functional role of interaction topological properties in conjunction with the dynamic structure of the subsystems. Along with the examination of bipartite consensusability, neutralizability is taken into account as well and is characterized by sufficient and necessary conditions. With the emphasis on individual diversity, another significant contribution of this technical note is to extend the procured results to heterogeneous opinion dynamics. Criteria to examine the polarizability, consensusability, and neutralizability of non-identical opinion dynamics are explored. In particular, some common algebraic properties shared among individuals play an essential role in establishing polarization, consensus, and neutralization.

The materials presented in Chapter 4 has been published in IEEE Transactions on Automatic Control [49].

Modeling and Analysis of Information Epidemics

Information spreading via diverse media, e.g., face-to-face conversations, television and Internet, is indispensable in our daily lives. It is inevitably influential to our decision making, opinions and even activities. Modeling and analysis of information diffusion process become attractive topics and have drawn wide interests in the fields of sociology, psychology, computer science and control in recent years [55]–[57].

As a fundamental issue, mathematical modeling of information diffusion has been thoroughly studied and multitudes of models have been reported [58], [59]. Among the models from diverse points of view, epidemic models have received great attention taking advantage of the analogy between diffusion process of viruses and the status of individuals during information dissemination [22]. The term, *information epidemics* [60], is deployed to describe the disease-like spread of information, e.g., the propagation of a commercial advertisement or a piece of rumor. An obvious common feature of the information epidemic models is that populations are classified into different *compartments*. Susceptible (S) and infected (I) are primary compartments in most literature, since they are natural analogies with people's accessibility of news (unaware or aware) or opinion of innovation (cons or pros). Further compartments, e.g., recovered/removed (R), can be introduced for different situations, which leads to numerous models, e.g., SIR and SIRS models [61].

Among all the information epidemic models, the main focus in this chapter is on the SIS and SIRS models. We first introduce the node-based SIS and SIRS models in both single-layer and multi-layer networks. The analysis of these models, especially the existence, uniqueness, and stability of the equilibria, is provided afterwards.

2.1 Information Epidemics Models

In this subsection, the node-based information epidemic models on both single-layer and multi-layer social networks are introduced. Specifically, on single-layer networks, the SIS and SIRS models are considered in continuous-time manner, whereas on multi-layer networks, the general form of the discrete-time SIS model is proposed.

2.1.1 Single-Layer Models

As is discussed in multitudes of literature works, the node-based epidemic models are able to characterized the information diffusion on graphs. To distinguish the model on multi-layer networks, in this subsection, only the single-layer SIS and SIRS model are introduced.

The Node-based SIS model Among all the information epidemic models, there exist several common compartments, e.g., susceptible (S) and infected (I). These compartments are naturally connected to the individual states, e.g., unawareness and awareness, or to refuse and to accept in the context of information diffusion. The susceptible-infected-susceptible (SIS) model [61] is a basic epidemic model, which is widely used in viral marketing and information diffusion processes.

The mechanism of the transitions in the SIS model can be described by a Markov chain with 2^N states, where N is the number of nodes in the network. Specifically, we denote the random variable $X_i(t)$ as the state of node i at time t . For the convenience of the further analysis, binary numbers are assigned, i.e., $X_i = 0$ or $X_i = 1$ if node i is in state S or I, respectively. Without loss of generality, the communication topology is assumed to be a strongly connected weighted digraph $\mathcal{G}(\mathcal{V}, \mathcal{E}, W)$, where $\mathcal{V} = \{1, 2, \dots, N\}$ and $\mathcal{E} \subseteq \mathcal{V} \times \mathcal{V}$ are the sets of vertices and edges, respectively; and $W = [w_{ij}] \in \mathbb{R}^{N \times N}$ is the nonnegative adjacency matrix. It is assumed that $w_{ij} > 0$ if and only if there exists a link from j to i ; $w_{ij} = 0$, otherwise. The local rule of the SIS model consists of two possible actions modeled as Poisson processes: i) the infection process: a susceptible node can be infected by its infected neighbors and ii) the curing process: an infected node can cure and become susceptible again. The infection process is considered as a proactive action, i.e., each infected individual i infects his/her susceptible social neighbors with rate α_i [62]. Whereas, the curing process is assumed to be passive with rate β_i . Note that generally there hold $\alpha_i \neq \alpha_j$ and $\beta_i \neq \beta_j$ for all $i, j \in \mathcal{V}, i \neq j$. It follows that the node-based SIS model is heterogeneous in view of both the communication topology and the transition process.

The local nodal dynamics can be modeled as a two-state Markov chain in continuous time. For a sufficiently small time Δt , there hold

$$\begin{aligned} \text{Prob}[X_i(t + \Delta t) = 1 | X_i(t) = 0] &= \sum_{j \in \mathcal{N}^{\text{in}}} \alpha_j w_{ij} X_j(t) \Delta t \\ \text{Prob}[X_i(t + \Delta t) = 0 | X_i(t) = 1] &= \beta_i X_i(t) \Delta t. \end{aligned} \quad (2.1)$$

By using the mean field approximation (MFA), the actual infection rate $\sum_{j \in \mathcal{N}^{\text{in}}} \alpha_j w_{ij} X_j(t)$ is replaced by $\sum_{j=1}^N \alpha_j w_{ij} \mathbf{E}[X_j(t)]$. This replacement is accurate if the states of the neighbors are sufficiently independent and the number of the in-neighbors of node i is large. In this case, the Central Limit Theorem [63] is applicable. It follows that if $\Delta t \rightarrow 0$, we have

$$\begin{aligned} \frac{d\mathbf{E}[X_i]}{dt} &= \mathbf{E}[(1 - X_i(t)) \sum_{j=1}^N \alpha_j w_{ij} X_j(t) - \beta_i X_i(t)] \\ &= \sum_{j=1}^N \alpha_j w_{ij} \mathbf{E}[X_j(t)] - \beta_i \mathbf{E}[X_i(t)] - \sum_{j=1}^N \alpha_j w_{ij} \mathbf{E}[X_i(t) X_j(t)] \\ &= (1 - \mathbf{E}[X_i(t)]) \sum_{j=1}^N \alpha_j w_{ij} \mathbf{E}[X_j(t)] - \beta_i \mathbf{E}[X_i(t)] - \sum_{j=1}^N \alpha_j w_{ij} \text{cov}[X_i, X_j], \end{aligned} \quad (2.2)$$

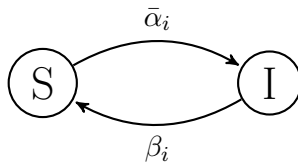


Figure 2.1.: Transitions between different states (S and I) of node i with rates $\bar{\alpha}_i = \sum_{j=1}^N \alpha_j w_{ij} p_j$ and β_i in the node-based SIS model

where the equation $\mathbf{E}[X_i] = \mathbf{Prob}[X_i = 1]$ is utilized. It is worth noting that the last equation is obtained by using

$$\mathbf{E}[X_i X_j] = \mathbf{E}[X_i] \mathbf{E}[X_j] - \mathbf{cov}[X_i, X_j]. \quad (2.3)$$

The covariance plays a fundamental role in (2.2) and it has been reported that $\mathbf{cov}[X_i, X_j] \geq 0$ for the SIS model in any graph [64]. Notice that $\mathbf{Prob}[X_i = 1] = \mathbf{E}[X_i]$. It yields that if $\mathbf{cov}[X_i, X_j] = 0$, by denoting $p_i(t) = \mathbf{Prob}[X_i = 1]$, one can have the node-based SIS model as follows

$$\dot{p}_i = (1 - p_i) \sum_{j=1}^N \alpha_j w_{ij} p_j - \beta_i p_i. \quad (2.4)$$

The interpretation of the node-base SIS model (2.4) is as follows: The change of the infection probability of node i during a time interval dt consists of two parts, i.e. the influence of the infected neighbors if node i is susceptible; and the curing probability if node i is infected. The equal transition map is presented in Figure 2.1. Note that $\bar{\alpha}$ is the equivalent infection rate which covers all the influence of the infected in-neighbors of node i .

The node-based SIS model (2.4) is a nonlinear differential equation which gives insights into the information diffusion process from the nodal point of view. Especially, it is efficient for large scale networks compared with the Markov chain model. Although the model (2.4) has been widely used and many existing literature works directly ignore the dynamics (2.2), the fundamental problem of the applicability of the node-based SIS model is of great importance. Apparently, the accuracy of the model (2.4) relies on the value of $\mathbf{cov}[X_i, X_j]$. To this end, the normalized accuracy criterion

$$r_T = \frac{2}{|\mathcal{E}|} \sum_{i=1}^N \sum_{j=1}^N \alpha_j w_{ij} \mathbf{cov}[X_i, X_j] \quad (2.5)$$

is introduced in [65] for the SIS model on undirected graphs and homogeneous diffusion processes. It is pointed out that the worst accuracy of the model (2.4) increases with average degree of the graph as well as the network scale. It implies that the node-based SIS model (2.4) is generally sufficiently accurate on large scale networks. To this end, the variable p_i in (2.4) is considered as the infection probability of node i in this dissertation.

The Node-based SIRS model In the epidemic processes, there exist not only susceptible and infected compartments but also short-term immunity [66]. It follows that the recovered or the removed state is necessary to be taken into account, which forms the SIRS model [67]. Akin to the short-term immunity phenomenon, the temporary oblivion is inevitable in the information diffusion processes. In Blogspace and web forums, the temporary oblivion or boredom regarding certain topic is vividly characterized by the process from R to S

[68], [69]. Apart from that, the SIRS model is also naturally applicable in marketing. The individuals, to whom a firm wants to sell the product, can be in one of three states: potential customer (susceptible), willing to buy (infected), and ignoring all the related information of the product (recovered). Additionally, this model is valuable to the long-term brand strategy [70] and viral marketing.

The underneath mechanism of the transition of the SIRS model can be described by a Markov chain with 3^N states. As an MFA of the Markov chain, a continuous-time node-based SIRS model taking into considerations of heterogeneity in networks and diffusion processes is adopted in this paragraph in the context of information diffusion.

We assume that there are three possible states in each node, i.e. susceptible (S), infected (I) and recovered (R) where an individual could fall into when facing a disease. Analogously, these three states refer to unawareness, awareness and oblivion of the information, respectively. In the SIRS model, it is assumed that the individual is infectious (willing to spread the news) once he/she is infected. Another widely adopted assumption is that the disease propagates only via interactions between people. Thus individuals have no chance of getting infected unless at least one of her neighbors is infectious.

The SIRS model could be naturally modeled as a Markov chain. Inspired by the model (2.1), we introduce ternary numbers for the compartments in SIRS model, i.e., the random variable $X_i(t) = 0, 1$ or 2 represents the state of node i to be S, I, and R at time instant t , respectively. It yields that the following conditional probabilities hold

$$\begin{aligned} \text{Prob}[X_i(t + \Delta t) = 1 | X_i(t) = 0] &= \sum_{j \in \mathcal{N}^{\text{in}}} \alpha_j w_{ij} \delta_{X_j(t), 1} \Delta t, \\ \text{Prob}[X_i(t + \Delta t) = 2 | X_i(t) = 1] &= \beta_i \Delta t, \\ \text{Prob}[X_i(t + \Delta t) = 0 | X_i(t) = 2] &= \gamma_i \Delta t, \end{aligned} \tag{2.6}$$

where $\delta_{m,n}$ is the Kronecker delta function defined as

$$\delta_{m,n} = \begin{cases} 1, & \text{if } m = n \\ 0, & \text{if } m \neq n. \end{cases} \tag{2.7}$$

It follows that the time derivative of the expectation of $\delta_{X_i,1}$ and $\delta_{X_i,2}$ can be respectively attained as

$$\begin{aligned} \frac{d\mathbf{E}[\delta_{X_i,1}]}{dt} &= \mathbf{E}[(1 - \delta_{X_i,1} - \delta_{X_i,2}) \sum_{j=1}^N \alpha_j w_{ij} \delta_{X_j,1} - \beta_i \delta_{X_i,1}] \\ &= \sum_{j=1}^N \alpha_j w_{ij} \mathbf{E}[\delta_{X_j,1}] - \beta_i \mathbf{E}[\delta_{X_i,1}] - \sum_{j=1}^N \alpha_j w_{ij} (\mathbf{E}[\delta_{X_i,1} \delta_{X_j,1}] + \mathbf{E}[\delta_{X_i,2} \delta_{X_j,1}]) \\ &= (1 - \mathbf{E}[\delta_{X_i,1}] - \mathbf{E}[\delta_{X_i,2}]) \sum_{j=1}^N \alpha_j w_{ij} \mathbf{E}[\delta_{X_j,1}] - \beta_i \mathbf{E}[\delta_{X_i,1}] \\ &\quad - \sum_{j=1}^N \alpha_j w_{ij} (\text{cov}[\delta_{X_i,1}, \delta_{X_j,1}] + \text{cov}[\delta_{X_i,2}, \delta_{X_j,1}]) \\ \frac{d\mathbf{E}[\delta_{X_i,2}]}{dt} &= \beta_i \mathbf{E}[\delta_{X_i,1}] - \gamma_i \mathbf{E}[\delta_{X_i,2}]. \end{aligned} \tag{2.8}$$

The covariances $\text{cov}[\delta_{X_i,1}, \delta_{X_j,1}]$ and $\text{cov}[\delta_{X_i,2}, \delta_{X_j,1}]$ can be neglected since the corresponding variables are assumed to be independent. Denote $p_i^I(t) = \text{Prob}[X_i(t) = 1]$ and $p_i^R(t) =$

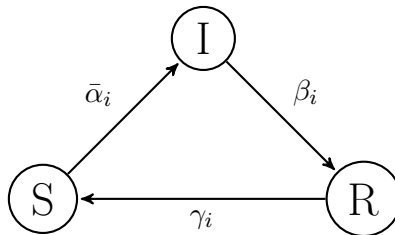


Figure 2.2.: Node-based SIRS model of node i with transition rates $\bar{\alpha}_i = \sum_{j=1}^N \alpha_j w_{ij} p_j^I$, β_i and γ_i between different states

$\text{Prob}[X_i(t) = 2]$. By using the MFA, the heterogeneous node-based SIRS model for node i in a directed network $\mathcal{G} = (\mathcal{V}, \mathcal{E}, W)$ can be described as

$$\begin{aligned} \dot{p}_i^I(t) &= (1 - p_i^I(t) - p_i^R(t)) \sum_{j=1}^N \alpha_j w_{ij} p_j^I(t) - \beta_i p_i^I(t), \\ \dot{p}_i^R(t) &= \beta_i p_i^I(t) - \gamma_i p_i^R(t), \end{aligned} \quad (2.9)$$

Note that $p_i^S(t)$ is redundant due to the fact that every node must be in one of the three states, i.e. the equality $p_i^S(t) + p_i^I(t) + p_i^R(t) = 1$ always holds. The interpretation of the node-base SIRS model (2.9) is as follows: i) The change of the infection probability of node i during a time interval dt consists of two parts, i.e. the influence of the infected neighbors if node i is susceptible; and the recovery probability if node i is infected. ii) The change of the recovery probability of node i during time interval dt is also made of two parts, i.e. the recovery probability if node i is infected; and the probability of being susceptible if node i is recovered.

The state variables in node-based SIRS model (2.9) are actually approximations of $v_i^I := \mathbf{E}[\delta_{X_i,1}]$ and $v_i^R := \mathbf{E}[\delta_{X_i,2}]$ in (2.8), respectively. In the case where the actions of node i due to each of his/her infectious in-neighbors are independent, one could know that the approximations behave well thanks to the central limit theorem. Unfortunately, it is evident that the independence condition can hardly hold in information diffusion processes. Nevertheless, the node-based SIRS model (2.9) is utilized taking into consideration its comprehensive physical meaning and far less computational consumption, especially in large-scale networks. Akin to the previous works [28], [71], [72], we still name p_i^I and p_i^R as the probabilities of infection and recovery for node i due to convenience of presentation in case of no ambiguity. To evaluate the validation of this node-based SIRS model, numerical experiments are conducted to compare the performance of the Markov chain and the node-based SIRS model in digraphs.

Comparison of node-based SIRS model and 3^N -state Markov chain In this subsection we focus on the detailed comparisons between the 3^N -state Markov chain and the node-based SIRS model over strongly connected directed networks.

The simulations are conducted with homogeneous coefficients over line graphs, E-R random graphs, small scale graphs and complete graphs with 5 nodes. The 5-node graphs used in these simulations are presented in Figure 2.3. Bearing in mind that the computation capacity and also the fact that the node-based model approximates the behavior of Markov chain less well in small networks, the number of nodes in the examples are chosen to be small. The value of the transition rates α, β and γ are all limited in the set $\{0.1, 1\}$

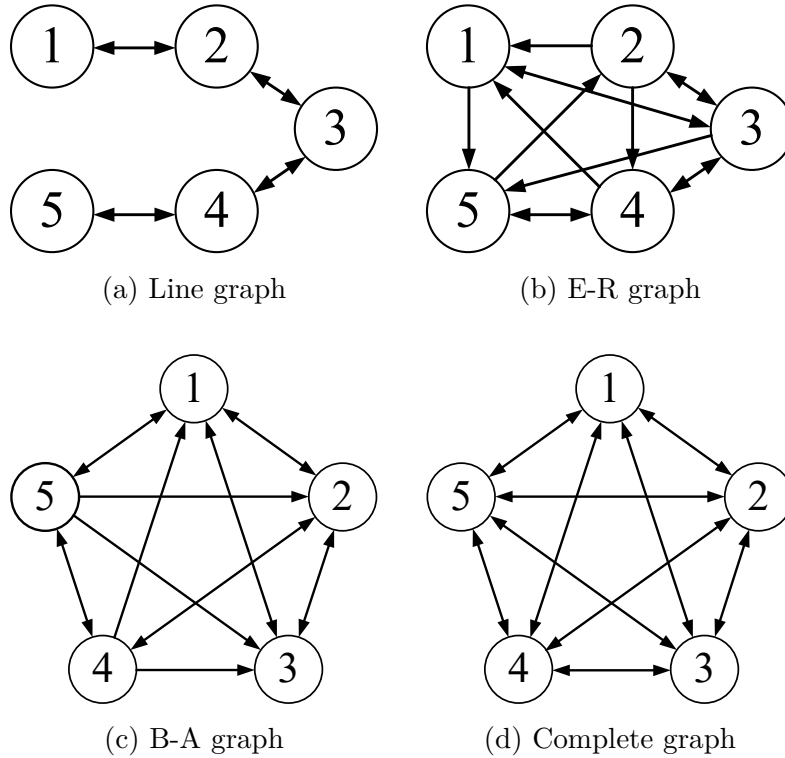


Figure 2.3.: Examples of 5-node graphs

such that the results can cover major range of the coefficients. For each simulation in the graphs with the same number of nodes, the initial values are the same. Specifically, the initial sates are randomly chosen as $(01020)_3$ and $(0120110)_3$. The corresponding initial states for the node-based SIRS model are then set as $((0, 0), (0, 1), (0, 0), (1, 0), (0, 0))$. We run all the simulations with sampling period 0.001 and $t_f = 50$. The differences between the infected and removed probabilities at t_f are obtained as $\Delta p^I(t_f) = v^I(t_f) - p^I(t_f)$ and $\Delta p^R(t_f) = v^R(t_f) - p^R(t_f)$. In Table 2.1, the results are listed in the form of 2-norm. The errors less than 0.005 is recorded as 0 in both tables. It is evident that for the same type of graph, the node-based SIRS model approximate the Markov chain best when $\alpha/\beta = 1/10$. In this setting, the process finally reaches the rumor free equilibrium. However, for the case when $\alpha/\gamma = 10$, the difference could be extremely large (1.18) and the process reaches the nontrivial equilibrium. Thus we conclude that the node-based SIRS model performs generally better with rumor free configurations. As for different kinds of graphs, the two models have the most similar final values in complete graphs. The largest error occurs in B-A networks and a potential reason is the heterogeneity caused by directed connections. The results in E-R and B-A networks may vary with respect to different connection settings.

2.1.2 Multi-Layer Model

Although the node-based models in subsection 2.1.1 is able to describe the information diffusion processes on social networks, only single epidemic and single layer network is considered, which is not general enough for diverse information dissemination phenomena. In this subsection, we extend the SIS model on single-layer network into multi-information SIS model on multi-layer networks.

Table 2.1.: $(\|\Delta p^I(t_f)\|_2, \|\Delta p^R(t_f)\|_2)$ in 5-node graphs

$\alpha : \beta : \gamma$	Line	E-R	B-A	Complete
1:1:1	(0.31,0.20)	(0.27,0.19)	(0.50,0.39)	(0.04,0.01)
1:1:10	(0.55,0.05)	(0.46,0.05)	(0.67,0.07)	(0.09,0.01)
1:10:1	(0,0.01)	(0,0.01)	(0,0.01)	(0,0.01)
1:10:10	(0,0)	(0,0)	(0,0)	(0,0)
10:1:1	(0.73,0.62)	(0.77,0.68)	(0.62,0.51)	(0.56,0.45)
10:1:10	(0.15,0.01)	(0.17,0.02)	(0.07,0.01)	(0.16,0.02)
10:10:1	(0.08,0.74)	(0.07,0.68)	(0.12,1.18)	(0,0.01)

A multilayer network structure is introduced to describe the interconnection in the population with fixed capacity via diverse media, e.g., face-to-face conversation and online chatting. Generally, we consider a multilayer network consists of L layers ($L \in \mathbb{N}_{\geq 0}$). This setting precisely mimics the scenario that the contact networks are non-identical via various media for certain group of population.

Inspired by [73], we denote $\mathcal{G}_i = (\mathcal{V}, \mathcal{E}_i, W_i), i \in \mathbb{N}_{[1:L]}$ as the i th layer of the multilayer network, where \mathcal{V} and $\mathcal{E}_i \subseteq \mathcal{V} \times \mathcal{V}$ are the sets of vertices and edges, respectively. The nonnegative matrix $W_i = [w_{i,jk}] \in \mathbb{R}^{N \times N}$ is the adjacency matrix. $w_{i,jk} > 0$ if and only if there exists a link from node j to k in the i th layer network. In this case, we say node j listens to node k or node k can influence node j via communication topology \mathcal{G}_i . Bearing in mind that multitudes of communications like campaigning and news propagation are not mutual but with direction, digraphs are considered. To this end, $w_{i,jk} = w_{i,kj}$ does not generally hold. It is also assumed that there exists no self loop, i.e., $w_{i,jj} = 0, \forall j \in \mathcal{V}$. For the convenience of further presentation, the in-neighborhood of node $j \in \mathcal{V}$ in the i th layer is introduced as

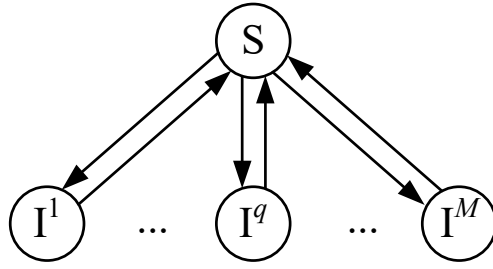
$$\mathcal{N}_{i,j}^{in} = \{k : w_{i,jk} > 0, k \in \mathcal{V}_i\}. \quad (2.10)$$

Note that we do not require the graph in each layer to be strongly connected. It reflects the fact that not all the individuals in the inspected group of population are accessible via every social media. For the case when $L = 1$, the multilayer network degenerates to a single network.

In this subsection, the competitive information epidemics is described as the discrete-time SIS model with heterogeneous transition rates. We take into account the SIS model where there are two states i.e., susceptible (S) and infected (I). Specially, to distinguish the infected states due to different pathogens, we assume that there exist $M (M \in \mathbb{N}_{\geq 0})$ independent epidemics labeled as $I^m, m = 1, \dots, M$. The transition relation between the states is presented in Figure 2.4. Specifically, there exist M stochastic transitions in this SIS model. By denoting $X_k(t)$ as the random variable standing for the state of node k at time instant t , one could obtain the following conditionally probabilities.

- i) The infection process: A susceptible agent k can get infected by epidemic m from its infected neighbor j in the i th layer network with infection rate $\alpha_{i,j}^m$. Under the assumption of independent Poisson process, the transition probability is the sum of all the k 's neighbors infected by epidemic m in every layer, i.e.,

$$\text{Prob}[X_k(t+1) = I^m | X_k(t) = S] = h \sum_{i=1}^L \sum_{j=1}^N \alpha_{i,j}^m w_{i,kj} \delta_{X_j, I^m}, \quad (2.11)$$


 Figure 2.4.: State transitions of the SIS model for M -competitive information

ii) The curing process: An agent k infected by epidemic m can get cured with rate β_k^m

$$\text{Prob}[X_k(t+1) = \text{S} | X_k(t) = \text{I}^m] = \beta_k^m h \quad (2.12)$$

Apart from the transition processes, a widely adopted assumption in the competitive epidemics is that the case when any node is infected by both epidemics is excluded. By denoting $p_k^m(t) = \text{Prob}[X_k(t) = \text{I}^m]$, one can obtain the following dynamics

$$p_k^m(t+1) = (1 - \sum_{q=1}^M p_k^q(t))h \sum_{i=1}^L \sum_{j=1}^N \alpha_{i,kj}^m p_j^m(t) + (p_k^m(t) - \beta_k^m h p_k^m(t)) \quad (2.13)$$

where $\alpha_{i,kj}^m = \alpha_{i,j}^m w_{i,kj}$. By encapsulating the states as $p^m = (p_1^m, \dots, p_n^m)$, $m \in \mathbb{N}_{[1:M]}$, the compact form of the SIS model then reads

$$p^m(t+1) = (I + h\tilde{A}^m - h \sum_{q=1}^M P^q(t)\tilde{A}^m - hB^m)p^m(t), m \in \mathbb{N}_{[1:M]}, \quad (2.14)$$

where $\tilde{A}^m = \sum_{i=1}^L A_i^m$, $A_i^m = [\alpha_{i,kj}^m] = \text{diag}(\alpha_{i,1}^m, \dots, \alpha_{i,N}^m)W_i$, $B^m = \text{diag}(\beta_{i,1}^m, \dots, \beta_{i,N}^m)$, and $P^q = \text{diag}(p^q)$.

The model in (2.14) is equivalent to the scenario of multiple competitive information epidemics spreading on one single layer network $\tilde{\mathcal{G}} = (\mathcal{V}, \tilde{\mathcal{E}})$ with different adjacency matrices, i.e., \tilde{A}^m . In other words, the spreading paths for the two competitive information are identical whereas the spreading rates differ. As is shown in Figure 2.5, the equivalent graph can be regarded as a compressed version of all the layers. Note that not all the nodes are active in each layer which vividly characterizes the fact that people are only into certain kinds of social media.

2.2 Equilibria and Stability Analysis of Single-Layer Information Epidemics

The equilibria are of great significance for dynamic systems from control theoretical point of view. As for the information epidemics systems, the equilibria are also important since they imply the steady states of the information diffusion processes. Evidently, the origin is an equilibrium of the SIS model in (2.4), as well as the SIRS model in (2.9). Thus it is referred to as the *nontrivial* equilibrium or the *disease-free* equilibrium (DFE) in the context

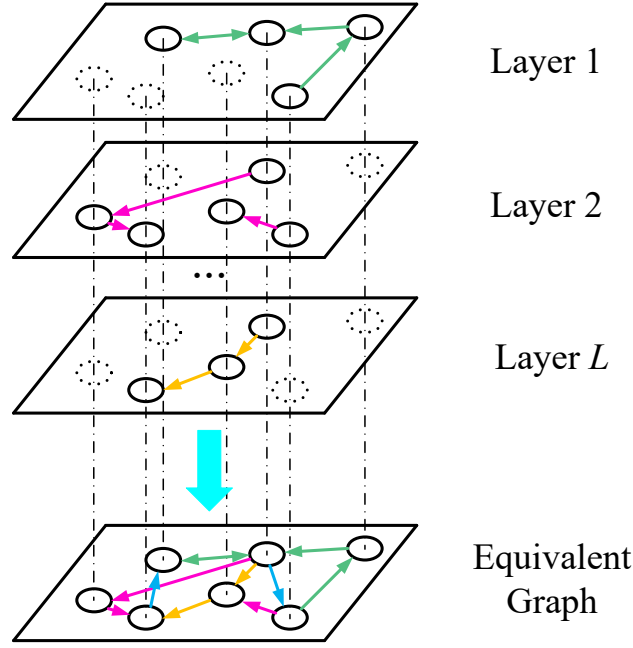


Figure 2.5.: Multi-layer networks and its equivalent graph on which the information spreads

of dynamical systems or the epidemiology, respectively. This zero equilibrium is naturally essential since its stability conditions infers the way for immunization. On the other hand, there may exist *trivial* equilibrium or the *endemic* equilibrium of the information epidemic models. The endemic equilibrium is straightforwardly associated with the propagation performance at the finite time so that more inspection is needed.

Since the SIRS model contains more compartments compared with the SIS model, we focus on the equilibrium analysis of the SIRS model in (2.9) as an instance and provide the stability conditions in this subsection. The results regarding the SIS model can be referred to in [27], [28].

By encapsulating the state variables as $p^I = [p_1^I, \dots, p_N^I]^T$ and $p^R = [p_1^R, \dots, p_N^R]^T$, the compact form of the SIRS reads

$$\begin{aligned} \dot{p}^I &= (I - P^I - P^R)WAp^I - Bp^I, \\ \dot{p}^R &= Bp^I - \Gamma p^R, \end{aligned} \quad (2.15)$$

where $A = \text{diag}(\alpha_1, \dots, \alpha_N)$, $B = \text{diag}(\beta_1, \dots, \beta_N)$ and $\Gamma = \text{diag}(\gamma_1, \dots, \gamma_N)$. $P^I = \text{diag}(p^I)$ and $P^R = \text{diag}(p^R)$ are diagonal matrices whose entries are the infection and recovering probabilities of each node at time instant t , respectively.

Henceforth we denote $p_i = [p_i^I, p_i^R]^T$ which should take value in the domain described as

$$\Delta := \{p_i | p_i^I \in [0, 1], p_i^R \in [0, 1], p_i^I + p_i^R \in [0, 1]\}. \quad (2.16)$$

Before embarking on the equilibria of the SIRS model, the boundaries of the state variables are first studied, whose result is concluded in the following lemma.

Lemma 1. *Consider the system described in (2.15), if $p_i(0) \in \Delta$, $p_i(t) \in \Delta$, $\forall t > 0$.*

Proof. Assume that for a time instant $\tau \geq 0$ there exist $p_i(\tau) \in \Delta$. Then we have the following three cases (a) if $p_i^I(\tau) = 0, \dot{p}_i^I(\tau) \geq 0, \forall p_i^R(\tau) \in [0, 1]$, (b) if $p_i^R(\tau) = 0, \dot{p}_i^R(\tau) \geq 0, \forall p_i^I(\tau) \in [0, 1]$ and (c) if $p_i^I(\tau) + p_i^R(\tau) = 0, \dot{p}_i^I(\tau) + \dot{p}_i^R(\tau) \leq 0$. From (a) and (b), we have $p_i^I, p_i^R \geq 0$ and along with (c), we have $p_i^I + p_i^R \leq 1$, which is equal to $p_i(t) \in \Delta, \forall t > 0$, if $p_i(0) \in \Delta$. \square

From Lemma 1, one can straightforwardly conclude that $p_i(t) \in \Delta$ always hold with reasonable initial condition, i.e., Δ^N is an invariant set of the system (2.15). In the remaining part, $p_i(0) \in \Delta$ is omitted for simplicity if there is no ambiguity.

For the convenience of the further analysis, we first fix some notations that will be used in this section. For matrix $X = [x_{ij}], Y = [y_{ij}] \in \mathbb{R}^{m \times n}$, we introduce the entry-wise comparison symbols. $X \leq (\ll, \geq, \gg) Y$ represents there holds $x_{ij} \leq (<, \geq, >) y_{ij}$ for all the responding entries in X and Y . $X > (<) Y$ means that $X \leq (\geq) Y$ and $X \neq Y$. These symbols are also valid for vectors. Hence, we denote $\rho(X)$ and $s(M)$ as the spectral radius and the largest real part of the eigenvalues of a square matrix X , respectively.

2.2.1 Preliminaries

For the convenience of the analysis, we the background knowledge on Metzler matrix and dynamical systems are briefly introduced.

Metzler Matrix A matrix $M \in \mathbb{R}^{n \times n}$ is a Metzler matrix if its off diagonal entries are nonnegative. The properties related to the analysis of the node-based SIRS model are provided in the following lemmas.

Lemma 2. *Given an irreducible Metzler matrix M , there holds that $s(M)$ is a simple eigenvalue of M and the associated eigenvector of $s(M)$ is unique (up to scalar multiple) and strictly positive.*

Lemma 3. *Given a irreducible Metzler matrix $M \in \mathbb{R}^{n \times n}$ and a vector $x > 0_n$, there hold: For any scalar μ ,*

- i) if $Mx > \mu x$, then $s(M) > \mu$;*
- ii) if $Mx = \mu x$, then $s(M) = \mu$;*
- iii) if $Mx < \mu x$, then $s(M) < \mu$.*

Lemma 4. [74] *If a Metzler matrix M is Hurwitz, then there exists a positive definite diagonal matrix D such that $M^T D + DM = -Q$ where Q is positive definite.*

Lemma 5. *Given an irreducible Metzler matrix M , there exists a positive definite diagonal matrix D such that $M^T D + DM = -Q$ where Q is positive semi-definite.*

Lemma 2 and 3 are originally given in [75] for nonnegative matrices. They also hold for Metzler matrices taking into consideration that $\text{sp}\{M + \zeta I\} = \text{sp}\{M\} + \zeta$ for any real scalar ζ .

Equilibrium and Stability Apart from the preliminaries on Metzler matrix, we recall some fundamental definitions on equilibrium and domain of attraction from [76], which are necessary for the analysis in the following subsections.

Consider the general form of autonomous systems:

$$\dot{x}(t) = f(x(t)), \quad x(0) = x_0, \quad (2.17)$$

where $f : \mathcal{X} \rightarrow \mathbb{R}^n$ is locally Lipschitz and $\mathcal{X} \subseteq \mathbb{R}^n$. The equilibrium of (2.17) is defined as follows.

Definition 1 (Equilibrium). Consider the system in (2.17). $x_e \in \mathcal{X}_e$ ($\mathcal{X}_e \subseteq \mathcal{X}$) is an equilibrium if there holds

$$f(x_e) = 0. \quad (2.18)$$

The stability of an equilibrium is of great significance in dynamical systems. In this dissertation, we highlight the asymptotic stability, which is rigorously defined as follows.

Definition 2 (Asymptotic stability). Consider the system in (2.17) with equilibrium $x_e \in \mathcal{X}_e$. This equilibrium is asymptotically stable, if for any $x(0) \in \mathcal{X}_e$ there holds $\lim_{t \rightarrow \infty} x(t) = x_e$. Then \mathcal{X}_e is said to be a domain of attraction for x_e . x_e is unstable if it is not stable.

Based on the above background, we can proceed on the analysis of the equilibria of the SIRS model.

2.2.2 The Disease-Free Equilibrium

Trivial equilibrium of is associated with rumor-free case. For certain kind of rumor diffusion, there exist no one to believe it after a period of time. Typical examples are the rumors refuted by science like the heavier object falls faster than the lighter. Specifically, for the SIRS model, we have the following theorem.

Theorem 1. *Given the node-based SIRS model (2.15), the origin is asymptotically stable with domain of attraction Δ^N , if $s(WA - B) \leq 0$.*

Proof. Since the graph \mathcal{G} is strongly connected, W is an irreducible nonnegative matrix. In addition, A and B are positive definite diagonal matrices, which implies that $(WA - B)$ is an irreducible Metzler matrix. For the case $s(WA - B) < 0$, according to Lemma 4, there exists a positive diagonal matrix \mathcal{P} such that $(WA - B)^\top \mathcal{P} + \mathcal{P}(WA - B)$ is negative definite. For the dynamics of p^I , consider a Lyapunov function $V(p^I(t)) = (p^I)^\top(t) \mathcal{P} p^I(t)$. The time derivative of V then reads

$$\begin{aligned} \dot{V}(p^I(t)) &= 2(p^I)^\top \mathcal{P} [(I - P^I - P^R)WA - B] p^I \\ &\leq 2(p^I)^\top \mathcal{P} (WA - B) p^I \\ &< 0 \end{aligned} \quad (2.19)$$

The inequality holds because $2(p^I)^\top (P^I + P^R) W A p^I \geq 0$ for all t . It yields that p^I approaches 0_N asymptotically. Additionally, since $\Gamma \succ 0$ and p^I and p^R are bounded by Lemma 1, it is apparent that $p^R \rightarrow 0_N$ as $t \rightarrow \infty$.

For the case when $s(WA - B) = 0$, there exists a positive diagonal matrix \mathcal{Q} such that $(WA - B)^\top \mathcal{Q} + \mathcal{Q}(WA - B)$ is negative semi-definite. By choosing the Lyapunov function $V(p^I(t)) = (p^I)^\top(t) \mathcal{Q} p^I(t)$, one can obtain the time derivative of V as

$$\begin{aligned} \dot{V}(p^I(t)) &= 2(p^I)^\top \mathcal{Q} [(I - P^I - P^R)WA - B] p^I \\ &= 2(p^I)^\top \mathcal{Q}(WA - B) p^I - 2(p^I)^\top \mathcal{Q}(P^I + P^R) W A p^I \\ &\leq 0 \end{aligned} \quad (2.20)$$

If $\dot{V} = 0$, one has $(p^I)^\top [(WA - B)^\top \mathcal{Q} + \mathcal{Q}(WA - B)] p^I = 0$. We then show $p^I = \mathbb{0}_N$ is the only solution by contradiction. Suppose $p^I \gg \mathbb{0}_N$. Since WA is irreducible Metzler, there holds $W A p^I \gg \mathbb{0}_N$. In addition, \mathcal{Q} and $P^I + P^R$ is positive definite. It is evident that $(p^I)^\top \mathcal{Q}(P^I + P^R) W A p^I > 0$, which implies that $\dot{V} < 0$. Suppose $p^I > \mathbb{0}_N$ and at least one of p^I 's element is 0. Taking into consideration that $(WA - B)^\top \mathcal{Q} + \mathcal{Q}(WA - B)$ is negative semi-definite, we have $s((WA - B)^\top \mathcal{Q} + \mathcal{Q}(WA - B)) = 0$. By Lemma 2, 0 is a simple eigenvalue associated with a unique strictly positive eigenvector. Thus the considered p^I is not the eigenvalue since it possesses at least one 0 element. It yields that $2(p^I)^\top \mathcal{Q}(WA - B) p^I < 0$. Hence, $\dot{V} < 0$. Then we conclude that neither of the aforementioned situations of p^I is possible to achieve $\dot{V} = 0$. It follows that $\dot{V} = 0$ if and only if $p^I = 0$. By La Salle's invariant principle, the system of p^I is asymptotically in the origin. Following the same techniques for the case when $s(WA - B) < 0$, one can conclude that the dynamics of p^R also converge to $\mathbb{0}_N$ asymptotically. Apart from the stability analysis, one can notice that no further requirements are needed for the region of p^I and p^R . Thus the whole region of Δ^N is the domain of attraction. Thus we complete the proof. \square

According to Theorem 1, $s(WA - B)$ plays the key role for the stability of the DFE of the SIRS model. Moreover, by directly inspect the dynamics in (2.15), we can obtain

$$\dot{p}^I \leq (WA - B) p^I. \quad (2.21)$$

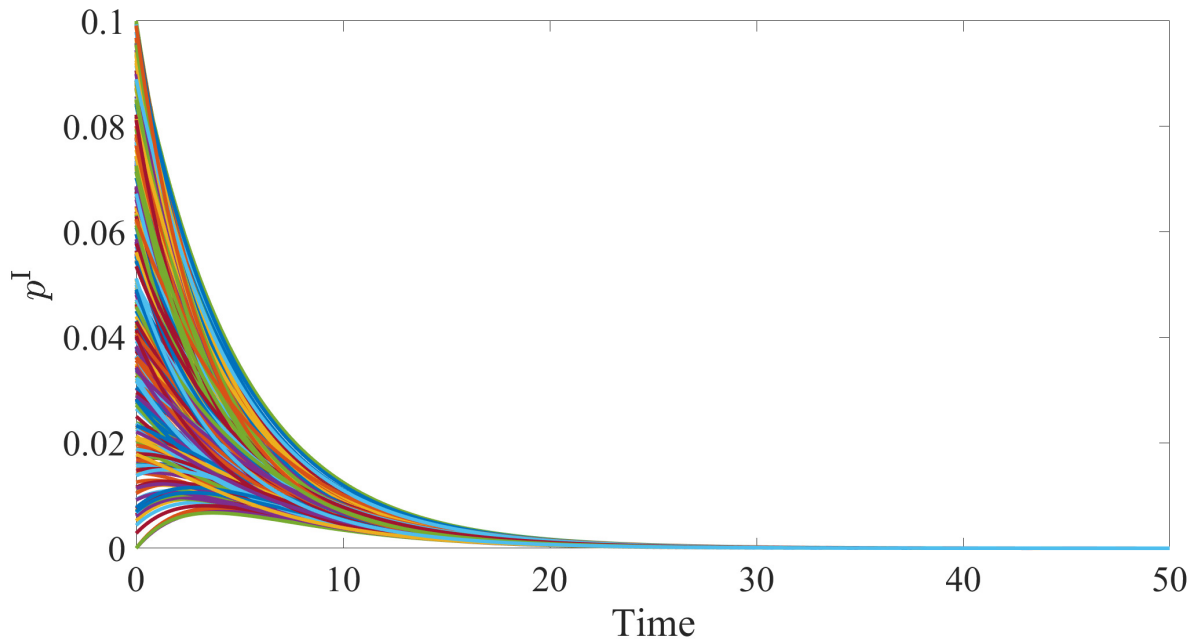
Since p^I is nonnegative, the comparison principle is applicable. It yields that the dynamics of p^I is upper bounded by (2.21). Thus one can easily obtain the origin is asymptotically stable if $s(WA - B) < 0$.

To visualize the results for the DEF, a numerical experiment is conducted on a strongly connected random network with 300 nodes and connection probability 0.3. The transition rates, α_i , β_i , and γ_i , are randomly selected in the intervals (0.05, 0.15), (0.25, 0.35), and (0.2, 0.3), respectively. As is shown in Figure 2.6, the DEF is achieved. Note that in this case $s(WA - B) = -0.1890 < 0$, i.e., the condition given in Theorem 1 is satisfied.

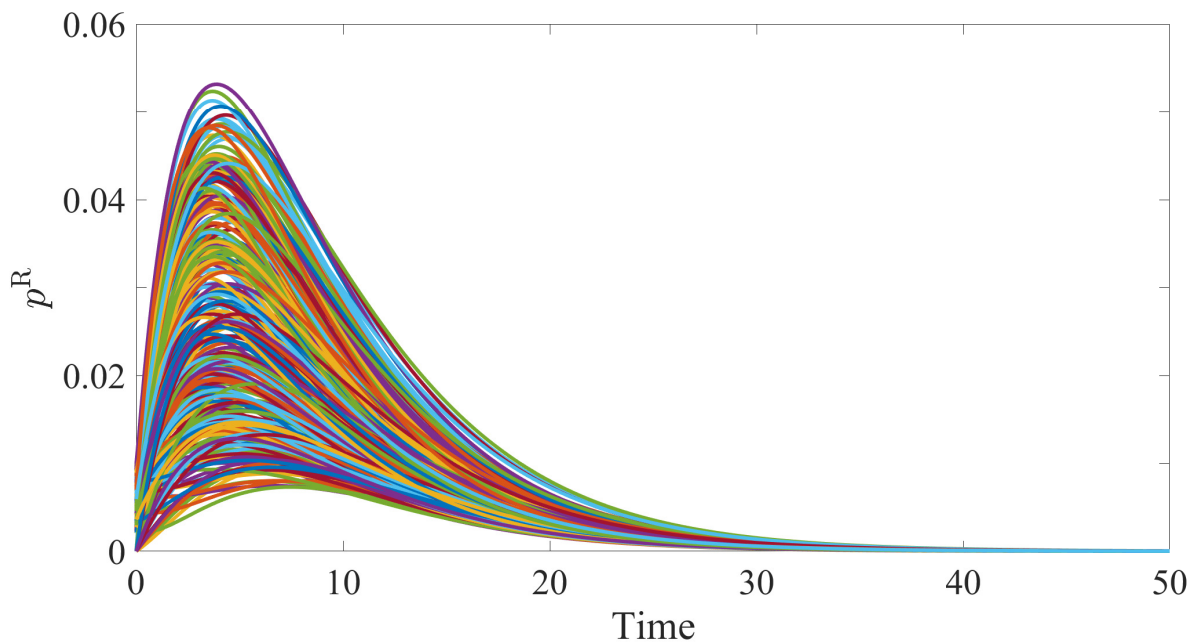
Until now, we only focus on the analysis of the DFE. However, for information diffusion, the endemic equilibrium is also significant. To this end, we continue this subsection to analyze the nontrivial equilibrium.

2.2.3 The Endemic Equilibrium

Unlike the obvious existence of the DEF, there may not exist an endemic equilibrium of the SIRS model in (2.15). To this end, prior to the stability analysis, the existence of the endemic equilibrium needs to be inspected. Let us first look into some properties of the endemic equilibrium if it does exist.



(a) Infection probabilities overtime



(b) Recovery probabilities overtime

Figure 2.6.: The infection and recovery probabilities reach the DFE on a strongly connected random network with 300 nodes and connection probability 0.3. The transition rates, α_i , β_i , and γ_i , are randomly selected in the intervals $(0.05, 0.15)$, $(0.25, 0.35)$, and $(0.2, 0.3)$, respectively. In this figure, $s(WA - B) = -0.1890 < 0$. The initial conditions are chosen in the intervals $[0, 0.1)$ and $[0, 0.01)$ for $p_i^I(0)$ and $p_i^R(0)$, respectively.

Lemma 6. *If there exists an endemic equilibrium $p^* = [(p^{I^*})^\top, (p^{R^*})^\top]^\top$ of the SIRS model (2.15), there holds $p^* \gg 0$.*

Proof. Since $p^* = [(p^{I^*})^\top, (p^{R^*})^\top]^\top$ is an equilibrium of the system (2.15), there hold

$$f(p^{I^*}, p^{R^*}) = 0, \quad g(p^{I^*}, p^{R^*}) = 0. \quad (2.22)$$

Without loss of generality, we consider two cases. First, suppose $p_i^{I^*} = 0$ for some $i \in \mathcal{V}$. By (2.9), we have

$$(1 - p_i^{R^*}) \sum_{j=1}^N \alpha_j w_{ij} p_j^{I^*} = 0, \quad \gamma_i p_i^{R^*} = 0. \quad (2.23)$$

Thus $p_i^{R^*} = 0$. In addition, since the graph is strongly connected, for any node i , $\mathcal{N}_i^{\text{in}} \neq \emptyset$. It follows that, there exists at least one $j \in \mathcal{V}$ such that $w_{ij} > 0$. In conjugation with $\alpha_j > 0$, we have $p_j^{I^*} = 0$ and hence $p_j^{R^*} = 0$. It implies that for any other node $k \in \mathcal{V} \setminus \{i, j\}$, if node k is in the in-neighborhood of either of the inspected nodes i and j , there hold $p_k^{I^*} = 0$ and $p_k^{R^*} = 0$. Since the graph \mathcal{G} is strongly connected, it is obvious by induction that $p^{I^*} = p^{R^*} = 0$. Thus our assumption $p_i^{I^*} = 0$ is impossible to derive an endemic equilibrium.

We then suppose $p_i^{R^*} = 0$ for some $i \in \mathcal{V}$. Similarly, by (2.9), we have

$$(1 - p_i^{I^*}) \sum_{j=1}^N \alpha_j w_{ij} p_j^{I^*} = 0, \quad \beta_i p_i^{I^*} = 0. \quad (2.24)$$

Thus one can obtain $p_i^{I^*} = 0$. Following the same approaches for the first case, one can conclude that $p_i^{R^*} = 0$ is impossible to derive an endemic equilibrium. To conclude, the opposite is true and there must hold $p^* \gg 0$. \square

It can be implied from Lemma 6 that if there exists an endemic equilibrium of the node-based SIRS model, it is strictly positive. Bearing in mind that if $s(WA - B) \leq 0$, the DFE is asymptotically stable for any initial condition in Δ^N , the case when $s(WA - B) > 0$, as the other side of condition in Theorem 1 should be discussed. Inspired by this idea, we obtain the following theorem.

Theorem 2. *Consider the node-based SIRS model (2.15). There exist two equilibria, the origin, which is unstable and a nontrivial equilibrium $p^* \gg 0$, which is unique, if $s(WA - B) > 0$.*

Proof. We first prove the instability of the origin. The Jacobian of (2.15) at the origin reads

$$J(0) = \begin{bmatrix} (WA - B)^\top & 0 \\ B & -\Gamma \end{bmatrix}. \quad (2.25)$$

Since $s(WA - B) > 0$, the origin is not stable because not all the eigenvalues of $J(0)$ are in the left complex plane.

We then prove the existence of p^* if $s(WA - B) > 0$ by Brouwer's fixed-point theorem. This proof is inspired by the proof in [77] and we extend the proof for the SIRS model.

For any p^* , there holds

$$(WA - B)p^{I^*} = (I + \Gamma^{-1}B)P^{I^*}WAp^{I^*}, \quad (2.26)$$

where the equation

$$p^{\text{R}^*} = \Gamma^{-1} B p^{\text{I}^*} \quad (2.27)$$

is used. By (2.26), one can derive

$$p^{\text{I}^*} = [I + (I + \Gamma^{-1} B) \text{diag}(B^{-1} W A p^{\text{I}^*})]^{-1} B^{-1} W A p^{\text{I}^*}. \quad (2.28)$$

Inspired by the above equation, we consider a continuous map $\bar{f}(x) : (0, 1]^N \rightarrow [0, 1]^N$ defined as

$$\bar{f}(x) = [I + (I + \Gamma^{-1} B) \text{diag}(B^{-1} W A x)]^{-1} B^{-1} W A x. \quad (2.29)$$

Note that $\bar{f}(p^{\text{I}^*}) = p^{\text{I}^*}$. We then look for a compact invariant set of the map $\bar{f}(x)$. The i -th entry of $\bar{f}(x)$ reads

$$\begin{aligned} \bar{f}_i(x) &= \frac{(B^{-1} W A x)_i}{1 + (1 + \gamma_i^{-1} \beta_i)(B^{-1} W A x)_i} \\ &= \frac{1}{1 + \gamma_i^{-1} \beta_i} \left(1 - \frac{1}{1 + (1 + \gamma_i^{-1} \beta_i)(B^{-1} W A x)_i} \right). \end{aligned} \quad (2.30)$$

Since $1 + \gamma_i^{-1} \beta_i > 0$ and $B^{-1} W A$ is nonnegative, it follows that for any $x, y \in (0, 1]^N$, there holds $\bar{f}(x) \leq \bar{f}(y)$ if $x \leq y$.

Besides, taking into account $s(WA - B) > 0$, one can derive $\rho := \rho(B^{-1} W A) > 1$. In addition, $B^{-1} W A$ is an irreducible nonnegative matrix. Thus by Perron-Frobenius theorem, there exists a vector $v \gg \mathbf{0}_N$ such that

$$B^{-1} W A v = \rho v. \quad (2.31)$$

It follows that there must exist a sufficiently small scalar $\epsilon > 0$ such that

$$\rho = 1 + \epsilon \rho v_i, \quad (2.32)$$

where v_i is the i th entry of v . It implies that $\epsilon v \leq \mathbf{1}_N$. By substituting $x = \epsilon v$ into $\bar{f}_i(x)$, in conjugation with (2.31), one has

$$\bar{f}_i(\epsilon v) = \frac{\epsilon \rho v_i}{1 + (1 + \gamma_i^{-1} \beta_i) \epsilon \rho v_i} \quad (2.33)$$

Since ϵ is sufficiently small, it can be chosen such that

$$\epsilon < \min_i \frac{\rho - 1}{\rho(1 + \gamma_i^{-1} \beta_i) v_i}. \quad (2.34)$$

Under this condition, there holds

$$\bar{f}(\epsilon v) \geq \epsilon v. \quad (2.35)$$

Recalling the results that for any $x, y \in (0, 1]^N$, there holds $\bar{f}(x) \leq \bar{f}(y)$ if $x \leq y$, we conclude that \bar{f} maps the compact convex set $[\epsilon v, \mathbf{1}_N]$ to itself. Thus by Brouwer's fixed-point theorem, there exists a fixed point in $[\epsilon v, \mathbf{1}_N]$. Moreover this fixed point is strictly positive since $\epsilon v \gg \mathbf{0}_N$. Additionally, since $\Gamma^{-1} B$ is invertible, $p^{\text{R}^*} \gg \mathbf{0}_N$ also exists. Thus we confirm the existence of the endemic equilibrium under the condition $s(WA - B)$.

It remains to show the endemic equilibrium is unique. Since the mapping from p^{I^*} to p^{R^*} is one-on-one, only the uniqueness of p^{I^*} needs to be shown by taking advantage of (2.27). Suppose there exist two distinct endemic equilibria $x, y \in [\epsilon v, \mathbf{1}_N]$ of the SIRS model. This assumption is valid since ϵ can be selected sufficiently small. Consider

$$\eta = \max_{i \in \mathcal{V}} \frac{x_i}{y_i}. \quad (2.36)$$

It implies that $x \leq \eta y$ and there exists $k \in \mathcal{V}$ such that $x_k = \eta y_k$. A fundamental step to show the uniqueness of the endemic equilibrium is to illustrate that $\eta \leq 1$. We then prove it by contradiction, i.e., we suppose $\eta > 1$.

Since for any $x, y \in (0, 1]^N$, there holds $\bar{f}(x) \leq \bar{f}(y)$ if $x \leq y$, it follows that

$$\begin{aligned} x_j &= \frac{(B^{-1}W Ax)_j}{1 + (1 + \gamma_i^{-1}\beta_i)(B^{-1}W Ax)_j} \\ &\leq \frac{\eta(B^{-1}W Ay)_j}{1 + \eta(1 + \gamma_i^{-1}\beta_i)(B^{-1}W Ay)_j} \end{aligned} \quad (2.37)$$

By assumption that $\eta < 1$, one has

$$x_j < \frac{\eta(B^{-1}W Ay)_j}{1 + (1 + \gamma_i^{-1}\beta_i)(B^{-1}W Ay)_j}. \quad (2.38)$$

In addition, y is a fixed point of \bar{f} , there holds

$$y_j = \frac{(B^{-1}W Ay)_j}{1 + (1 + \gamma_i^{-1}\beta_i)(B^{-1}W Ay)_j}. \quad (2.39)$$

By combining the above two expressions, it yields that

$$x_j < \eta y_j = x_j, \quad (2.40)$$

which is naturally a contradiction. Thus there holds $x \leq y$. Dually, by exchanging x and y in the relation (2.36), one can show that $y \leq x$ by using the similar approach. To conclude, we have $x = y$, which is equivalent with the uniqueness of the endemic equilibrium. \square

Theorem 2 reveals that the endemic equilibrium does exist and is unique under the condition $s(WA - B) > 0$. However, the detailed information of this equilibrium is still unknown. To this end we provide the following theorem.

Theorem 3. *The endemic equilibrium of node-based SIRS model (2.15) is expressed as an iteration*

$$\begin{aligned} p_i^{I^*} &= \kappa_i \left(1 - \frac{1}{1 + \xi_i \sum_{j=1}^N \alpha_j w_{ij} \xi_j \left(1 - \frac{1}{1 + \xi_j \sum_{k=1}^N \alpha_k w_{jk} \xi_k (1 - \dots)} \right)} \right), \\ p_i^{R^*} &= \delta_i \kappa_i \left(1 - \frac{1}{1 + \xi_i \sum_{j=1}^N \alpha_j w_{ij} \xi_j \left(1 - \frac{1}{1 + \xi_j \sum_{k=1}^N \alpha_k w_{jk} \xi_k (1 - \dots)} \right)} \right) \end{aligned} \quad (2.41)$$

where $\delta_i = \frac{\beta_i}{\gamma_i}$, $\xi_i = \frac{1+\delta_i}{\beta_i}$, and $\kappa_i = \frac{1}{1+\delta_i}$. Hence, the equilibria is bounded by

$$\begin{aligned} 0 < p_i^{\text{I}^*} &\leq \kappa_i \left(1 - \frac{1}{1 + \xi_i \alpha_{\max}} \right), \\ 0 < p_i^{\text{R}^*} &\leq \delta_i \kappa_i \left(1 - \frac{1}{1 + \xi_i \alpha_{\max}} \right). \end{aligned} \quad (2.42)$$

Proof. Since $(p^{\text{I}^*}, p^{\text{R}^*})$ is the endemic equilibrium of the SIRS model (2.15), there hold

$$p_i^{\text{I}^*} = \frac{\bar{\alpha}_i}{(1 + \delta_i)\bar{\alpha}_i + \beta_i}, \quad p_i^{\text{R}^*} = \frac{\delta_i \bar{\alpha}_i}{(1 + \delta_i)\bar{\alpha}_i + \beta_i}, \quad (2.43)$$

where $\bar{\alpha}_i := \sum_{j=1}^N \alpha_j w_{ij} p_j^{\text{I}^*}$. Along with the notation ξ_i and κ_i , we have

$$\begin{aligned} p_i^{\text{I}^*} &= \frac{1}{1 + \delta_i} \frac{\sum_{j=1}^N \alpha_j w_{ij} p_j^{\text{I}^*}}{\sum_{j=1}^N \alpha_j w_{ij} p_j^{\text{I}^*} + \beta_i / (1 + \delta_i)} \\ &= \kappa_i \left(1 - \frac{1}{1 + \xi_i \sum_{j=1}^N \alpha_j w_{ij} p_j^{\text{I}^*}} \right). \end{aligned} \quad (2.44)$$

Thus in conjugation with $p_j^{\text{R}^*} = \delta_i p_j^{\text{I}^*}$, we can obtain (2.41) by iteration.

It remains to show that the equilibrium is bounded. Since $p_j^{\text{R}^*} \leq 1$, we have

$$\begin{aligned} p_i^{\text{I}^*} &\leq \kappa_i \left(1 - \frac{1}{1 + \kappa_i \alpha_{\max} \sum_{j=1}^N w_{ij}} \right) \\ &= \kappa_i \left(1 - \frac{1}{1 + \xi_i \alpha_{\max}} \right), \end{aligned} \quad (2.45)$$

where $\alpha_{\max} = \max_{i \in \mathcal{V}} \alpha_i$. In light of $\sum_{j=1}^N \alpha_j w_{ij} p_j^{\text{I}^*} \geq 0$ and $p_j^{\text{R}^*} = \delta_i p_j^{\text{I}^*}$, one can simply obtain (2.42). Thus we complete the proof. \square

From Theorem 3, the endemic equilibrium is strictly smaller than $\mathbb{1}$. The upcoming question is whether this endemic equilibrium is stable or not. We have the following conjecture.

Conjecture 1. *Given the node-based SIRS model (2.15), the epidemic equilibrium p^* is asymptotically stable with domain of attraction $\Delta^N \setminus \{0_{2N}\}$, if $s(WA - B) > 0$.*

This conjecture is proposed based on the result regarding the SIS model given in [77], where the properties of the Metzler matrix is utilized. Here we provide a potential way leading to the proof of the conjecture.

Let $x_i(t) = p_i^{\text{I}} - p_i^{\text{I}^*}$ and $y_i(t) = p_i^{\text{R}} - p_i^{\text{R}^*}$. By using the dynamics (2.9), the time derivatives of $x_i(t)$ and $y_i(t)$ read

$$\begin{aligned} \dot{x}_i &= (1 - p_i^{\text{I}^*} - p_i^{\text{R}^*}) \sum_{j=1}^N \alpha_j w_{ij} x_j - (x_i + y_i) \sum_{j=1}^N \alpha_j w_{ij} (p_j^{\text{I}^*} + x_j) - \beta_i x_i \\ \dot{y}_i &= \beta_i x_i - \gamma_i y_i, \end{aligned} \quad (2.46)$$

where the relations

$$\begin{aligned} (1 - p_i^{\text{I}^*} - p_i^{\text{R}^*}) \sum_{j=1}^N \alpha_j w_{ij} p_j^{\text{I}^*} - \beta_i p_i^{\text{I}^*} &= 0 \\ \beta_i p_i^{\text{I}^*} - \gamma_i p_i^{\text{R}^*} &= 0 \end{aligned} \quad (2.47)$$

are used.

By denoting $x = [x_1, \dots, x_N]^\top$, $y = [y_1, \dots, y_N]^\top$ and $z = [x^\top, y^\top]^\top$, the compact form of (2.46) reads

$$\dot{z} = S(x)z, \quad (2.48)$$

where

$$S(x) = \begin{bmatrix} S_1(x) & -\text{diag}(WA(p^{\text{I}^*} + x)) \\ B & -C \end{bmatrix}, \quad S_1(x) = (I - P^{\text{I}^*} - P^{\text{R}^*})WA - \text{diag}(WA(p^{\text{I}^*} + x)) - B. \quad (2.49)$$

In conjugation with (2.42), the domain of the state variables can be directly obtained as follows.

$$-\kappa_i < x_i < 1, \quad -\kappa_i \delta_i < y_i < 1. \quad (2.50)$$

Thus the node-based SIRS model (2.15) is asymptotically stable at the endemic equilibrium if and only if the system (2.48) is asymptotically stable at the origin.

We then on the way to show that $S(x)$ is essentially negative definite, i.e., $S(x) + S^\top(x)$ is negative definite for all proper x . For any two nonzero vectors v_x and v_y satisfying the domain of x and y , respectively, we have

$$\begin{aligned} H_v &= [v_x^\top, v_y^\top] S(x) [v_x^\top, v_y^\top]^\top \\ &= v_x^\top S_1(x) v_x - v_x^\top \text{diag}(WA(p^{\text{I}^*} + x)) v_y + v_y^\top B v_x - v_y^\top C v_y \end{aligned} \quad (2.51)$$

Denote the first three items as

$$\tilde{H}_v = v_x^\top S_1(x) v_x - v_x^\top \text{diag}(WA(p^{\text{I}^*} + x)) v_y + v_y^\top B v_x. \quad (2.52)$$

The extremum of \tilde{H}_v can be achieved at the point where the gradient is zero. Thus we set

$$\nabla \tilde{H}_v = \left[\left(\frac{\partial \tilde{H}_v}{\partial v_x} \right)^\top, \left(\frac{\partial \tilde{H}_v}{\partial v_y} \right)^\top \right]^\top = 0, \quad (2.53)$$

where

$$\begin{aligned} \frac{\partial \tilde{H}_v}{\partial v_x} &= (S(x) + S^\top(x)) v_x - \text{diag}(WA(p^{\text{I}^*} + x)) v_y + B v_y \\ \frac{\partial \tilde{H}_v}{\partial v_y} &= -\text{diag}(WA(p^{\text{I}^*} + x)) v_x + B v_x. \end{aligned} \quad (2.54)$$

By combining the above equations and bearing in mind that

$$v_x^\top S_1(x) v_x = \frac{1}{2} v_x^\top (S_1(x) + S_1^\top(x)) v_x, \quad (2.55)$$

it is clear that the extremum of \tilde{H}_v is 0. If the extremum is the maximum, the essentially negativeness of $S(x)$ is obtained, which is a critical milestone to build a common Lyapunov

function for all x . However, this result seems not apparent unless looking into the row sum and column sum of $S(x)$ [78]. The major obstacle is that a Hurwitz matrix is not naturally to be essentially negative definite but with further condition [79].

To visualize the results for the endemic equilibrium, a numerical experiment is conducted on a strongly connected random network with 300 nodes and connection probability 0.3. The transition rates, α_i , β_i , and γ_i , are randomly selected in the intervals (0.55, 0.65), (0.15, 0.25), and (0.3, 0.4), respectively. Figure 2.7 manifests that the model converges to the endemic equilibrium. In this case, $s(WA - B) = 0.4018 > 0$, i.e., the condition given in the conjecture is satisfied.

2.3 Equilibria and Stability Analysis of Multi-Layer Information Epidemics

Prior to the analysis of the multi-layer information epidemics (2.14), the following lemma is necessary.

Lemma 7. *Given an irreducible nonnegative matrix Q , there exists a positive diagonal matrix \mathcal{P} such that $Q^\top \mathcal{P} Q - \mathcal{P}$ is negative (semi-)definite, if $s(Q) \leq 1$.*

It is clear that Lemma 7 is the discrete-time version of Lemma 5. Hence, for the ease of the remaining analysis, we have the following assumptions.

Assumption 1. *For system (2.14), there hold $p^m(0) \in [0, 1]^N, \forall m \in \mathbb{N}_{[1:M]}$ and $\sum_{q=1}^M p^q(0) \in [0, 1]^N$.*

Assumption 2. *For all $k \in \mathcal{V}$, there hold $h\beta_k^m \leq 1, \forall m \in \mathbb{N}_{[1:M]}$ and $h \sum_{i=1}^L \sum_{j=1}^N \max_{m \in \mathbb{N}_{[1:M]}} \{\alpha_{i,kj}^m\} \leq 1$.*

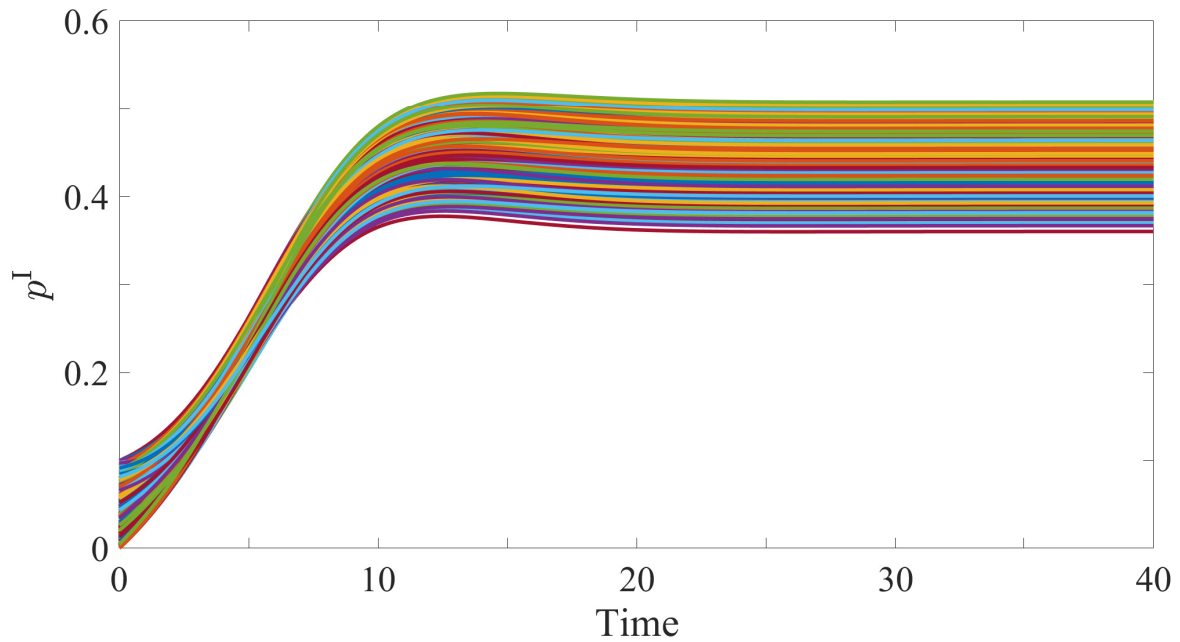
Assumption 3. *\tilde{A}^m is irreducible for all $m \in \mathbb{N}_{[1:M]}$, i.e., the equivalent network $\tilde{\mathcal{G}}$ is strongly connected.*

Assumption 1 is natural to make sure that the initial condition of the system is reasonable. In conjugation with 2, we will show that the multi-layer information epidemics model is well-defined. Besides, in Assumption 3, the strong connectivity of the equivalent network guarantees the information flow among always the agents.

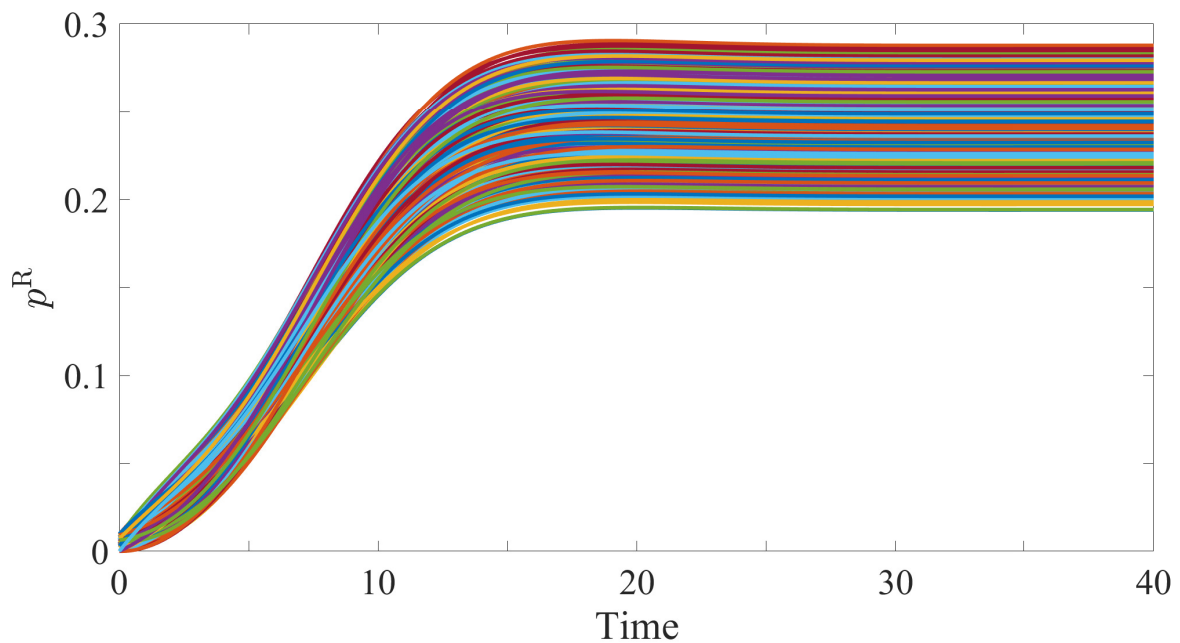
Before embarking on the equilibrium analysis of the system (2.14), we first provide the following lemma to bound the infection probabilities.

Lemma 8. *Given Assumptions 1 and 2, for the system in (2.13), there hold $p_k^m(t) \in [0, 1]$ for all $m \in \mathbb{N}_{[1:M]}$ and $\sum_{q=1}^N p_k^q(t) \in [0, 1]$ for all $k \in \mathcal{V}$ and $t \in \mathbb{N}_{\geq 0}$.*

Proof. We prove the lemma by using mathematical induction. Based on Assumption 1, at time $t = 0$, the results hold straightforwardly. Suppose that at time instant $\tau \in \mathbb{N}_{\geq 0}$, there hold $p_k^m(\tau) \in [0, 1]$ and $\sum_{q=1}^N p_k^q(\tau) \in [0, 1]$. Apparently, $p_k^m(\tau + 1) \geq 0$ holds since each item of the right hand side of (2.13) is nonnegative. It implies that $\sum_{q=1}^N p_k^q(\tau + 1) \geq 0$. Thus



(a) Infection probability overtime



(b) Recovery probability overtime

Figure 2.7.: The infection and recovery probabilities reach the endemic equilibrium on a strongly connected random network with 300 nodes and connection probability 0.3. The transition rates, α_i , β_i , and γ_i , are randomly selected in the intervals $(0.55, 0.65)$, $(0.15, 0.25)$, and $(0.3, 0.4)$, respectively. In this figure, $s(WA - B) = 0.4018 > 0$. The initial conditions are chosen in the intervals $[0, 0.1)$ and $[0, 0.01)$ for $p_i^I(0)$ and $p_i^R(0)$, respectively.

we only have to show they are upper bounded by 1. By rearranging the dynamics of p_k^m as follows

$$\begin{aligned} p_k^m(\tau + 1) &= (1 - p_k^m(\tau))h \sum_{i=1}^L \sum_{j=1}^N \alpha_{i,kj}^m p_j^m(\tau) + p_k^m(\tau)(1 - \beta_k^m h) \\ &\quad - \sum_{q=1, q \neq m}^M p_k^q(\tau) \sum_{i=1}^L \sum_{j=1}^N \alpha_{i,kj}^m p_j^m(\tau), \end{aligned} \quad (2.56)$$

we have $p_k^m(\tau + 1)$ equals a sum of the convex combination of $h \sum_{i=1}^L \sum_{j=1}^N \alpha_{i,kj}^m p_j^m(\tau)$ and $(1 - \beta_k^m h)$, and a nonpositive term. Since Assumption 2 holds, it follows that $h \sum_{j=1}^N \alpha_{i,kj} p_j(\tau) \leq 1$ and $(1 - \beta_k h) \leq 1$. Thus the convex combination is upper bounded by 1. Therefore there holds $p_k^m(t) \leq 1$. Furthermore one can compute

$$\begin{aligned} \sum_{q=1}^M p_k^q(\tau + 1) &= (1 - \sum_{q=1}^M p_k^q(\tau))h \sum_{i=1}^L \sum_{j=1}^N \sum_{q=1}^M \alpha_{i,kj}^q p_j^q(\tau) + \sum_{q=1}^M p_k^q(\tau)(1 - \beta_k^q h) \\ &\leq (1 - \sum_{q=1}^M p_k^q(\tau))h \sum_{i=1}^L \sum_{j=1}^N \max_{m \in \mathbb{N}_{[1:M]}} \{\alpha_{i,kj}^m\} + \sum_{q=1}^M p_k^q(\tau) \max_{m \in \mathbb{N}_{[1:M]}} \{1 - \beta_k^m h\} \end{aligned} \quad (2.57)$$

According to Assumption 2, one can attain $\sum_{q=1}^M p_k^q(\tau + 1) \leq 1$. By mathematical induction, we have $p_k^m(t) \in [0, 1]$ for all $m \in \mathbb{N}_{[1:M]}$ and $\sum_{q=1}^M p_k^q(t) \in [0, 1]$ for all $k \in \mathcal{V}$ and $t \in \mathbb{N}_{\geq 0}$. \square

Lemma 8 reveals that there exists a invariance set \mathcal{P} denoted as

$$\mathcal{P} = \{p^m \in \mathbb{R}^N, m \in \mathbb{N}_{[1:M]} : 0 \leq p^m, \sum_{q=1}^M p_k^q \leq \mathbb{1}\}, \quad (2.58)$$

if the system (2.14) is properly configured.

2.3.1 The Disease-Free Equilibrium

Akin to the single-layer models, the disease-free equilibrium (DFE) is the origin of the system (2.14), i.e., $p_e = 0$. This equilibrium is of great importance for information diffusion where the DFE means the rumor-free case. The existence, uniqueness and stability analysis of the DFE are inspected in this subsection.

In order to deal with the issues of competitive information diffusion processes, the prior step is the analysis of the DFE of the single epidemic spreading model as follows.

$$x(t + 1) = (I + h\tilde{A} - hX(t)\tilde{A} - hB)x(t), \quad (2.59)$$

where $x(t) \in [0, 1]^N$ is the vector consists of the individual infection probabilities at time t and $X(t) = \text{diag}(x(t))$. \tilde{A} and B are similarly defined as \tilde{A}^m and B^m . Since only single epidemic is considered, m can only be 1 and is omitted. This discrete-time SIS model has been validated in [80] by using the Snow dataset and the USDA dataset. The following lemma provide a condition leading to the asymptotic stability of the DFE of the model (2.59).

Lemma 9. *Given Assumptions 2 and 3, 0 is the unique equilibrium of the system (2.59), which is asymptotically stable with the domain of attraction $[0, 1]^N$ if $s(I + h\tilde{A} - hB) \leq 1$.*

Proof. Denote $Q = I + h\tilde{A} - hB$. Based on Assumption 2 and 3, Q is an irreducible nonnegative matrix. Since $s(Q) \leq 1$, by using Lemma 7, there exists a positive diagonal matrix P such that $Q^\top \mathcal{P}Q - \mathcal{P}$ is negative definite. Consider the Lyapunov function $V(x(t)) = x^\top(t) \mathcal{P}x(t)$. The increment of $V(x(t))$ can be calculated as

$$\begin{aligned} \Delta V(t) &= V(t+1) - V(t) \\ &= x^\top(t+1) \mathcal{P}x(t+1) - x^\top(t) \mathcal{P}x(t) \\ &= x^\top(Q - hX\tilde{A})^\top \mathcal{P}(Q - hX\tilde{A})x - x^\top \mathcal{P}x \\ &= x^\top(Q^\top \mathcal{P}Q - \mathcal{P})x - 2hx^\top \tilde{A}^\top X \mathcal{P}Qx + h^2x^\top \tilde{A}^\top X \mathcal{P}X\tilde{A}x \end{aligned} \quad (2.60)$$

Since $s(Q) \leq 1$, we have

$$\begin{aligned} \Delta V(t) &\leq -2hx^\top \tilde{A}^\top X \mathcal{P}Qx + h^2x^\top \tilde{A}^\top X \mathcal{P}X\tilde{A}x \\ &= h^2x^\top \tilde{A}^\top X \mathcal{P}X\tilde{A}x - 2hx^\top \tilde{A}^\top X \mathcal{P}(I + h\tilde{A} - hB)x \\ &= -h^2x^\top \tilde{A}^\top X \mathcal{P}X\tilde{A}x - 2hx^\top \tilde{A}^\top X \mathcal{P}(I - hB)x \end{aligned} \quad (2.61)$$

Based on Assumption 2, we have $I - hB \leq O$. It yields that $\Delta V \leq 0$. Note that if $s(Q) < 1$, one can attain $\Delta V < 0$ because the first row in (2.61) is strict. If $s(Q) = 1$, it is straight forward that the last row in (2.61) is equal to 0 if and only if $x = 0$. Therefore, 0 is an asymptotically stable equilibrium by La Salle's invariance principle. Meanwhile, since all the states in $[0, 1]^N$ are included in the above derivation, the origin is the unique equilibrium. \square

A numerical experiment is conducted to validate Lemma 9. Taking into consideration an SC random network of 300 nodes and 0.3 connection probability, the single-layer SIS model (2.59) is simulated with configurations: $\alpha_{kj} \in (0.05, 0.15)$, $\beta_k \in (0.25, 0.35)$ and $h = 1$. It is clear by calculation that $s(I + h\tilde{A} - hB) \leq 1$ is satisfied. Thus x approaches 0 asymptotically as is shown in Figure 2.8 (in this case $s(I + h\tilde{A} - hB) = 0.8034$).

The result in Lemma 9 reminds us of the condition given in Theorem 1. More specifically, the result above can be regarded as a discrete-time version of the condition in Theorem 1. It implies that $s(I + h\tilde{A} - hB)$ plays an important role in the equilibrium and stability of the model (2.59). This inspires us to come up with the following lemma which is significant for the result of the multi-layer model.

Lemma 10. [80][Proposition 2] *Given Assumptions 2 and 3, there exists two equilibria of the system (2.59): 0 and $0 \ll x^* \ll \mathbb{1}$, if $s(I + h\tilde{A} - hB) > 1$.*

The proof is similar with the proof for Lemma 2 and is saved for triviality. Note that we point out $x^* \ll \mathbb{1}$, which is straight forward by checking the model (2.59).

A numerical experiment is conducted to show the endemic equilibrium in Lemma 10. Taking into consideration an SC random network of 300 nodes and 0.3 connection probability, the single-layer SIS model (2.59) is simulated with configurations: $\alpha_{kj} \in (0.45, 0.55)$, $\beta_k \in (0.25, 0.35)$ and $h = 1$. It is clear by calculation that $s(I + h\tilde{A} - hB) > 1$ is satisfied. Thus x approaches 0 asymptotically as is shown in Figure 2.9 (in this case $s(I + h\tilde{A} - hB) = 1.2059$).

Based on the aforementioned results on the equilibria of the single-layer model, we are on our way to provide the condition for the stability of the DFE of the multi-layer SIS model, which is presented in the following theorem.

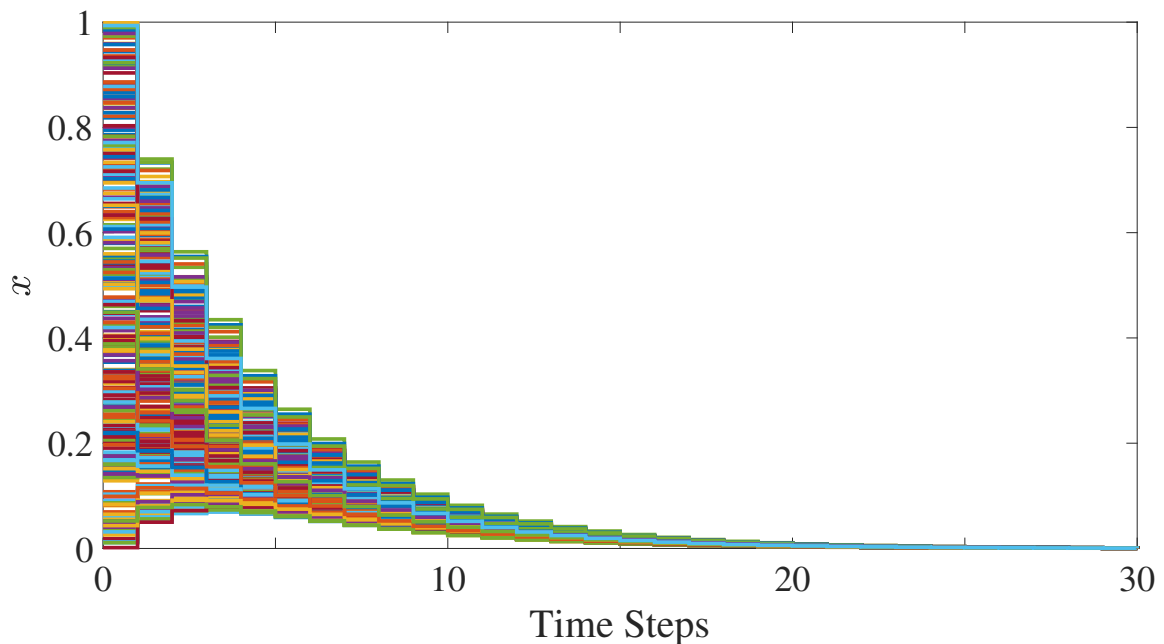


Figure 2.8.: The infection probabilities in the model (2.59) reaches the DFE on a strongly connected network of 300 nodes and 0.3 connection probability. The transition rates are randomly selected as $\alpha_{kj} \in (0.05, 0.15)$, $\beta_k \in (0.25, 0.35)$. The sampling period is set to $h = 1$. In this figure, $s(I + h\tilde{A} - hB) = 0.8034 < 1$.

Theorem 4. *Given Assumptions 1, 2 and 3, there exists the DFE of the system (2.14), which is unique and asymptotically stable with domain of attraction \mathcal{P} , if and only if $s(I + h\tilde{A}^m - hB^m) \leq 1$ for all $m \in \mathbb{N}_{[1:M]}$.*

Proof. Sufficiency: Since Assumption 1 holds, according to Lemma 8, $p_k^m(t)$ is always non-negative. In light of the system (2.14), we have

$$p^m(t+1) \leq (I + h\tilde{A}^m - hP^m(t)\tilde{A}^m - hB^m)p^m(t), \quad (2.62)$$

which shows that the trajectory of $p^m(t)$ is bounded by the single epidemic spreading model (2.59). Thus based on Lemma 9 and the comparison principle [76], $p^m(t)$ converges to the unique equilibrium $\mathbb{0}$ asymptotically for all initial states satisfying Assumption 1. Hence by Lemma 8, the domain of attraction is \mathcal{P} .

Necessity: The necessity part can be proved by contradiction. Suppose there holds $s(I + h\tilde{A}^m - hB^m) > 1$ for certain m and $p^q = \mathbb{0}$ for all $q \neq m, q \in \mathbb{N}_{[1:M]}$. Under this circumstance, the dynamics (2.14) degenerates to (2.59). Therefore we only have to show that the model in (2.59) converge to a nontrivial equilibrium, which is contradictory to the uniqueness of the DFE. This nontrivial equilibrium does exist based on Lemma 10. Thus we complete the proof. \square

This theorem is validated on a two layer network where each layer is a random graph of 300 nodes and 0.3 connection probability. Consider three kinds of information with the transition rates presented in Table 2.2. By choosing the sampling period as 1, we show the performance of the infection probabilities in Figure 2.10, where $p^m, m = 1, 2, 3$ reaches the

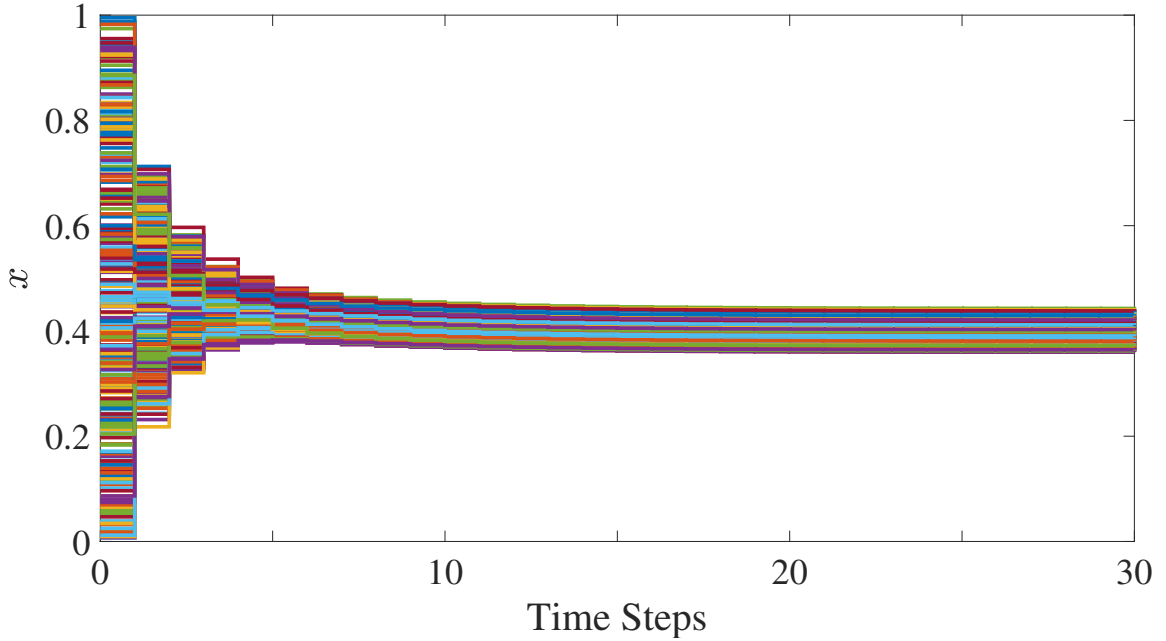


Figure 2.9.: The infection probabilities in the model (2.59) reaches the endemic equilibrium on a strongly connected random network of 300 nodes and 0.3 connection probability. The transition rates are randomly selected as $\alpha_{kj} \in (0.45, 0.55)$, $\beta_k \in (0.25, 0.35)$. The sampling period is set to $h = 1$. In this figure, $s(I + h\tilde{A} - hB) = 1.2059 > 1$.

Table 2.2.: Transition rates of three kinds of information reaching the DFE in a two-layer network.

	$m = 1$	$m = 2$	$m = 3$
$\alpha_{i,jk}^m (i = 1, 2)$	(0.05,0.15)	(0.15,0.25)	(0.05,0.35)
β_k^m	(0.25,0.35)	(0.35,0.45)	(0.35,0.45)

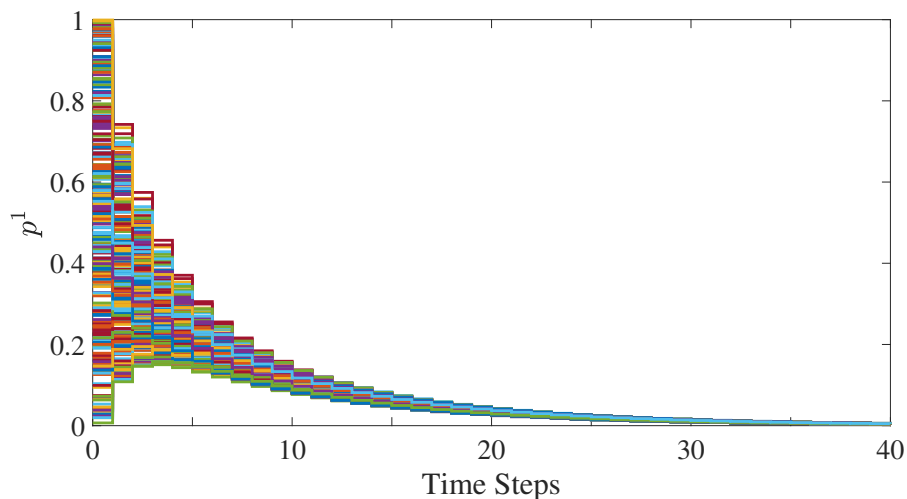
DFE asymptotically. In this case, we have $s(I + h\tilde{A}^1 - hB^1) = 0.9034$, $s(I + h\tilde{A}^2 - hB^2) = 0.9942$, and $s(I + h\tilde{A}^3 - hB^3) = 0.8024$, i.e., the condition given in Theorem 4 is satisfied.

2.3.2 The Endemic Equilibrium

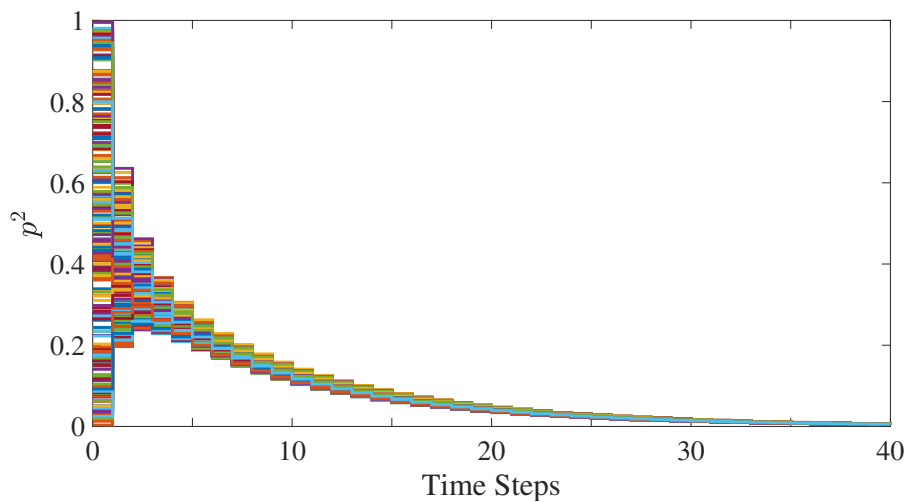
It has been already shown in Lemma 9, for the single-layer discrete-time SIS model, there exist a unique strictly positive endemic equilibrium if $s(I + h\tilde{A} - hB) > 1$. We then investigate the stability of this endemic equilibrium, which is necessary for the analysis of the multi-layer case.

Lemma 11. *Given Assumptions 2 and 3, the endemic equilibrium of the discrete-time single-layer SIS model (2.59) is locally asymptotically stable, if $s(I + h\tilde{A} - hB) > 1$.*

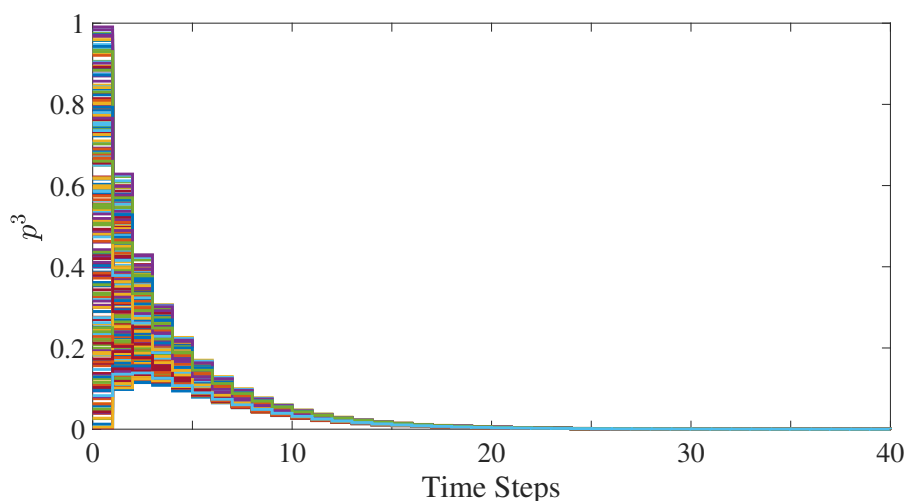
Proof. Since $s(I + h\tilde{A} - hB) > 1$, there exists a unique endemic equilibrium x^* based on Lemma 10. Let $y(t) = x(t) - x^*$ be the error variable. It follows that the difference equation



(a) Infection probabilities of information 1 reach the DFE



(b) Infection probabilities of information 2 reach the DFE



(c) Infection probabilities of information 3 reach the DFE

Figure 2.10.: The multi-layer SIS model reaches the DFE on a two layer network where each layer is a random graph of 300 nodes and 0.3 connection probability. The transition rates are listed in Table 2.2. The sampling period is set to $h = 1$. In each subfigure, there holds $s(I + h\tilde{A}^1 - hB^1) = 0.9034 < 1$, $s(I + h\tilde{A}^2 - hB^2) = 0.9942 < 1$, and $s(I + h\tilde{A}^3 - hB^3) = 0.8024 < 1$, respectively.

for $y(t)$ reads

$$y(t+1) = (I + h\tilde{A} - hB - h(Y(t) + X^*)\tilde{A} - h\text{diag}(\tilde{A}x^*))y(t), \quad (2.63)$$

where $Y(t) = \text{diag}(y(t))$ and the relation

$$(\tilde{A} - X^*\tilde{A} - B)x^* = 0 \quad (2.64)$$

is utilized. It is clear that $y = 0$ at the equilibrium x^* . The Jacobian of (2.63) at $y = 0$ can be obtained as

$$\begin{aligned} J|_{y=0} &= \left[(I + h\tilde{A} - hB - h(Y + X^*)\tilde{A} - h\text{diag}(\tilde{A}x^*))^\top - h\text{diag}(\tilde{A}y) \right] |_{y=0} \\ &= (I + h\tilde{A} - hB - hX^*\tilde{A} - h\text{diag}(\tilde{A}x^*))^\top. \end{aligned} \quad (2.65)$$

One can check that $J|_{y=0}$ is irreducible and Metzler. Notice that

$$(x^*)^\top J|_{y=0} = [(I - h\text{diag}(\tilde{A}x^*))x^*]^\top. \quad (2.66)$$

Since Assumption 2 holds, in conjugation with Lemma 10, one can attain $(I - h\text{diag}(\tilde{A}x^*))x^* \gg x^*$. It implies that $s(J|_{y=0}) < 1$ by Lemma 2. Thus for any autonomous discrete-time linear time-invariant system $z(t+1) = J|_{y=0}z(t)$, $z(t)$ is asymptotically stable by Lemma 7. It is equivalent that all the eigenvalues of $J|_{y=0}$ lay in the unit circle. To this end, we conclude that the Jacobian at 0 is Schur stable, which yields that the equilibrium $y = 0$ is locally asymptotically stable. This completes the proof. \square

In Lemma 11, the local stability of the endemic equilibrium is guaranteed. However, the global $(\mathcal{P} \setminus \{0\})$ in this case) stability of the endemic equilibrium of the single-layer discrete-time SIS model is still an open problem. We provide a conjecture as follows.

Conjecture 2. *Given Assumptions 2 and 3, the endemic equilibrium of the discrete-time single-layer SIS model (2.59) is asymptotically stable with domain of attraction $\mathcal{P} \setminus \{0\}$, if $s(I + h\tilde{A} - hB) > 1$.*

This conjecture is inspired not only by the local stability condition in Lemma 11, but also the result for the continuous SIS model [77]. Here we provide a brief idea towards the proof of Conjecture 2.

Denote

$$A(y(t)) = I + h\tilde{A} - hB - h(Y(t) + X^*)\tilde{A} - h\text{diag}(\tilde{A}x^*) \quad (2.67)$$

as the system matrix in the error dynamics (2.63). It is clear that $A(y(t))$ is an irreducible Metzler matrix for any $y(t)$. Furthermore, there holds

$$A(y(t))x^* = (I - hX(t)\tilde{A})x^* < x^*. \quad (2.68)$$

It implies that $s(A(y(t))) \leq 1$ for all $y(t)$. To this end, if there exists a common Lyapunov function $V = y^\top \mathcal{P}y$ where \mathcal{P} is the positive diagonal matrix in Lemma 7 and is valid for all t , the stability of endemic equilibrium can be obtained. Further application of the LaSalle's invariance principle can be expected to finally prove the asymptotic stability.

Back to the endemic equilibrium of the multi-layer SIS model, it is interesting to note that there may exist different situations. Here we give one example of the equilibrium where only one piece of information is dominant.

Table 2.3.: Transition rates of three kinds of information reaching the SDIE in a two-layer network.

	$m = 1$	$m = 2$	$m = 3$
$\alpha_{i,jk}^m (i = 1, 2)$	(0.05,0.15)	(0.25,0.35)	(0.05,0.35)
β_k^m	(0.25,0.35)	(0.05,0.15)	(0.35,0.45)

Single Dominant Information Equilibrium In the multi-layer SIS model, there could exist a situation when one piece of information dominates the steady state while other information vanishes. This case reflects the case when one of the company defeats other competitors and its advertisements is well spread.

The rigorous condition to achieve this single dominant information equilibrium (SDIE) remains to be inspected. Here we provide a conjecture based on Lemma 11.

Conjecture 3. *Given Assumptions 1, 2 and 3, the system (2.14) possesses two equilibria, i.e., the DFE and a unique endemic equilibrium $(p^{m*}, 0)$ with $p^{m*} \gg 0$, if $s(I + h\tilde{A}^m - hB^m) > 1$ and $s(I + h\tilde{A}^q - hB^q) \leq 1$ for all $q \in \mathbb{N}_{[1:M]}$, $q \neq m$. Furthermore, the DFE is asymptotically stable with domain of attraction $\{p : p^m = 0\}$ and $(p^{m*}, 0)$ is asymptotically stable with domain of attraction $\mathcal{P} \setminus \{p : p^m = 0\}$.*

We provide an idea to prove this conjecture as follows.

By using the similar approach in the proof of Theorem 4, one can straightforwardly obtain that p^q converges to 0 asymptotically for initial conditions $p^m \in [0, 1]^N$ since $s(I + h\tilde{A}^q - hB^q) \leq 1$ for all $q \in \mathbb{N}_{[1:M]}$, $q \neq m$. If $p^m(0) = 0$, $p^m(t) \equiv 0$ for all $t \in \mathbb{N}_{\geq 0}$. Thus the claims regarding the DFE is proved.

If $p^m(0) \neq 0$, the dynamics (2.14) can be regarded as an autonomous system

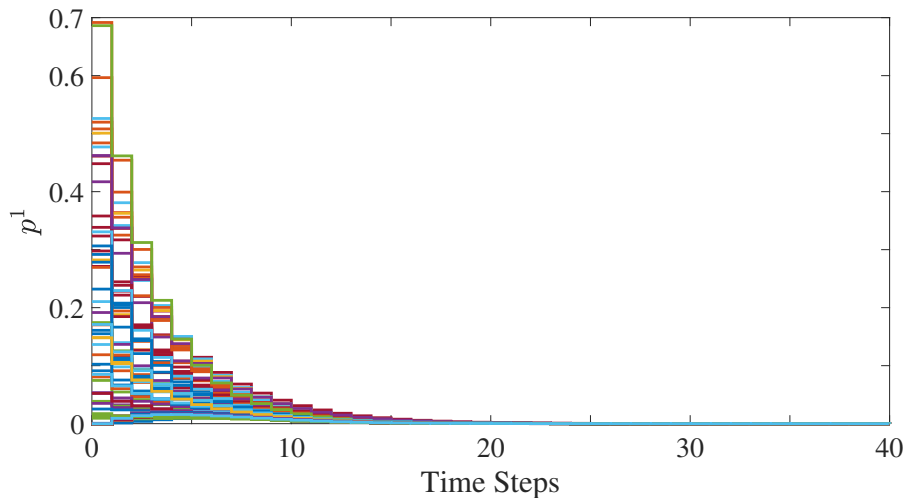
$$p^m(t+1) = (I + h\tilde{A}^m - hP^m(t)\tilde{A}^m - hB^m)p^m(t) \quad (2.69)$$

since the item $-h \sum_{q=1}^M P^q(t)\tilde{A}^m p^m(t)$ converges to 0 asymptotically. Thus the problem degenerates to the stability endemic equilibrium of the single-layer discrete-time SIS model (2.59). It yields that Conjecture 3 is true, if Conjecture 2 is confirmed.

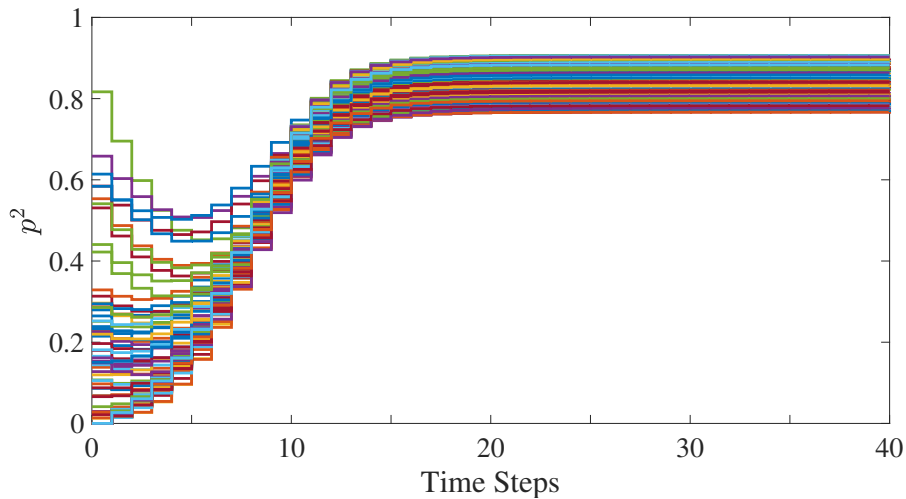
This conjecture is tested in a two-layer network where each layer is a random graph of 300 nodes and 0.3 connection probability. Consider three kinds of information with the transition rates presented in Table 2.3. By choosing the sampling period as 1, we show the performance of the infection probabilities in Figure 2.11, where p^1 and p^3 reach the DFE asymptotically while p^2 reaches the endemic equilibrium. In this case, we have $s(I + h\tilde{A}^1 - hB^1) = 0.9051$, $s(I + h\tilde{A}^2 - hB^2) = 1.5022$, and $s(I + h\tilde{A}^3 - hB^3) = 0.8105$, i.e., the condition given in Conjecture 3 is satisfied.

2.4 Discussion

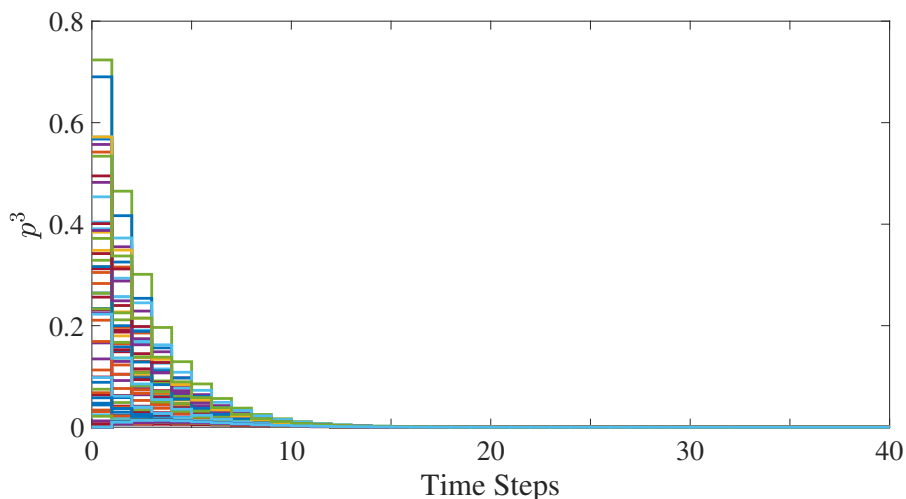
In this chapter, we focus on the modeling and analysis of the information diffusion processes on social networks. By adopting epidemics models and using the mean-field approximation, the node-based SIS and SIRS model are introduced. Distinct from the existing models, the heterogeneities in both the communication topology and the diffusion process itself are



(a) Infection probabilities of information 1 reach the DFE



(b) Infection probabilities of information 2 reach the endemic equilibrium



(c) Infection probabilities of information 3 reach the DFE

Figure 2.11.: The multi-layer SIS model reaches the SDIE on a two layer network where each layer is a random graph of 300 nodes and 0.3 connection probability. The transition rates are listed in Table 2.3. The sampling period is set to $h = 1$. In each subfigure, there holds $s(I + h\tilde{A}^1 - hB^1) = 0.9051 < 1$, $s(I + h\tilde{A}^2 - hB^2) = 1.5022 > 1$, and $s(I + h\tilde{A}^3 - hB^3) = 0.8105 < 1$, respectively.

considered. We then extend the continuous single-layer single epidemic model into discrete-time multi-layer multiple epidemics model.

The analysis of the information epidemic models emphasizes the existence, uniqueness, and stability of the equilibria. Specifically, the node-based SIRS model may possess the DFE and the endemic equilibrium under different conditions. The parameters associated with the transition rates and the underneath networks play the dominant role. This result is also valid for the uniqueness and stability. For the multi-layer model, similar results are obtained in combination with the requirement in the sampling period.

The main contribution in this chapter are twofolds:

- i) We propose the heterogeneous node-based SIRS model and provide the equilibrium analysis results. Although there exist many macroscopic and microscopic epidemics models, very few consider the SIRS model. By associating the temporary immunity in epidemics spreading and the oblivion phenomenon in information diffusion process, the SIRS model is adopted. Distinct from the conventional literature, we take into account both the influence of the network topology and the heterogeneous transition rates. For the proposed model, there exist two equilibria: the disease-free equilibrium (DFE) and the endemic equilibrium. By using the properties of Metzler matrix, the condition $s(WA - B) \leq 0$ is obtained which can guarantee the asymptotic stability of the DFE. Besides, if there holds $s(WA - B) > 0$, the node-based SIRS possesses a unique endemic equilibrium.
- ii) We propose the multi-layer node-based SIS model for multiple information spreading processes. The multi-layer network characterizes the diverse media from which the information is propagated. Apart from the network structure, we consider multiple information diffusion processes. By assuming the infection states caused by different information are mutually exclusive, the competitive spreading are investigated. This model vividly describe the marketing competition of companies by propagating their product from diverse media. The equilibrium analysis of this model is based on the newly reported results for the discrete-time SIS model on single-layer networks. Specifically, the DFE of the multi-layer node-based SIS model is asymptotically stable if and only if $s(I + h\tilde{A}^m - hB^m) \leq 1$. Thus the network topology, the transition rates of the information diffusion process, and the sampling period play dominant role for the limit behavior of the proposed model.

The nonlinear nature of the proposed models is the major difficulty to achieve the aforementioned results. Furthermore, the influence of the network topology makes the analysis more complicated. Due to these reasons, several immediate problems are still open.

- i) The stability of the endemic equilibrium of the node-based SIRS model. In Section 2.2, we provide a conjecture as the stability condition as well as the promising way leading to the proof. The precise and rigorous proof are left for the future work.
- ii) The stability of the endemic equilibrium of the discrete-time single-layer SIS model. In Section 2.3, we provide a conjecture for the stability condition inspired by the results for the continuous-time SIS model. If this conjecture is confirmed, the condition for the asymptotic stability of the single dominant information equilibrium (SDIE) can be attained.

- iii) Existence and stability of other endemic equilibria of the multi-layer SIS model. In the last part of Section 2.3, an example is provided to show the existence of the SDIE. An interesting question is whether there exist other kinds of endemic equilibria. Inspired by the co-exist equilibrium of the single-layer bi-virus SIS model, the limit behavior of the proposed model could also be the co-exist state, i.e., there exists $p_i^m > 0$ for some $i \in \mathcal{V}$ and all $m \in \mathbb{N}_{[1:M]}$.
- iv) Computationally cheap algorithms to check the existence, uniqueness, and stability of the DFE and endemic equilibria. In the proposed conditions, the eigenvalues of the matrices of dimension N are need to be calculated. It is of high computational burden for large scale networks. In order to solve this problem, an attractive way is to develop fast algorithms taking into consideration the network structure, e.g., the sparseness of the network.
- v) General epidemics model. Although there exist many different kinds of epidemics models, no general one has been reported in literature. The recent the generalized susceptible-exposed-infected-vigilant (G-SEIV) model paves the way to this target. However, to develop a generic model that covers all the possible compartments, as well as the time-varying network topology, and the potential noise, is still an open problem.

Control Design for Information Epidemics

Apart from modeling and analysis problems addressed in Chapter 2, an attractive topic for information epidemics is to design an optimal control strategy that guides information propagation in complex networks as a desired way. Although there exist several very recent works regarding optimal control or model predictive control for epidemic models, e.g., [81]–[83], none of them considers time-dependent control rules, which naturally belongs to optimal resource allocation or optimization. Other related papers dealing with control problem for epidemic models [84], [85], but very few inspect the node-based models. Besides, according to the recent survey [86], the optimal control design for information epidemics is still an open problem. The previous study [87] inspects the node-based model, however, in their approach, the model needs to be linearized and only the disease free case is set to be the target. From information epidemics' perspective, in Section 3.1 we introduce two practical scenarios: to impede the rumor spreading and to improve propagation for marketing or campaigning. Furthermore, the robust optimal control problem is considered in Section 3.2 taking into account the noisy transition rates.

3.1 Optimal Control for the SIRS Information Epidemics

In this section, we address the optimal control problem for the SIRS information epidemics and propose optimal control rules for two practical situations.

To guide the information diffusion process, we introduce the word-of-mouth communication which is a common way to influence social neighbors. As is shown in Figure 3.1, we take enhancing (or impeding) the information spreading to node 1 for example. By influencing in infection way with respect to his/her in-neighbors (node 5), the infection probability of node 1 could be increased (or decreased). This word-of-mouth way is based on the fact that the decision-making of individuals will be influenced by their social neighbors. To this end, a control signal is introduced to interact with the infection rate. Note that although this kind of strategy is widely used in the control design for epidemics and information diffusion processes [88], [89], seldom works have implemented it for the node-based models. Specifically, for the node-based SIRS model (2.9), the controlled system can be written as

$$\begin{aligned}\dot{p}_i^I &= (1 - p_i^I - p_i^R) \sum_{j=1}^N (\alpha_j + u_j) w_{ij} p_j^I - \beta_i p_i^I, \\ \dot{p}_i^R &= \beta_i p_i^I - \gamma_i p_i^R.\end{aligned}\tag{3.1}$$

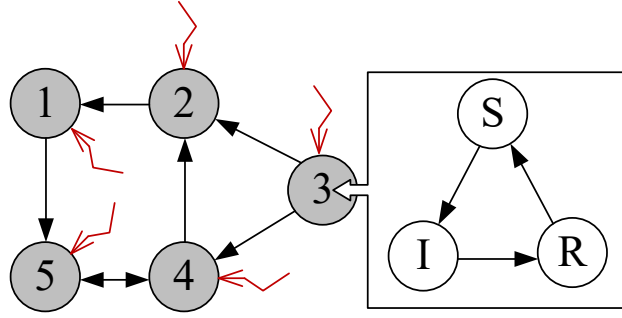


Figure 3.1.: Control frame for node-based SIRS model

The stacked control input is denoted as $u = [u_1, \dots, u_N]^T$. Let $U(t) = \text{diag}(u(t))$, the compact form of the controlled information epidemics reads

$$\begin{aligned} \dot{p}^I &= (I - P^I - P^R)W(A + U)p^I - Bp^I, \\ \dot{p}^R &= Bp^I - \Gamma p^R. \end{aligned} \quad (3.2)$$

Note that we have the following admissible set for the control inputs.

$$u \in \mathcal{U} \triangleq \{u : u_i \text{ is Lebesgue integrable, } u_{\min} \leq u_i(t) \leq u_{\max}, \forall i \in \mathcal{V}\}, \quad (3.3)$$

where u_{\min} and u_{\max} are real scalars to bound all the functions in \mathcal{U} . We assume that $u_{\min}u_{\max} \geq 0$. Taking enhancing the diffusion for example, there is no doubt that to increase the infection rates is the intuitive option, i.e., the bounds are both nonnegative in this case. u_{\min} is usually chosen as the worst acceptable increment of the infection rates while u_{\max} is roughly calculated according to the budget. It is required that $u_{\min}(t) + \alpha_i \geq 0$ such that the underneath mechanism of the SIRS model is satisfied. Notice that $u_i(t) + \alpha_i = 0$ indicates that there is no infection procedure activated by node i . Based on the above settings, we propose the two optimal control problems for information epidemics.

Situation 1: Aiming at impeding the spread of rumors, we introduce the following optimal control problem.

$$\begin{aligned} \min_{u(t) \in \mathcal{U}} J_1 &= \int_0^{t_f} r \mathbf{1}^T p^I(t) + u^T(t) Q u(t) dt, \\ \text{s.t. (3.2), } &p^I(0) = p_0^I, p^R(0) = p_0^R, p_i(t) \in \Delta, \forall i \in \mathcal{V}, \end{aligned} \quad (3.4)$$

where r is a positive scalar and Q is a constant positive definite diagonal matrix. p_0^I and p_0^R are the given initial conditions, i.e. the probabilities of each people being infected and recovered in the very beginning. The terms $\mathbf{1}^T p^I(t)$ is the sum of the infection probability of people at time instant t . It also describes the (approximated) mathematical expectations of the number of people being infected. The first item of the cost function in (3.4) represents the penalty corresponding to the number of individuals who believe the rumor. Note that since rumor-free is the desired performance, we do not distinguish states S and R, which leads to no item contain p^R explicitly. Apart from the penalty, the consumption of the control is also considered. The inputs can be explained as the incentive for each individual so that they can act as desired. Inspired by the related works e.g., [89], [90], the quadratic form is chosen to model the cost. The non-quadratic forms of consumption can be referred to in [83], [86], which is covered by the second situation.

Situation 2: Aiming at enhancing the information diffusion of campaign and marketing, we consider the optimal control problem as follows.

$$\begin{aligned} \min_{u(t) \in \mathcal{U}} J_2 &= -s_I \mathbb{1}^\top p^I(t_f) - s_R \mathbb{1}^\top p^R(t_f), \\ \text{s.t. (3.2), } p^I(0) &= p_0^I, p^R(0) = p_0^R, \\ \int_0^{t_f} \sum_{i=1}^N b_i(u_i(t)) dt &\leq \mathcal{B}, p_i(t) \in \Delta, \forall i \in \mathcal{V}, \end{aligned} \quad (3.5)$$

where s_I and s_R are positive scalars, $b_i(u_i(t))$ is the budget function and $\mathcal{B} \in \mathbb{R}$ is the fixed budget. The cost function in (3.5) only considers the terminal performance because for the political campaign nothing counts but the final number of supporters on the voting day. Furthermore, the infected and the recovered are not of the same importance for the campaigner or product manager and generally there holds $s_I > s_R > 0$. Apart from the cost function, it is rationally assumed that in the constraint, $b_i(\cdot)$ is continuous, positive and increasing in u_i . This is based on the fact that the more increment of the infection rate, the more budget is needed as the incentives. Since companies or the campaign teams usually have limited budget, the constant \mathcal{B} is introduced as the upper bound for the overtime cost. It is worth noting that one can calculate the maximum resource needed by substituting u_{\max} into the budget function. In this paper we only consider the case when $\mathcal{B} < \sum b_i(u_{\max})$. There is no doubt that the value of \mathcal{B} plays an significant role in the performance of the information diffusion process, which is further illustrated in the numerical experiments.

3.1.1 Existence of the Solutions

From practical point of view, the existence issue should be examined to ensure that an optimal control problem has a solution before attempting to calculate the solution. The existence of the solutions is confirmed by the following theorem.

Theorem 5. *Given optimal control problems (3.4) and (3.5), there exist control signals in \mathcal{U} such that the cost functions are minimized, respectively.*

In order to prove Theorem 5, We first show the properties of the node-based SIRS model in the following Lemma.

Lemma 12. *The node-based SIRS model (3.2) is globally Lipschitz continuous in $p(t)$, where $p(t) := [(p^I)^\top, (p^R)^\top]^\top$.*

Proof. The system in (3.2) is denoted as $\dot{p}(t) = F(p(t), u(t))$ for simplicity. Since $u(t)$ is a function of t , we can directly consider the Lipschitz continuity of $F(p, t)$ in p . Let $\hat{p} := [\hat{p}^I, \hat{p}^R]$ satisfy (3.2). Then we use 1-norm to prove the Lipschitz continuity.

$$\begin{aligned} \|F(p, t) - F(\hat{p}, t)\|_1 &= \|\dot{p}^I - \dot{\hat{p}}^I\|_1 + \|\dot{p}^R - \dot{\hat{p}}^R\|_1 \\ &\leq N(\alpha_{\max} + u_{\max}) \|p^I - \hat{p}^I\|_1 + \beta_{\max} \|p^I - \hat{p}^I\|_1 \\ &\quad + (\alpha_{\max} + u_{\max}) \sum_{i=1}^N \sum_{j=1}^N |p_i^I p_j^I - \hat{p}_i^I \hat{p}_j^I| \\ &\quad + (\alpha_{\max} + u_{\max}) \sum_{i=1}^N \sum_{j=1}^N |p_i^R p_j^I - \hat{p}_i^R \hat{p}_j^I|. \end{aligned} \quad (3.6)$$

By rewriting $(p_i^I p_j^I - \hat{p}_i^I \hat{p}_j^I)$ as $(p_i^I p_j^I - p_i^I \hat{p}_j^I + p_i^I \hat{p}_j^I - \hat{p}_i^I \hat{p}_j^I)$, one can have

$$\begin{aligned} & \sum_{i=1}^N \sum_{j=1}^N |p_i^I p_j^I - \hat{p}_i^I \hat{p}_j^I| \\ & \leq \sum_{i=1}^N |p_i^I| \sum_{j=1}^N |p_j^I - \hat{p}_j^I| + \sum_{j=1}^N |\hat{p}_j^I| \sum_{i=1}^N |p_i^I - \hat{p}_i^I| \\ & \leq N \|p^I - \hat{p}^I\|_1. \end{aligned} \quad (3.7)$$

and similarly there holds

$$\sum_{i=1}^N \sum_{j=1}^N |p_i^R p_j^R - \hat{p}_i^R \hat{p}_j^R| \leq N (\|p^R - \hat{p}^R\|_1 + \|p^R - \hat{p}^R\|_1). \quad (3.8)$$

Substitute (3.7) and (3.8) into (3.6), it follows that

$$\|F(p, t) - F(\hat{p}, t)\|_1 \leq L \|p - \hat{p}\|_1, \quad (3.9)$$

where $L = 3N(\alpha_{\max} + u_{\max}) + \beta_{\max} > 0$ is the Lipschitz constant. \square

Based on Lemma 1 and 12, we provide the following proof for the existence of the solution to (3.4) by examining the conditions given by Cesari Theorem in [91].

- 1) The admissible input set \mathcal{U} and the set of solutions to Cauchy problem, i.e. $\dot{p} = F(p, u)$, $p^I(0) = p_0^I$, $p^R(0) = p_0^R$, is apparently non-empty since $F(p, u)$ is Lipschitz in p [76, Theorem 3.2].
- 2) We prove that $F(p, u)$ is bounded by $\hat{C}_1(1 + \|p\| + \|u\|)$. Since u is bounded, it is needed to show $C_1(1 + \|p\|)$. Similar to the calculation above, we have

$$\begin{aligned} \|F(p, u)\|_1 & \leq (\alpha_{\max} + u_{\max}) \sum_{i=1}^N (1 + p_i^I + p_i^R) |w_{ij} p_j^I| \\ & \quad + \sum_{i=1}^N |\beta_i p_i^I| + \sum_{i=1}^N |\beta_i p_i^I - \gamma_i p_i^R| \end{aligned} \quad (3.10)$$

Generally, since $N \gg \gamma_{\max}$, we choose $C_1 = 2[N(\alpha_{\max} + u_{\max}) + \beta_{\max}]$ such that $\|F(p, u)\| \leq C_1(1 + \|p\|)$.

- 3) $F(p, u)$ is linear in u and the integrand satisfies the inequality $r \mathbf{1}^\top p^I + u^\top Q u \geq C_2 \|u\|_2^{C_3} - C_4$. It is required that $C_2 > 0$, $C_3 > 1$, which can be fulfilled by choosing $C_2 = \lambda_{\min}\{Q\}$, $C_3 = 2$ and $C_4 = 0$.

Thus all the conditions of Cesari Theorem are satisfied, which infers the existence of the solution to the problem described as (3.4).

For Situation 2, taking into consideration that the optimum is unlikely to be achieved without sufficient use of the budget, we rewrite the limited budget constraint as

$$\dot{h}(t) = \sum_{i=1}^N b_i(u_i(t)), \quad h(0) = 0, \quad h(t_f) = \mathcal{B}. \quad (3.11)$$

However, since the convexity of $b_i(u_i(t))$ in u_i is not guaranteed, the proof for (3.4) is not applicable for (3.5). Therefore an alternative approach based on extreme value theorem is provided.

Based on the extreme value theorem [92, Theorem 4.16], we prove the existence of the solution to (3.5). First we show that the solution of the node-based SIRS model (3.2) is continuous. From Lemma 12, the model (3.2) is Lipschitz continuous. Moreover, $F(p(t), u(t))$ is obviously bounded. To attain the continuous dependence on parameter $u(t)$, the following proposition needs to be validated.

Proposition 1. *Give $\|u - \hat{u}\| < \delta$, $\delta > 0$, there exist $\mu > 0$ such that $\|F(p, u) - F(p, \hat{u})\| < \mu$.*

Proof. 1-norm is utilized here to prove the proposition. By directly calculation, we have

$$\begin{aligned} & \|F(p, u) - F(p, \hat{u})\|_1 \\ &= \sum_{i=1}^N \left| (1 - p_i^I - p_i^R) \sum_{j=1}^N (u_j - \hat{u}_j) w_{ij} p_j^I \right| \\ &\leq \sum_{i=1}^N \left| 1 - p_i^I - p_i^R \right| \sum_{j=1}^N |u_j - \hat{u}_j| \\ &\leq N \|u - \hat{u}\|_1 \end{aligned} \tag{3.12}$$

Let $\mu = N\delta$, the result in the proposition can be obtained. \square

Now we can come to the result that $F(p, u)$ is continuous in u . Define the following set for the constraint

$$\mathcal{S} = \left\{ u : \int_0^{t_f} \sum_{i=1}^N b_i(u_i(\tau)) d\tau = \mathcal{B}, u_{\min} \leq u_i(t) \leq u_{\max} \right\}, \tag{3.13}$$

which is compact. Along with the compact set \mathcal{U} , the product $\mathcal{S} \times \mathcal{U}$ is also compact. Since the conditions of [92, Theorem 4.16] are all satisfied, there exist a solution to (3.5).

3.1.2 Solutions to the Optimal Control Problems

Since the existence of the solution is guaranteed, we are now focusing on solving the optimal control problem (3.4) and (3.5).

Solution to (3.4): Pontryagin's Maximum Principle is utilized here. Denote $p = (p^I, p^R)$ and rewrite the system (3.2) as $\dot{p} = F(p, u)$. the Hamiltonian of the optimal control problem reads:

$$H_1(p, u, \lambda) = -r \mathbf{1}^\top p^I - u^\top Q u + \lambda^\top F(p, u), \tag{3.14}$$

where $\lambda(t) \in \mathbb{R}^{2N}$ denotes the costate vector and the integrand in (3.4) is multiplied by -1 to form a maximization problem. Let $\lambda = (\lambda^I, \lambda^R)$, where $\lambda^I, \lambda^R \in \mathbb{R}^N$ are the Lagrange multipliers. Then we can compute the costate equations as follows

$$\begin{aligned} \dot{\lambda}^I(t) &= -\frac{\partial H_1(p, u, \lambda)}{\partial p^I(t)} \\ &= r \mathbf{1} - [(A + U)W^\top(I - P^R) - B]\lambda^I - B\lambda^R \\ &\quad + \Lambda^I W(A + U)p^I + [\Lambda^I W(A + U)]^\top p^I, \\ \dot{\lambda}^R(t) &= -\frac{\partial H_1(p, u, \lambda)}{\partial p^R(t)} = \Lambda^I W(A + U)p^I + \Gamma \lambda^R, \end{aligned} \tag{3.15}$$

where $\Lambda^I = \text{diag}(\lambda^I)$ and $\Lambda^R = \text{diag}(\lambda^R)$. By solving $\frac{\partial H}{\partial u} = 0$ at $p = p^*, u = u^*$ and $\lambda = \lambda^*$, the optimal control rule can be expressed as

$$u^*(t) = \frac{1}{2}Q^{-1}P^{I*}(t)W^T(I - P^{I*}(t) - P^{R*}(t))\lambda^{I*}(t), u^*(t) \in \mathcal{U}, \quad (3.16)$$

or more specifically, for each node we have

$$u_i^*(t) = \min \left\{ \max \left\{ \frac{p_i^{I*}(t)}{2q_i} \sum_{j=1}^N w_{ji}(1 - p_j^{I*}(t) - p_j^{R*}(t))\lambda_j^{I*}(t), u_{\min} \right\}, u_{\max} \right\}. \quad (3.17)$$

Moreover, we have the following further property of the solution.

Theorem 6. *The solution (3.17) to the optimal control problem (3.4) is unique.*

Proof. This proof follows the idea of the proof in [91, Theorem 6.2]. It is evident that p^* and λ are continuous on interval $[t_0, t_f]$, hence they are bounded therein. In conjugation with of 2) and 3) in the proof of Theorem 5, it follows that

$$\begin{aligned} |\lambda^T F(p, u)| &\leq C_5(1 + \|u\|), \\ -H_1 &\geq C_2\|u\|^2 - C_5(1 + \|u\|) \end{aligned} \quad (3.18)$$

for some constant C_5 . Then $-\|u\|^{-1}H_1 \rightarrow \infty$ as $\|u\| \rightarrow \infty$. Besides, Q is positive definite implies H_1 is strictly concave in u . Thus H_1 reaches its maximum at a unique u^* on \mathcal{U} . \square

According to the terminal term of the cost function, the transversality conditions read

$$\lambda^I(t_f) = 0, \quad \lambda^R(t_f) = 0. \quad (3.19)$$

Although the optimal control inputs can be analytically presented as (3.17), it cannot be directly calculated because $p^*(t)$ and $\lambda^*(t)$ are unknown beforehand. To tackle this issue, the shooting method is used in [89]. However, in that case, the arbitrary initial condition of a scalar costate is hard to choose, let alone the situation in equation (3.15) with $2N$ -dimension costate vector. Thus we introduce the forward backward sweep method (FBSM) with modification such that it can be used in this N -dimension optimal control problem as follows.

In the FBSM above, Euler method is used such that the continuous model is discretized with sampling period ΔT . The convergence and further properties of FBSM can be referred to in [93].

Solution to (3.5): The Hamiltonian here is written as

$$\begin{aligned} H_2(p, u, \sigma) &= (\sigma^I)^T [(I - P^I - P^R W(A + U)p^I \\ &\quad - Bp^I] + (\sigma^R)^T (Bp^I - \Gamma p^R) + \sigma_h \sum_{i=1}^N b_i(u_i), \end{aligned} \quad (3.20)$$

where $\sigma^I \in \mathbb{R}^N$, $\sigma^R \in \mathbb{R}^N$ and $\sigma_h \in \mathbb{R}$ are the Lagrange multipliers and $\sigma := (\sigma^I, \sigma^R, \sigma_h)$. The costates dynamics of σ^I and σ^R are similar to those in (3.15) while

$$\dot{\sigma}_h = -\frac{\partial H_2}{\partial h} = 0, \quad (3.21)$$

Algorithm 1 Forward-backward sweep method

```

1: Input:  $p_0^I, p_0^R$ , initial guess  $\mathbf{u} = [u(0), \dots, u(end)]$ .
2: for  $k = 0 : 1 : end$  do
3:    $p^I(k+1) \leftarrow p^I(k) + \Delta T \dot{p}^I(k)$ 
4:    $p^R(k+1) \leftarrow p^R(k) + \Delta T \dot{p}^R(k)$ 
5: end for
6: for  $k = end : -1 : 2$  do
7:    $\lambda^I(k-1) \leftarrow \lambda^I(k) - \Delta T \dot{\lambda}^I(k-1)$ 
8:    $\lambda^R(k-1) \leftarrow \lambda^R(k) - \Delta T \dot{\lambda}^R(k-1)$ .
9: end for
10: Compute  $\hat{\mathbf{u}}$  according to (3.17).
11: if  $\|\mathbf{u} - \hat{\mathbf{u}}\|_2 > \epsilon$  then
12:    $\mathbf{u} \leftarrow \hat{\mathbf{u}}$ 
13:   goto line 2
14: else
15:   output  $\mathbf{u}^* = \hat{\mathbf{u}}$ .
16: end if
    
```

which infers that σ_h is a constant scalar but unknown. If the budget function is chosen as quadratic form as that in (3.4), by using similar techniques to obtain (3.16), we obtain the control law as

$$u^*(t) = \frac{1}{2\sigma_h} Q^{-1} P^{I*}(t) W^T (I - P^{I*}(t) - P^{R*}(t)) \sigma^{I*}(t), u^*(t) \in \mathcal{U}. \quad (3.22)$$

Thus to obtain the value of σ_h becomes a natural idea to solve the problem in (3.5). An approach combining the FBSM and the secant method has been reported to be implemented to solve a similar problem with low dimension in [94]. However, to propose an initial guess which leads to a convergent solution is technically hard, let alone with far larger scale of networks. One alternative method is proposed in [90] where the value of σ_h is obtained by trial-and-error. Moreover, the budget function $b_i(u_i)$ may not be differentiable which could be another obstacle to implement the mentioned approaches. To deal with this problem, the Matlab function `fmincon` is utilized to solve this problem numerically. The detailed configurations and further discussions are presented in the following subsections. Note that in this case the solution to optimal control problem (3.5) may not be unique since the solution is highly related to the property of $b_i(u_i)$.

3.1.3 Numerical Experiments

The performance of the node-based SIRS model under optimal control (3.4) and (3.5) are examined to show the effectiveness of the designed control strategy.

We implement the optimal control on a real network in [95] with slight modification. This network describes the friendships between boys in a small highschool in Illinois. The largest strongly connected subgraph containing 67 nodes is utilized. The weights of the in-edges are normalized such that the adjacency matrix is row stochastic. The transition rates α_i , β_i and γ_i are randomly chosen in the intervals (0.55, 0.65), (0.15, 0.25) and (0.3, 0.4), respectively. This guarantees the heterogeneity of the SIRS model. The initial condition

$p_i^I(0)$ and $p_i^R(0)$ are scalars in $[0, 0.01)$ for all $i \in \mathcal{V}$. Note that there are around 20% of the nodes with $p_i^I(0) = 0$ or $p_i^R(0) = 0$, respectively. These configurations are valid for both situations mentioned. Since the steady states of the diffusion process in fixed graphs are highly dependent on the transition rates, optimization rather than optimal control is a more direct way to reach the desired performance. To this end, we mainly focus on the transient states but not the steady states of the information epidemics. Thus in this subsection we set the terminal time as $t_f = 6$ and the sampling period as $\Delta T = 0.1$.

For Situation 1 to impede rumor spreading described in (3.4), the weight associated with the infected individuals is set to $r = 5$. Note that the weighting matrix Q is chosen to be diagonal whose entries read

$$q_i = q|\mathcal{N}_i^{\text{in}}|, \forall i \in \mathcal{V}, \quad (3.23)$$

where q is a scalar set as 0.1 in this case and $|\mathcal{N}_i^{\text{in}}|$ is the cardinality of the in-neighborhood set of node i . The weighting matrix Q mimics the fact that the more individuals one can influence, the resources he/she deserves to obtain to make sure that rumors are less possible to spread via his/her social connections. Thanks to the strongly connectivity of the network, one has $q_i > 0$, i.e., Q is positive definite. The bounds of inputs are set as $[-0.3, 0]$.

Figure 3.2 shows the performance of optimal control in (3.4) compared with those under no control as well as the cost overtime. It yields that the number of individuals who believe the rumor is diminished within the terminal time. To show the control implemented to the specific individuals, two typical nodes labeled 26 and 61 are selected. These two nodes possess (one of) the most and least in-neighbors (18 and 1 in-neighbors), respectively. As is presented in Figure 3.3, the probabilities of these two nodes getting infected are vastly decreased. It is notable to point out that during most of the controlled period, u_{61} stays on the boundary while u_{26} is only in a low level. This phenomenon is due to the fact that the consumption is linear in the number of in-neighbors. The control inputs, evidently, do not behave as bang-bang controllers but mostly in between -0.3 and 0. In the end of the control, i.e., around $t = 5.1$, the absolute value of u_i turns to decrease, which is a trade-off in light of the cost function in J_1 . The terminal value of u_i is zero based on the expression of control law in (3.17) and the transversality condition of λ^I in (3.19).

For Situation 2, the performance of optimal control to enhance the spread with a limited budget is validated. The bounds of input are now set as $u_{\min} = 0$ and $u_{\max} = 1$. The budget \mathcal{B} is chosen as 70. For simplicity, the budget function is still in quadratic form, i.e., $b_i(u(t)) = q_i u_i^2(t)$. Besides, the weights s_I and s_R are set as 5 and 1, respectively. The solution to (3.5) is obtained by `fmincon`, where we choose the initial guess of all the input as u_{\max} and the `sqp` algorithm is used. The performance of the controlled information epidemics is presented in Figure 3.4, which manifests that the optimal control can increase the diffusion extraordinarily and the budget is adequately utilized during the time interval. Detailed information of the two nodes with the most and the least in-neighbors are presented in Figure 3.5. The contributions to $-J_2$ of these two nodes are remarkably increased at t_f . The control input u_{61} stays at the upper bound most of the time while u_{26} stays at a low level. According to the input in Figure 3.5, it is apparent that the budget is not sufficiently enough to support the maximal resources allocated to each individual.

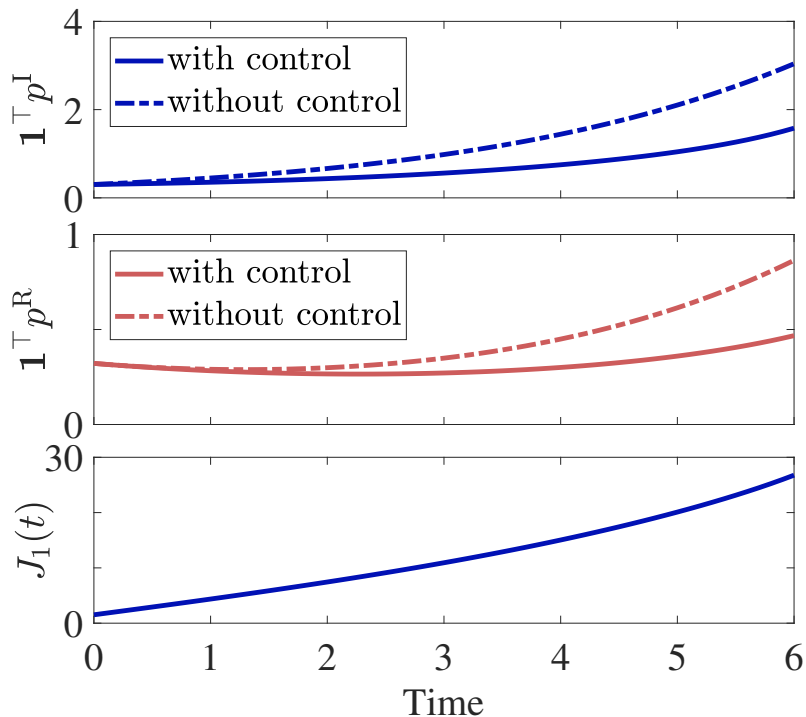


Figure 3.2.: Performance of information epidemics with optimal control in (3.4) and without control as well as the cost overtime. on the highschool network with 67 nodes. The transition rates α_i , β_i , and γ_i are randomly chosen in the intervals $(0.55, 0.65)$, $(0.15, 0.25)$ and $(0.3, 0.4)$, respectively. The initial condition $p_i^I(0)$ and $p_i^R(0)$ are scalars in $[0, 0.01)$. The terminal time is set to $t_f = 6$ and the sampling period $\Delta T = 0.1$. The configurations for the optimal control in (3.4) are: $r = 5$, $q_i = 0.1|\mathcal{N}_i^{\text{in}}|$, $u_{\min} = -0.3$, and $u_{\max} = 0$.

3.1.4 Discussions on Influence of the Parameters

The solutions to the optimal control problems (3.4) and (3.5) are inevitably influenced by the parameters therein. The impacts of the main parameters are discussed in this subsection. An E-R random graph of 30 nodes with connectivity probability 0.1 is generalized. The initial conditions are randomly chosen in the interval $[0, 0.01)$. The transition rates in Subsection 3.1.3 are adopted with slight modification.

In Situation 1, the boundary of the input and the terminal time play significant role to impede the rumor spreading. The comparisons among different configurations of u_{\min} and t_f are studied. In this case, α_i is within the interval $(0.75, 0.85)$ and u_{\max} is set to 0. The simulations are conducted under the same initial conditions and network topology while u_{\min} changes from -0.1 to -0.5 with step 0.1 and t_f increases from 3 to 7 with step 2. As is shown in Figure 3.6, we can conclude that generally with shorter terminal time and the larger input bound, the better performance can be achieved to impede rumor spreading. Specifically, with the same terminal time, the larger $|u_{\min}|$ is, the less people tend to believe the rumor. However, the decrement of the infected is retarded. From the view of time limit, with identical u_{\min} , the longer time we plan to impede the dissemination, the rumor spreads

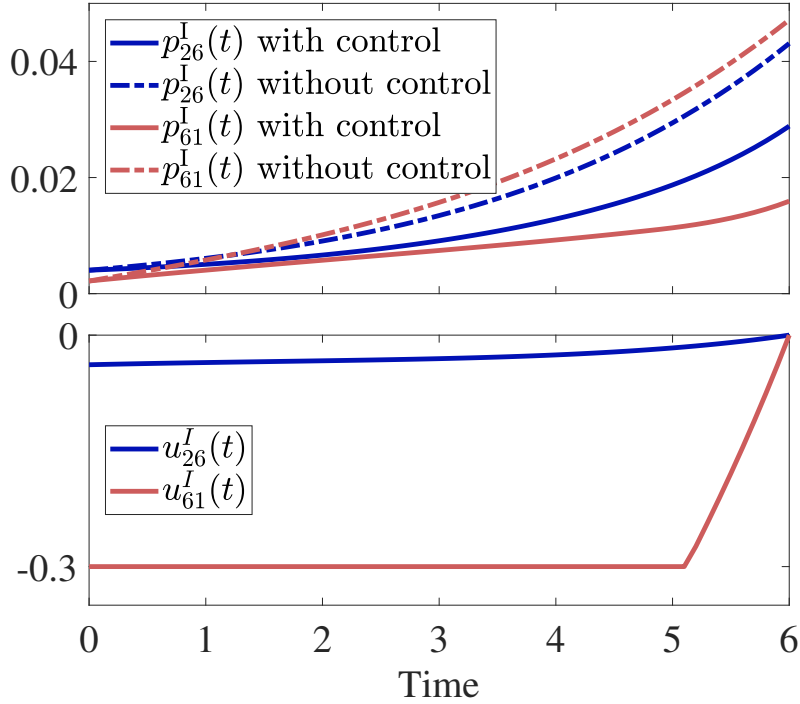


Figure 3.3.: Selected p_i^I for nodes labeled 26 and 61. The simulation is conducted on the highschool network with 67 nodes. The transition rates α_i , β_i and γ_i are randomly chosen in the intervals $(0.55, 0.65)$, $(0.15, 0.25)$ and $(0.3, 0.4)$, respectively. The initial condition $p_i^I(0)$ and $p_i^R(0)$ are scalars in $[0, 0.01]$. The terminal time is set to $t_f = 6$ and the sampling period $\Delta T = 0.1$. The configurations for the optimal control in (3.4) are: $r = 5$, $q_i = 0.1|\mathcal{N}_i^{\text{in}}|$, $u_{\min} = -0.3$, and $u_{\max} = 0$.

more widely. The reason underneath is that the rumor also spreads meanwhile we take the control action. Note that for the case when $u_{\min} = -0.5$, the approximated numbers of infected nodes at the terminal time are very similar for different t_f , which infers that for certain long period of time, the bound of input plays the dominant role in the performance of the system. Thus to impede the spread of rumors, we should wisely make decisions on the resources we can pay and start as early as possible.

In Situation 2, the role of the budget as well as terminal time are selected for further inspection. In this case, α_i is within the interval $(0.25, 0.35)$ and u_{\min} and u_{\max} are set to 0 and 1, respectively. The simulations are conducted via changing \mathcal{B} from 4 to 20 with step 4 and t_f from 4 to 6 with step 1. In Figure 3.7, we show the corresponding variation of $-J_2$ under different configurations. It yields that the more budget we have, the better diffusion we can obtain, which also means that more people would buy the product or vote for the desired campaigner. Similar to the result on impeding rumors, for identical budget, more people turn to be infected in longer diffusion time. However, the effect of time expansion is weakened as time interval increases because the limited sources are distributed for longer periods. To conclude, the budget is the dominant factor in marketing or campaigning in a short period of time.

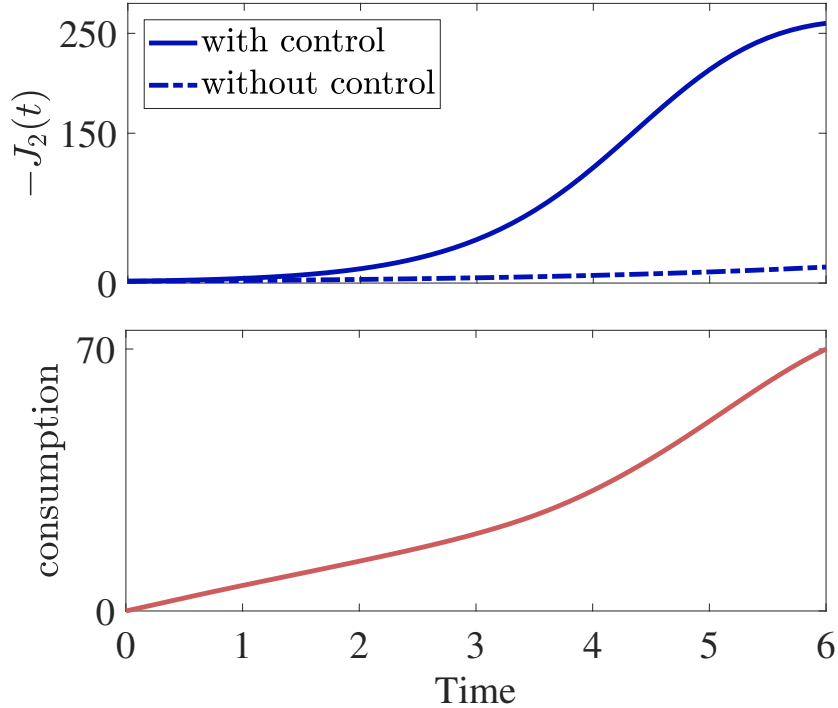


Figure 3.4.: Performance of information epidemics with optimal control in (3.5) and without control along with the consumption overtime on the highschool network with 67 nodes. The transition rates α_i , β_i and γ_i are randomly chosen in the intervals $(0.55, 0.65)$, $(0.15, 0.25)$ and $(0.3, 0.4)$, respectively. The initial condition $p_i^I(0)$ and $p_i^R(0)$ are scalars in $[0, 0.01]$. The terminal time is set to $t_f = 6$ and the sampling period $\Delta T = 0.1$. The configurations for the optimal control in (3.5) are: $s_I = 5$, $s_R = 1$, $q_i = 0.1|\mathcal{N}_i^{\text{in}}|$, $u_{\min} = 0$, $u_{\max} = 1$, and $\mathcal{B} = 70$.

3.2 Robust Optimal Control for Information Epidemics with Noisy Infection Rates

Until now, we only consider the modeling, analysis, and control for information epidemics without noise. Nevertheless, noise is inevitable in the diffusion processes in practical situations. For instance, the behavior of randomly accepting or refusing the information [96] and the individualization force in opinion dynamics [97] are regarded as noise in recent literature. Instead of the aforementioned scenarios, the transition processes between different compartments are sensitive to perturbation caused by external noise [62]. Whereas this topic is seldom inspected.

Moreover, since the optimal control design for information epidemics is still an open problem [86], the robust optimal controller design problem for information epidemics with noise is still untouched. To the best of our knowledge, there exist few literature regarding the control of such kind of model with perturbations. To this end, we address the robust optimal control problem for information epidemics with noisy transition rates.

This section is mainly based on our article [54]. For the first time, a robust optimal control

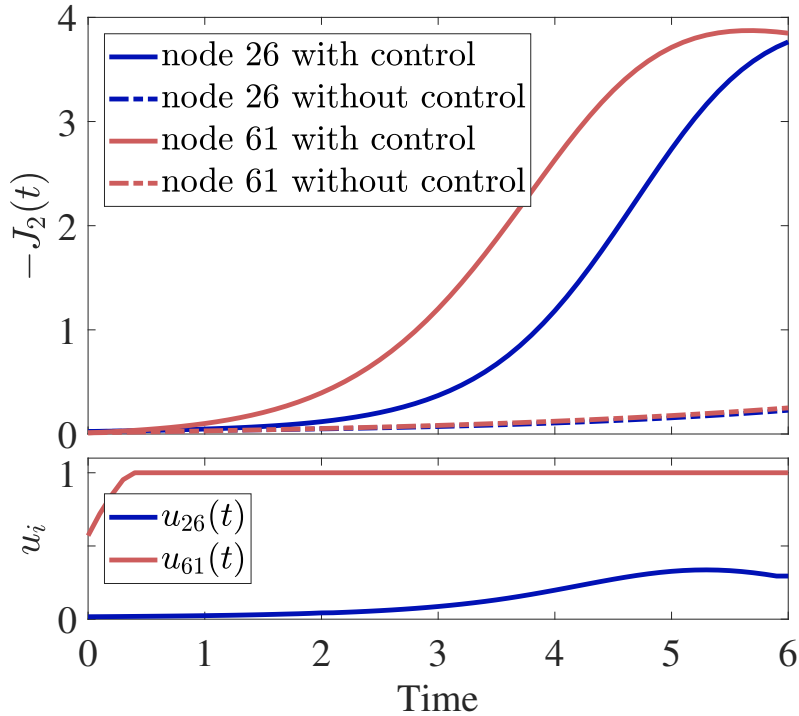


Figure 3.5.: Selected $-J_2(t)$ for nodes labeled 26 and 61. The simulation is conducted on the highschool network with 67 nodes. The transition rates α_i , β_i and γ_i are randomly chosen in the intervals $(0.55, 0.65)$, $(0.15, 0.25)$ and $(0.3, 0.4)$, respectively. The initial condition $p_i^I(0)$ and $p_i^R(0)$ are scalars in $[0, 0.01]$. The terminal time is set to $t_f = 6$ and the sampling period $\Delta T = 0.1$. The configurations for the optimal control in (3.5) are: $s_I = 5$, $s_R = 1$, $q_i = 0.1|\mathcal{N}_i^{\text{in}}|$, $u_{\min} = 0$, $u_{\max} = 1$, and $\mathcal{B} = 70$.

strategy enhancing the information diffusion with perturbed parameters is designed for information epidemics over heterogeneous communication networks. Both the heterogeneities in the network structure and the transition processes are considered by using directed graph description and different transition rates, such that the diversities rooted in the social environment and the individual character are considered. Moreover, the perturbation on the transition rates is introduced, which generally covers most types of uncertainties in information diffusion processes. By manipulating the infection rates, the control input which mimics word-of-mouth is to be designed to robustly maximizing the dissemination. In light of the practical scenarios, the fixed budget constraint is taken into account. Recalling the distribution analysis approach, the inspected problem is transformed into an optimal control problem with a cost function combining the nominal control performance and the influence of the noise. The solution to the proposed problem is achieved taking advantage of the Pontryagin Maximum Principle (PMP). To attain a practically efficient solution, a computationally cheap algorithm combining the forward backward sweep method (FBSM) and the secant method is provided. This result is especially significant for large scale social networks.

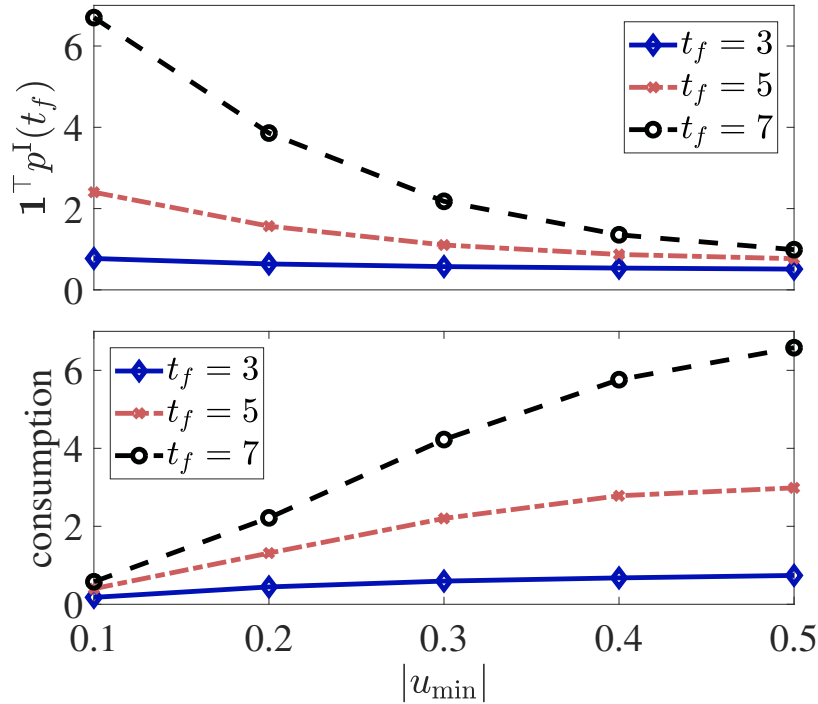


Figure 3.6.: Influence of u_{\min} and t_f in (3.4). This simulation is conducted on an E-R random graph of 30 nodes with connectivity probability 0.1. The initial conditions are randomly chosen in the interval $[0, 0.01)$. The transition rates α_i , β_i and γ_i are randomly chosen in the intervals $(0.75, 0.85)$, $(0.15, 0.25)$ and $(0.3, 0.4)$, respectively. The sampling period is set to $\Delta T = 0.1$. u_{\max} is set to 0. The configurations u_{\min} changes from -0.1 to -0.5 with step 0.1 and t_f increases from 3 to 7 with step 2.

3.2.1 The Node-Based SIS Model with Noisy Transition Rates

In this section, the information epidemics is described as the SIS model with heterogeneous transition rates. The SIS epidemic model could be naturally modeled as a Markov chain which possesses two possible states i.e. susceptible (S) and infected (I) [26]. Analogously, in the context of information diffusion, these two states may refer to unawareness and awareness, respectively. In this section, the infection process (from S to I) is considered as a proactive action, i.e., each infected individual i infects his/her susceptible social neighbors with rate α_i [62]. The curing process (from I to S) is assumed to be passive with rates β_i . In light of the diversity of individual character, the transition rates are assumed to be generally different for each agent. This setting as well as the directed communication networks leads to the heterogeneity of the inspected dynamics.

By denoting $p = [p_1, \dots, p_N]^T$, $\alpha = [\alpha_1, \dots, \alpha_N]^T$ and $\beta = [\beta_1, \dots, \beta_N]^T$, the compact form of (2.4) reads

$$\dot{p} = (I - P)WAp - Bp, \quad (3.24)$$

where $P = \text{diag}(p)$, $A = \text{diag}(\alpha)$ and $B = \text{diag}(\beta)$. Taking into consideration the noise in

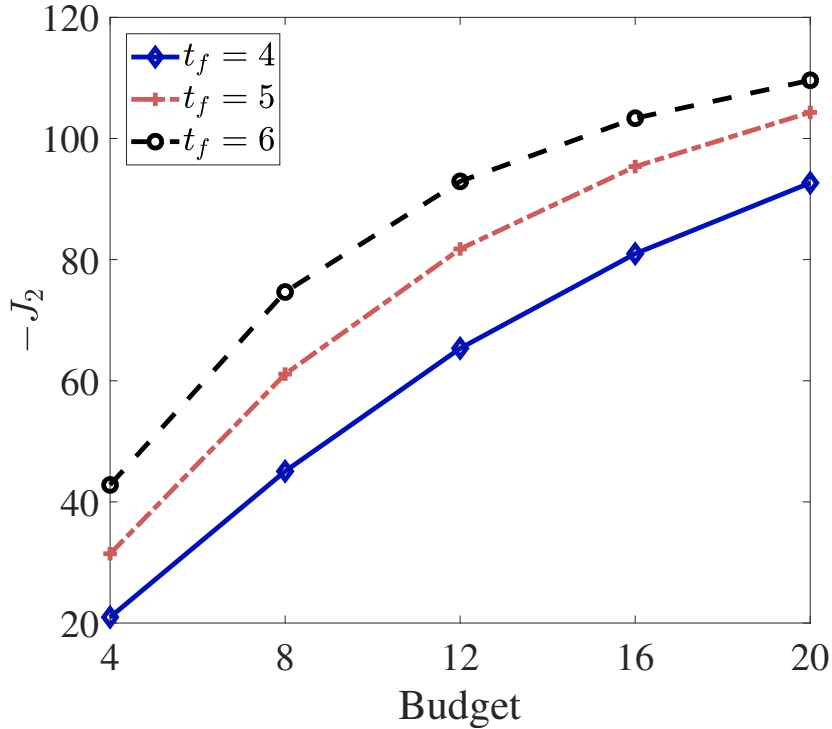


Figure 3.7.: Influence of u_{\max} and t_f in (3.5). This simulation is conducted on an E-R random graph of 30 nodes with connectivity probability 0.1. The initial conditions are randomly chosen in the interval $[0, 0.01)$. The transition rates α_i , β_i and γ_i are randomly chosen in the intervals $(0.25, 0.35)$, $(0.15, 0.25)$ and $(0.3, 0.4)$, respectively. The sampling period is set to $\Delta T = 0.1$. u_{\min} and u_{\max} are set to 0 and 1, respectively is set to 0. The configurations \mathcal{B} changes from 4 to 20 with step 4 and t_f from 4 to 6 with step 1.

the diffusion process, the transition rates in the system (2.4) are assumed to be perturbed, which is described as

$$\alpha = \hat{\alpha} + \delta\alpha, \quad \beta = \hat{\beta} + \delta\beta, \quad (3.25)$$

where $\hat{\alpha}$ and $\hat{\beta}$ are the deterministic nominal transition rates which could be obtained by statistics. $\delta\alpha$ and $\delta\beta$ are the noise reflecting the uncertainties in the transition process. They might be related to the characteristics and decisions of the individuals, as well as the disseminated information, in the social network. For example, to what extent an infected individual would like to share the information to his/her social neighbors is not constant. Without any further investigation to the distribution of the noise, it is natural to assume them as Gaussian Process and independent of each other. Specifically, suppose there holds the following probability density function (PDF)

$$f_{\text{p.d.}}(\theta) = \frac{1}{(2\pi)^{N/2} \det(V_\theta)^{1/2}} e^{-\frac{1}{2}\delta\theta^T V_\theta \delta\theta}, \quad \theta = \alpha \text{ or } \beta, \quad (3.26)$$

where $V_\alpha, V_\beta \in \mathbb{R}^{N \times N}$ are the positive definite covariance matrices. Similar arguments could be referred to in [62]. Based on the node-based SIS model, we are on the way to design the

optimal control strategy to enhance the information diffusion.

3.2.2 Problem formulation

By interacting with the infection rates, we introduce the control input $u_i \in \mathbb{R}$ to each individual, which yields the compact form of the control as $u = [u_1, \dots, u_N]^\top$. Thus the controlled information epidemics reads

$$\dot{p} = (I - P)W(A + U)p - Bp, \quad (3.27)$$

where $U = \text{diag}(u)$. The control input is required to be limited in the following admissible set

$$\mathcal{U} = \{u : u_i \in [u_{\min}, u_{\max}], \text{ Lebesgue integrable}, \forall i \in \mathcal{V}\}, \quad (3.28)$$

where $u_{\min}, u_{\max} \in \mathbb{R}$ are the lower and upper boundaries of the input. Since we consider enhancing the information spreading, it is assumed that $0 \leq u_{\min} < u_{\max}$.

The robust optimal control problem is described as follows.

$$\begin{aligned} \min_{u \in \mathcal{U}} J &= -\mathbf{1}^\top p(t_f), \\ \text{s.t. } (3.27), p(t_0) &= p_0, \\ \int_{t_0}^{t_f} \sum_{i=1}^N b_i(u_i) &\leq \mathcal{B}, \end{aligned} \quad (3.29)$$

where $\mathcal{B} > 0$ is the fixed budget. p_0 is the given initial condition, i.e. the probabilities of each people being infected in the very beginning. The term $|J(t_f)| = \mathbf{1}^\top p(t_f)$ describes the (approximated) mathematical expectations of the number of infected people at the fixed terminal time t_f . The cost function only considers the terminal performance mimics many practical scenarios. For example, in a political campaign nothing counts but the final number of supporters on the voting day. Apart from the cost, $b_i(\cdot) : \mathbb{R}^N \rightarrow \mathbb{R}$ is the *consumption function* and $\mathcal{B} \in \mathbb{R}$ is the fixed budget, which forms the constraint. It is rationally assumed that $b_i(\cdot)$ is continuous, positive and increasing in u_i . This is based on the fact that the more increment of the infection rate, the more budget is needed as the incentives. Since companies or the campaign teams usually have limited budget, the constant \mathcal{B} is introduced as the upper bound for the overtime consumption. It is worth noting that one can calculate the maximum resource needed by substituting u_{\max} into the consumption function. In this paper we only consider the case when $\mathcal{B} < \sum b_i(u_{\max})$. There is no doubt that the value of \mathcal{B} plays an significant role in the performance of the information diffusion process, which is further illustrated in Subsection 5. Inspired by the related works e.g., [89], [90], the quadratic form is chosen to model the consumption, i.e., we choose $u^\top Q u$ as the consumption function where Q is a constant positive definite diagonal matrix.

Based on the problem formulated in (3.29), we then provide the solution techniques to calculate the robust optimal control.

3.2.3 Solution to the Robust Control Problem

To deal with the optimal control for systems with noise, two fundamental ways are commonly used. In the case when the disturbance is deterministic, the optimal control problem

can be formulated as zero or non-zero differential games [98]. However, it is not suitable for the situation in information epidemics which is perturbed by the noise with stochastic nature, let alone the case in conjugation with the fixed time horizon. An alternative is the stochastic optimal control which takes the expectation as the cost function. Nonetheless, the standard approaches, e.g., solving the Hamilton-Jacobi-Bellman (HJB) equation and utilizing stochastic maximum principle [99], are computationally expensive, especially for systems with large scales which is a general characteristic owned by dynamics on social networks. To this end, a novel approach is provided to solve the problem in (3.29) approximately. Taking advantage of the property of the dynamics (3.27), the distribution analysis technique is used to solve the robust optimal control problem. As the fundamental of the proposed method, the optimal control of the nominal information epidemics is first introduced.

Optimal Control of Nominal Information Epidemics Before embarking on the robust optimal control problem (3.29), we investigate the *nominal control*, i.e., the optimal control of the nominal system. By ignoring the influence of the noise, the nominal system can be obtained as follows

$$\dot{\hat{p}} = (I - \hat{P})W(\hat{A} + \hat{U})\hat{p} - \hat{B}\hat{p}, \quad (3.30)$$

where the variables and parameters are similarly defined as those in (3.24). Based on the system (3.30), the problem in (3.29) can be rewritten as

$$\begin{aligned} \min_{\hat{u} \in \mathcal{U}} \hat{J} &= -\mathbf{1}^\top \hat{p}(t_f), \\ \text{s.t. (3.30), } \hat{p}(t_0) &= p_0, \\ \int_{t_0}^{t_f} \sum_{i=1}^N b_i(\hat{u}_i) &\leq \mathcal{B}. \end{aligned} \quad (3.31)$$

In order to solve the problem, the isoperimetric constraint in (3.31) is transformed into the following differential equation

$$\dot{h}(t) := \hat{u}^\top(t)Q\hat{u}(t), \quad h(0) = 0, \quad h(t_f) = \mathcal{B}. \quad (3.32)$$

Note that the equation of $h(t)$ in (3.32) is obtained based on the fact that the optimum is unlikely to be achieved unless the budget is sufficiently used. The optimal control problem (3.43) is then solved based on Pontryagin Maximum Principle (PMP). By introducing the Lagrangian multiplier $\hat{\lambda}_p \in \mathbb{R}^N$ and $\hat{\sigma} \in \mathbb{R}$, we have the Hamiltonian

$$\hat{H} = \hat{\lambda}_p^\top [(I - \hat{P})W(\hat{A} + \hat{U})\hat{p} - \hat{B}\hat{p}] + \hat{\sigma} \hat{u}^\top Q \hat{u}. \quad (3.33)$$

According to PMP, we have the dynamics of the costate as follows

$$\dot{\hat{\lambda}}_p = -\frac{\partial \hat{H}}{\partial \hat{p}} = -(\hat{A} + \hat{U})W^\top(I - \hat{P})\hat{\lambda}_p + B\hat{\lambda}_p - \hat{\Lambda}_p W(\hat{A} + \hat{U})\hat{p} \quad (3.34)$$

with the transversality conditions $\hat{\lambda}_p(t_f) = -\mathbf{1}$. Specially, by taking the constraint (3.32) into consideration, one has $\dot{\hat{\sigma}} = 0$, which implies that $\hat{\sigma}$ is a constant but to be fixed.

By setting $\frac{\partial \hat{H}}{\partial \hat{u}} = 0$, we can obtain the control input as follows

$$\hat{u}^* = -\frac{1}{2\hat{\sigma}^*} Q^{-1} [\hat{P}^* W^\top (I - \hat{P}^*) \hat{\lambda}_p^*], \quad \hat{u}^* \in \hat{\mathcal{U}}. \quad (3.35)$$

Although the solution can be analytically presented in the form of (3.35), the problem in (3.30) are unlikely to be directly solved following this approach and a numerical solution is necessary. However, inspired by the solution of the nominal information epidemics, the problem in (3.29) are transformed into a similar formulation in the underlying subsection.

Distribution Analysis Approach In order to solve the problem in (3.29), the distribution analysis approach is introduced. It is evident that p is linear in the infection and curing rates, respectively. According to [100], it implies that the covariance of $J(t) = -\mathbf{1}^\top p(t)$ can be computed by the covariance of α and β as

$$V_J = l_\alpha^\top V_\alpha l_\alpha + l_\beta^\top V_\beta l_\beta, \quad (3.36)$$

where

$$l_\alpha^\top(t) = \left. \frac{\partial J(t)}{\partial \alpha} \right|_{\alpha=\hat{\alpha}, \beta=\hat{\beta}}, \quad l_\beta^\top(t) = \left. \frac{\partial J(t)}{\partial \beta} \right|_{\alpha=\hat{\alpha}, \beta=\hat{\beta}}. \quad (3.37)$$

Note that the numerator layout notation of the matrix calculus is used. In order to calculate the terminal values of l_α and l_β , an additional set of sensitivity equations are integrated in [101]. However, this approach cannot be directly used in (3.29) because what we consider here is a functional. With slight modification, let

$$M_\alpha := \frac{\partial p}{\partial \alpha}, \quad M_\beta := \frac{\partial p}{\partial \beta}. \quad (3.38)$$

It is clear that

$$l_\alpha = -\mathbf{1}^\top M_\alpha|_{\alpha=\hat{\alpha}, \beta=\hat{\beta}}, \quad l_\beta = -\mathbf{1}^\top M_\beta|_{\alpha=\hat{\alpha}, \beta=\hat{\beta}}. \quad (3.39)$$

By using the chain rule and the rule for interchanging the order of differentiation for certain mixed partials, the time derivative of M_α and M_β can be obtained as follows

$$\begin{aligned} \dot{M}_\alpha &= \frac{\partial}{\partial t} M_\alpha = \frac{\partial}{\partial t} \frac{\partial p}{\partial \alpha} = \frac{\partial}{\partial \alpha} \dot{p} \\ &= \frac{\partial}{\partial \alpha} ((I - P)W(A + U)p - Bp) + \mathcal{J} \frac{\partial p}{\partial \alpha} \\ &= (I - P)WP + \mathcal{J} M_\alpha \\ \dot{M}_\beta &= -P + \mathcal{J} M_\beta, \end{aligned} \quad (3.40)$$

where \mathcal{J} is the Jacobian matrix and reads,

$$\mathcal{J} = \frac{\partial \dot{p}}{\partial p} = (I - P)W(A + U) - \text{diag}(W(A + U)p) - B. \quad (3.41)$$

To this end, the minimization of J in (3.29) can be approximated by the combination of the following two parts

$$J_1 = -\mathbf{1}^\top \hat{p}(t_f), \quad J_2 = V_J(t_f), \quad (3.42)$$

where J_1 is the nominal cost function with respect to the controlled nominal system (3.30) and J_2 is the variance of J around the nominal value caused by the parameter uncertainty. Note that by introducing the auxiliary systems (3.40), the problem with noise in (3.29) is transformed into the optimal control problem in deterministic systems. Rather than

formulating a multi-objective problem of $[J_1, J_2]$, we introduce the weighted sum of J_1 and J_2 , which yields the following optimal control problem.

$$\begin{aligned} & \min_{u \in \mathcal{U}} J_1 + rJ_2, \\ & \text{s.t. (3.30), (3.40), } \hat{p}(t_0) = p_0, \\ & \int_{t_0}^{t_f} u^\top Q u \leq \mathcal{B} \end{aligned} \quad (3.43)$$

where $r > 0$ is the weighting coefficient. It is worth noting that as a trade-off between the desired cost J_1 and the influence of the noise J_2 , the value of r is of great significance in (3.43). Generally, r is set in advance by the companies or the campaign teams based on their knowledge or prediction of the noise. Specifically, smaller r infers that the influence of noise is not considered as very important and vice versa. Further discussions are given in Subsection 3.2.5 to provide valuable insights on the selection of r .

Remark 1. By doing the distributional analysis, the robust optimal control problem in (3.29) is transformed into the optimal control problem in (3.43). As a sacrifice, the dynamics are augmented with $2N$ vector differential equations in (3.40). To deal with this problem, the simultaneous corrector method is proposed in [102] to solve this large-scale problem in an efficient manner. Bearing in mind the following solution to the optimal control problem, an alternative approach is used which is presented in detail in the last part of this section.

The optimal control problem (3.43) is then solved based on PMP. As a prior step, the dynamics in (3.40) should be reshaped in a vector form. By denoting $m_{\alpha,i}$ the i th column of $M_\alpha|_{\alpha=\hat{\alpha},\beta=\hat{\beta}}$, $\forall i \in \mathcal{V}$ and similarly for $m_{\beta,i}$, one has

$$\begin{aligned} \dot{m}_{\alpha,i} &= \hat{p}_i(I - \hat{P})W_i + \mathcal{J} m_{\alpha,i} \\ \dot{m}_{\beta,i} &= -\hat{p}_i \mathbf{e}_i + \mathcal{J} m_{\beta,i}, \forall i \in \mathcal{V}, \end{aligned} \quad (3.44)$$

where $\mathbf{e}_i \in \mathbb{R}^N$ is the i th column of the unity matrix and W_i is the i th column of the adjacency matrix W .

By introducing the Lagrangian multiplier $\lambda_p, \lambda_{\alpha,i}, \lambda_{\beta,i} \in \mathbb{R}^N$, $\forall i \in \mathcal{V}$ and $\sigma \in \mathbb{R}$, we have the Hamiltonian

$$\begin{aligned} H &= \lambda_p^\top [(I - \hat{P})W(\hat{A} + U)\hat{p} - \hat{B}\hat{p}] + \sigma u^\top Q u \\ &+ \sum_{i=1}^N \lambda_{\alpha,i}^\top [\hat{p}_i(I - \hat{P})W_i + \mathcal{J} m_{\alpha,i}] + \lambda_{\beta,i}^\top [-p_i \mathbf{e}_i + \mathcal{J} m_{\beta,i}]. \end{aligned} \quad (3.45)$$

According to PMP, the time-derivatives of the costates read

$$\begin{aligned} \dot{\lambda}_p &= -\frac{\partial H}{\partial \hat{p}} = -(\hat{A} + U)W^\top(I - \hat{P})\lambda_p + B\lambda_p - \Lambda_p W(\hat{A} + U)\hat{p} \\ &+ \sum_{i=1}^N \hat{p}_i \text{diag}(W_i)\lambda_{\alpha,i} - \mathbf{e}_i \lambda_{\alpha,i}^\top (I - \hat{P})W_i + \text{diag}(\mathbf{e}_i)\lambda_{\beta,i} \\ &+ \sum_{i=1}^N \Lambda_{\alpha,i} W(\hat{A} + U)m_{\alpha,i} + \Lambda_{\beta,i} W(\hat{A} + U)m_{\beta,i} \\ &+ (\hat{A} + U)W^\top(M_{\alpha,i}\lambda_{\alpha,i} + M_{\beta,i}\lambda_{\beta,i}), \\ \dot{\lambda}_{\alpha,i} &= -\frac{\partial H}{\partial m_{\alpha,i}} = -\mathcal{J}^\top \lambda_{\alpha,i}, \quad \dot{\lambda}_{\beta,i} = -\frac{\partial H}{\partial m_{\beta,i}} = -\mathcal{J}^\top \lambda_{\beta,i} \end{aligned} \quad (3.46)$$

with the transversality conditions

$$\begin{aligned}\lambda_p(t_f) &= -\mathbf{1}, \quad \lambda_{\alpha,i}(t_f) = -2r(\mathbf{1}^\top \otimes \mathbf{e}_i)V_\alpha M_\alpha(t_f)\mathbf{1}, \\ \lambda_{\beta,i}(t_f) &= -2r(\mathbf{1}^\top \otimes \mathbf{e}_i)V_\beta M_\beta(t_f)\mathbf{1}, \quad \forall i \in \mathcal{V}.\end{aligned}\tag{3.47}$$

Specially, in light of the constraint (3.32), one has $\dot{\sigma} = 0$, which implies that σ is a constant but to be fixed.

By setting $\frac{\partial H}{\partial u} = 0$, we can obtain the control input as follows

$$\begin{aligned}u^* &= -\frac{1}{2\sigma^*}Q^{-1}\left[\hat{P}^*W^\top(I - \hat{P}^*)\lambda_p^* + \sum_{i=1}^N M_{\alpha,i}W^\top(I - P)\lambda_{\alpha,i}\right. \\ &\quad \left.+ M_{\beta,i}W^\top(I - P)\lambda_{\beta,i} - PW^\top(M_{\alpha,i}\lambda_{\alpha,i} + M_{\beta,i}\lambda_{\beta,i})\right], u^* \in \mathcal{U}.\end{aligned}\tag{3.48}$$

Remark 2. On one hand, the terms in the dynamics of costates (3.34) and the input (3.35) of the nominal system are reserved in (3.46) and (3.48), respectively. On the other hand, the distinguishing terms shows the influence of the noise. To this end, the distribution analysis approach reveals the consistency associated with the nominal optimal control solution.

As with the control in (3.35), u^* in (3.48) cannot be directly calculated due to the impossibility of attaining the optimum in advance. Thus a novel algorithm is proposed to obtain the control input numerically, which is also applicable to the problem (3.31) with slight modification.

3.2.4 Solution Techniques for Robust Optimal Control of Information Epidemics

As a commonly adopted approach, the shooting method is used in [89]. However, in that case, the arbitrary initial condition of a scalar costate is hard to choose. Taking advantage of the fact that σ is a constant scalar, an alternative way to obtain its value becomes a natural idea to solve the problem in (3.43). Conventionally, the value of σ is obtained by trial-and-error [90] which is technically difficult and time-consuming to implement because a sufficiently small initial guess is needed and no efficient update law is given. As a modification, the secant method has been reported to be implemented to solve a similar problem in [94]. However, the issue tacked there is of low dimension and the algorithm is not precisely presented. Inspired by the previous works, we provide the a novel algorithm systematically. Apart from the secant method to search the value of σ , the forward backward sweep method (FBSM) is also utilized to calculate the control input iteratively. Thus we provide the combined approach as in Algorithm 1.

Apparently, once the costate σ is given, one can obtain a cost according to the consumption function. It implies that there exists a map $error = \mathcal{B} - f(\sigma)$ where $f(\cdot) : \mathbb{R} \rightarrow \mathbb{R}$ is a function of σ . It yields that σ is the root when the error equals zero. Based on this fact, the FBSM and the secant method can be combined together. Given the initial condition of p and initial guess of the control input, the states overtime can be obtained by forwardly implementing the dynamics (3.30). As a successive step, the costates can be computed backwardly. By utilizing the errors between the budget and the consumption resulted from two initial values of σ , the secant method can be applied to update this constant costate. This iteration ends when the errors reach certain tolerance. The convergence analysis of the FBSM can be referred to in

Algorithm 2 Forward-backward sweep with secant method

```

1: Input:  $p_0$ , initial guess  $\mathbf{u}^{[0]} = [u(0), \dots, u(end)]$ ,  $\sigma^{[1]}, \sigma^{[2]}$ , given tolerance  $\epsilon > 0$ , budget  $\mathcal{B}$ 
2: for  $k = 0 : 1 : end$  do
3:    $\hat{p}(k+1) \leftarrow \hat{p}(k) + \Delta T \dot{\hat{p}}(k)$ 
4: end for
5: for  $k = end : -1 : 2$  do
6:    $\lambda_p(k-1) \leftarrow \lambda_p(k) - \Delta T \dot{\lambda}_p(k)$ 
7:    $\lambda_\alpha(k-1) \leftarrow \lambda_\alpha(k) - \Delta T \dot{\lambda}_\alpha(k)$ 
8:    $\lambda_\beta(k-1) \leftarrow \lambda_\beta(k) - \Delta T \dot{\lambda}_\beta(k)$ 
9: end for
10: According to (3.48), compute  $\mathbf{u}^{[1]}$  using  $\sigma^{[1]}$ 
11:  $error^{[1]} \leftarrow \mathcal{B} - h^{[1]}(end)$ 
12: According to (3.48), compute  $\mathbf{u}^{[2]}$  using  $\sigma^{[2]}$ 
13:  $error^{[2]} \leftarrow \mathcal{B} - h^{[2]}(end)$ 
14: while ( $|error^{[1]}| > \epsilon$  or  $|error^{[2]}| > \epsilon$  or  $|error^{[1]} - error^{[2]}| > \epsilon$ ) do
15:    $error^{[1]} \leftarrow error^{[2]}$ ,  $\sigma^{[1]} \leftarrow \sigma^{[2]}$ 
16:    $\sigma^{[3]} \leftarrow \sigma^{[2]} - error^{[2]}(\sigma^{[2]} - \sigma^{[1]}) / (error^{[2]} - error^{[1]})$ 
17:    $\mathbf{u}^{[0]} \leftarrow \mathbf{u}^{[2]}$ 
18:   Compute  $error^{[3]}$  similarly as line 2 to 10
19:    $error^{[2]} \leftarrow error^{[3]}$ ,  $\sigma^{[2]} \leftarrow \sigma^{[3]}$ 
20: end while
21: Output  $\mathbf{u}^{[2]}$ 

```

[93] and is saved for triviality. Compared with conventional optimization algorithms, e.g., Matlab `fmincon`, the proposed approach is computationally much cheaper and also capable of dealing with high dimensional problems. Note that the proposed algorithm is able to be applied to the problem in (3.31) by replacing the respective equations of costates in lines 6 to 8 by the ones in (3.34). The detailed discussions are presented in Subsection 3.2.5.

3.2.5 Numerical Experiments

In this section, the performance of the node-based SIS model under robust optimal control (3.29) is examined to show the effectiveness of the designed control strategy.

We inspect the information epidemics on two real networks with slight modification. The first network describes the friendship between boys in a small highschool in Illinois [103] (referred as the highschool network), whose largest strongly connected subgraph containing 67 nodes is utilized. The second network shows the friendship between the residents living at a residence hall located on the Australian National University campus [104] (referred as the residence hall network). Similarly, a 214-node strongly connected subgraph is extracted. The weights of the in-edges are normalized such that the adjacency matrix is row stochastic. The effectiveness of the proposed robust optimal control and its comparison with the nominal control are examined in both networks such that the results are convincing. The nominal transition rates $\hat{\alpha}_i$ and $\hat{\beta}_i$ are randomly chosen in the intervals (0.05, 0.15) and (0.005, 0.015), respectively. This guarantees the heterogeneity of the SIS model. The covariance matrices V_α and V_β are selected to be diagonally dominant and their diagonal entries are randomly

chosen within $(0.3, 0.35)$. The diagonal weighting matrix Q is selected according to the cardinality of each node, i.e., the i th diagonal entry $q_i = 0.1|\mathcal{N}_i^{in}|$, which mimics the natural fact that more influential one individual is the more incentives should be paid to gain his/her help for information spreading.

The initial condition $p_i(0)$ is a scalar in $[0, 0.01)$ for all $i \in \mathcal{V}$. Note that there are around 20% of the nodes with initial value zero. These configurations are valid for all the simulations in this section. During all the simulations, the information epidemics is discretized with the sampling period $\Delta T = 0.01$. Other fixed parameters are the initial time instant $t_0 = 0$, $u_{\min} = 0$ and $u_{\max} = 0.5$.

The validation of the proposed robust optimal control is first conducted by comparing with the system under no control and heuristic control on the highschool network. By choosing the budget $\mathcal{B} = 30$, $t_f = 5$, the robust optimal control can be calculated by Algorithm 1. Note that according to [101], the initial conditions for $m_{\alpha,i}$ and $m_{\beta,i}$ are both set to $\mathbf{0}$. To make an evaluable comparison, a heuristic control is implemented such that the control input is identical for each node at every time instant. In light of the consumption function and the given budget \mathcal{B} , this control input equals 0.4088 entry-wise. The simulation results of the expectation of the number of infected people overtime ($|J(t)|$) are shown in Figure 3.8. A similar numerical experiment is conducted on the residence hall network. We set the budget as $\mathcal{B} = 30$ while other parameters remain unchanged. The respective heuristic control is 0.2602. The results are presented in Figure 3.9. It is evident that the controlled epidemics, both the heuristic and the robust optimal control, shows better performance, since the diffusion processes are extraordinarily enhanced compared with the uncontrolled. Apart from that, the proposed robust optimal control scheme reveals a superior performance in terms of $|J(t)|$. It is worth noting that this performance is achieved by making full use of the budget over the fixed control horizon which implies that the constraints are fulfilled.

We then compare the performance of the dynamics under robust control obtained by solving (3.43) with that of the nominal control using the same configuration as in the first simulations. The control inputs are calculated offline: the robust control is obtained by solving (3.43) while the nominal control by solving (3.29) but with respect to the nominal system (3.30). The simulations on both networks are conducted 1,000 times, each of which contains noise in both infection and curing rates. By taking the differences in $\mathbf{1}^\top p(t_f)$ ($|J(t_f)|$) as the index, the performance is shown in Figure 3.10. For the highschool network (Figure 3.10 (a) and (b)) and the residence hall network (Figure 3.10 (c) and (d)), almost all the simulations show that the robust optimal control results in slightly better performance than the nominal control. It implies that under this configuration, the information spreads generally wider under the robust control. Although the differences are not notably large, T-test for both scenario shows a two-tailed p -value far less than 0.001, which means that the results are significantly different and the results in Figure 3.10 are convincing. Note that if the control input is dominant compared with the transition rates and social networks with larger scale are considered, better performance can be expected.

Based on the problem formulation and the proposed solution technique, the weight r and the budget \mathcal{B} are two of the most influential factors. Specifically, r determines the trade-off between the real objective and the influence of the noise and \mathcal{B} stands for the upper bound of resources. By choosing r from 0 to 1 with step 0.1 and \mathcal{B} from 15 to 35 with step 5, we compare $|J(t_f)|$ under each settings on the highschool network. Other configurations are the same with those in the first simulation. As is presented in Figure 3.11, it is evident that for

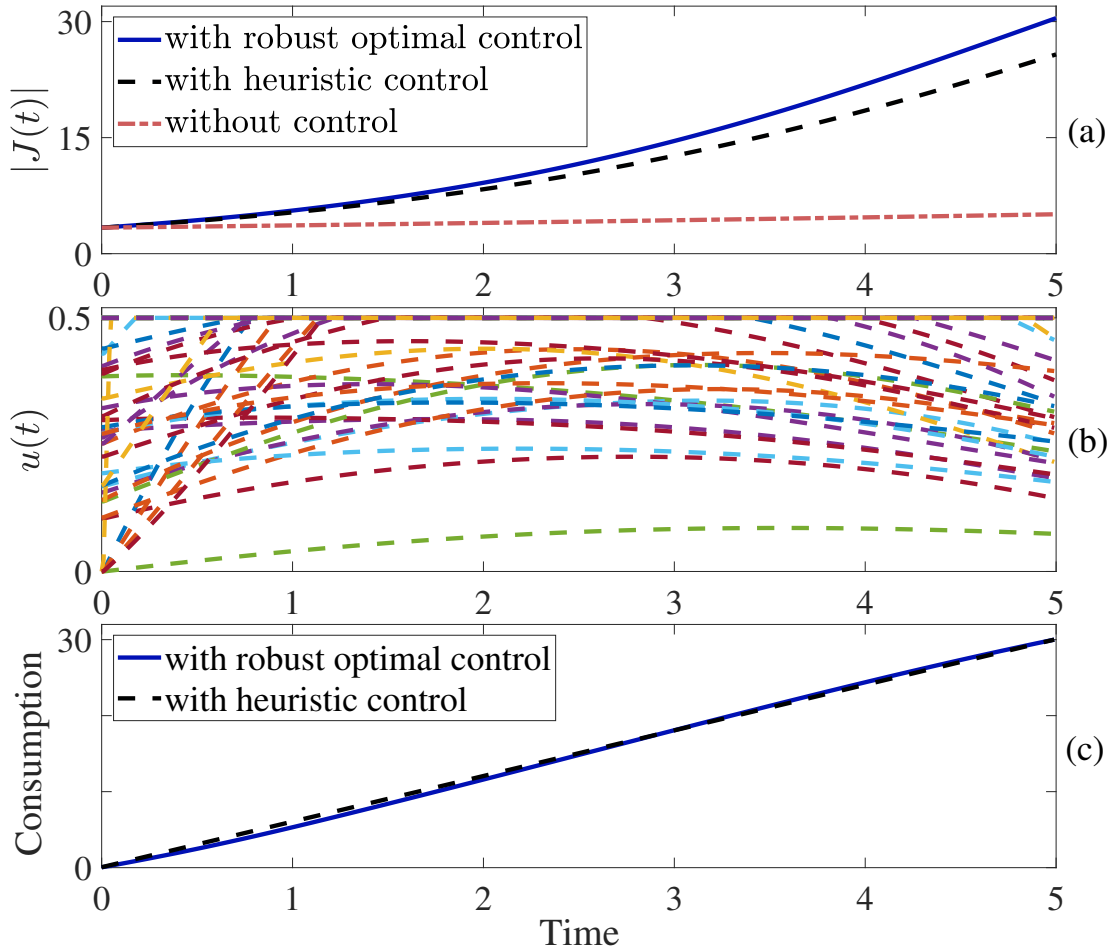


Figure 3.8.: The performance of the diffusion process on the highschool network with 67 nodes. (a) Comparison of $|J(t)|$ with no control, with heuristic control (identical control input, 0.4088, for each node at each time instant) and with robust optimal control. The robust optimal controller shows better performance than the heuristic control and uncontrolled epidemics. (b) The control input of the robust optimal control for each node, which is bounded in $[u_{\min}, u_{\max}]$. (c) The consumption over time. For both heuristic control and robust optimal control, the budget is adequately used. The initial condition is set as $p_i(0) \in [0, 0.01)$. Other parameters are: $\hat{\alpha} \in (0.05, 0.15)$, $\hat{\beta} \in (0.005, 0.015)$, $\mathcal{B} = 30$, $t_0 = 0$, $t_f = 5$, $u_{\min} = 0$ and $u_{\max} = 0.5$.

the same weight r , more budget results in better spreading performance. It is worth noting that the increment of $|J(t_f)|$ slows down as the budget increases. This yields that companies and campaign teams should wisely plan their budget to reach a balance between the resource and objective. As for the case when the budget is fixed, the performance of $|J(t_f)|$ fluctuate with respect to the change of r . Taking $\mathcal{B} = 20$ and 35 as examples, $|J(t_f)|$ reaches the peak when $r = 0.1$ and 0.2, respectively. To this end, the choice of r is nontrivial which may highly related with the feature of noise. Thus the prior knowledge and the estimation of the

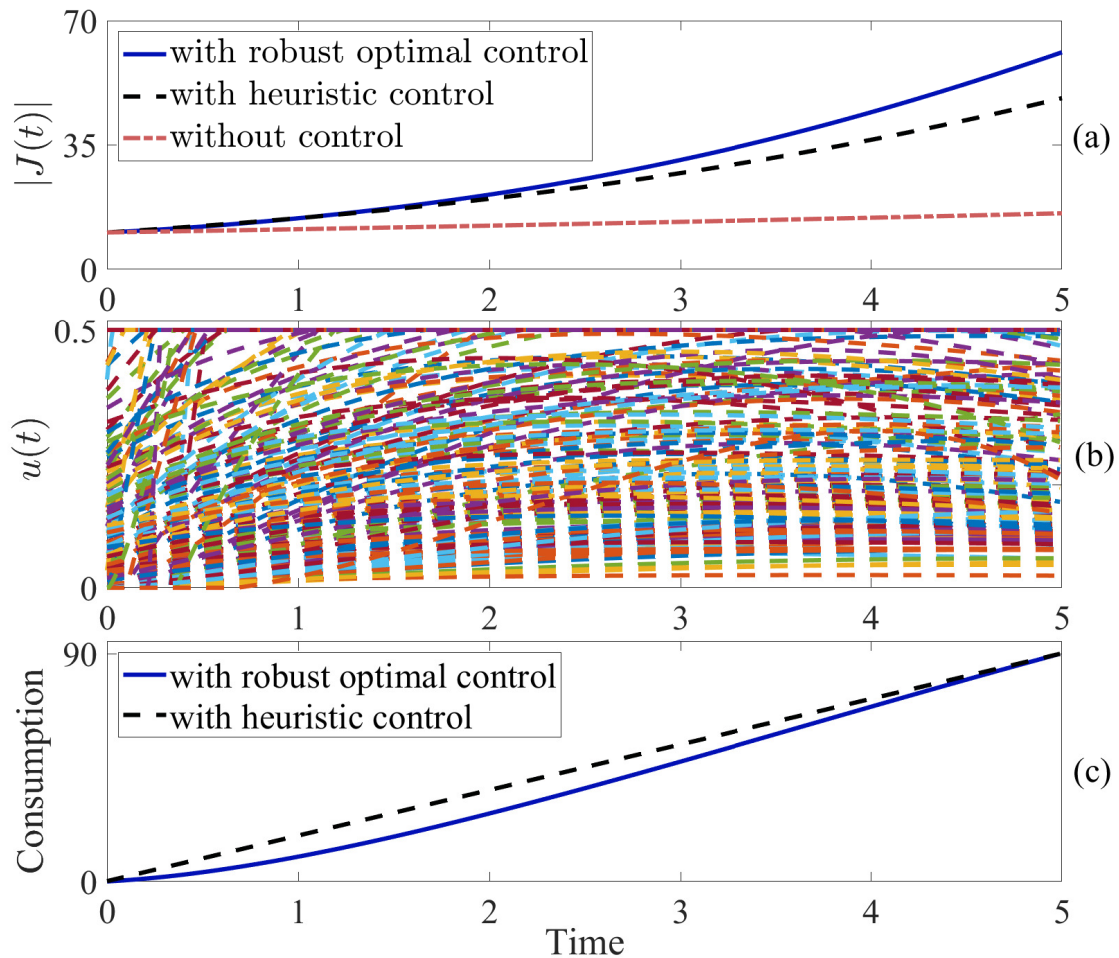


Figure 3.9.: This simulation is conducted over the residence hall network with 214 nodes. The initial condition is set as $p_i(0) \in [0, 0.01]$. Other parameters are chosen as: $\hat{\alpha} \in (0.05, 0.15)$, $\hat{\beta} \in (0.005, 0.015)$, $\mathcal{B} = 90$, $t_0 = 0$, $t_f = 5$, $u_{\min} = 0$ and $u_{\max} = 0.5$. (a) The performance of the diffusion process with no control, with heuristic control (identical control input, 0.2602, for each node at each time instant) and with optimal control is compared in the form of $|J(t)|$. The robust optimal controller shows better performance than the heuristic control and uncontrolled epidemics. (b) The control input of the optimal control for each node, which is bounded in $[u_{\min}, u_{\max}]$ (c) The consumption over time. For both heuristic control and robust optimal control, the budget is adequately used.

affordable impact of the noise are necessary.

3.3 Discussion

In this section, focusing on information diffusion processes in social networks, heterogeneous node-based SIRS model is introduced to describe the dissemination process. An optimal

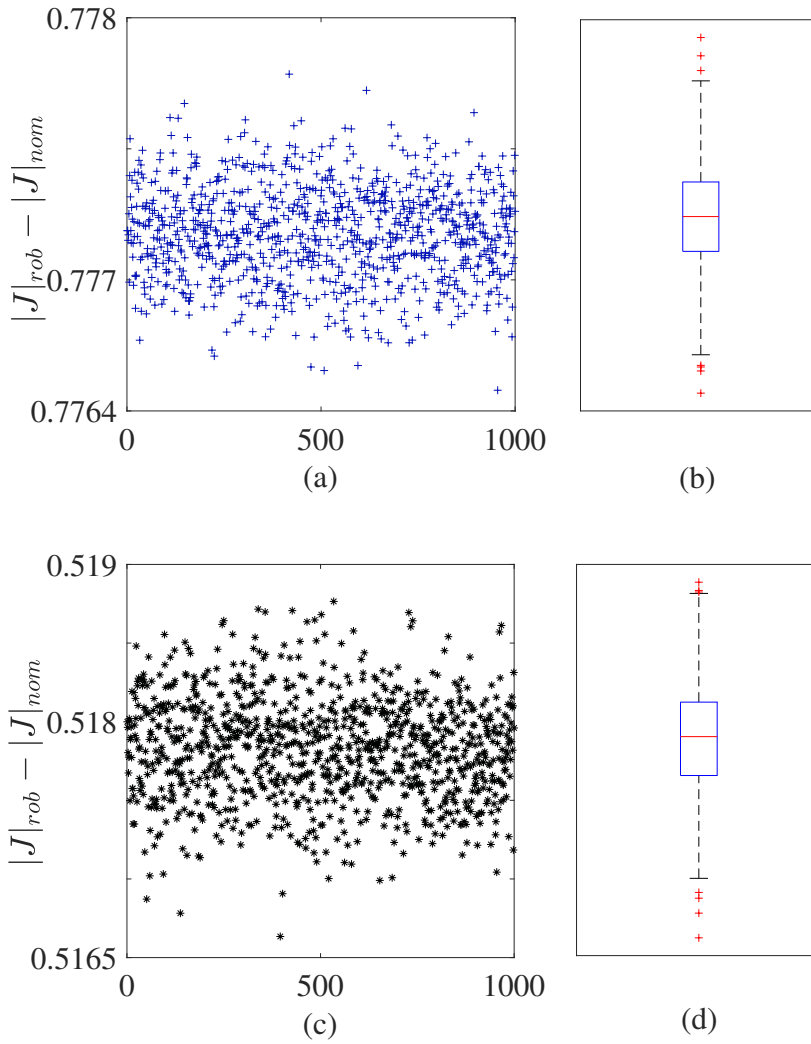


Figure 3.10.: Comparison between robust optimal control and nominal control in the form of $|J|_{rob} - |J|_{nom}$ on highschool network and residence hall network with 1000 runs. (a) and (b) are the scatter plot and box plot of the index for the scenario on the highschool network, respectively. (c) and (d) are for the scenario on the residence hall network. In both cases, the robust optimal control results in slightly better performance than the nominal control.

control framework on interacting the infection rate is proposed, following which two scenarios, i.e., to impede rumor spreading and to enhance the diffusion in marketing or campaign, are separately described. The solutions to the optimal control problems are proved to exist and obtained by Pontryagin Maximum Principle. Forward-backward sweep algorithm and `fmincon` are used to get the solution numerically. Several simulations are conducted to show effectiveness of the model as an approximation of the Markov chain and the performance of the optimal control law. By comparing the performance of the system under different configurations, we also conclude that: i) it is effective and critical to start to impede the

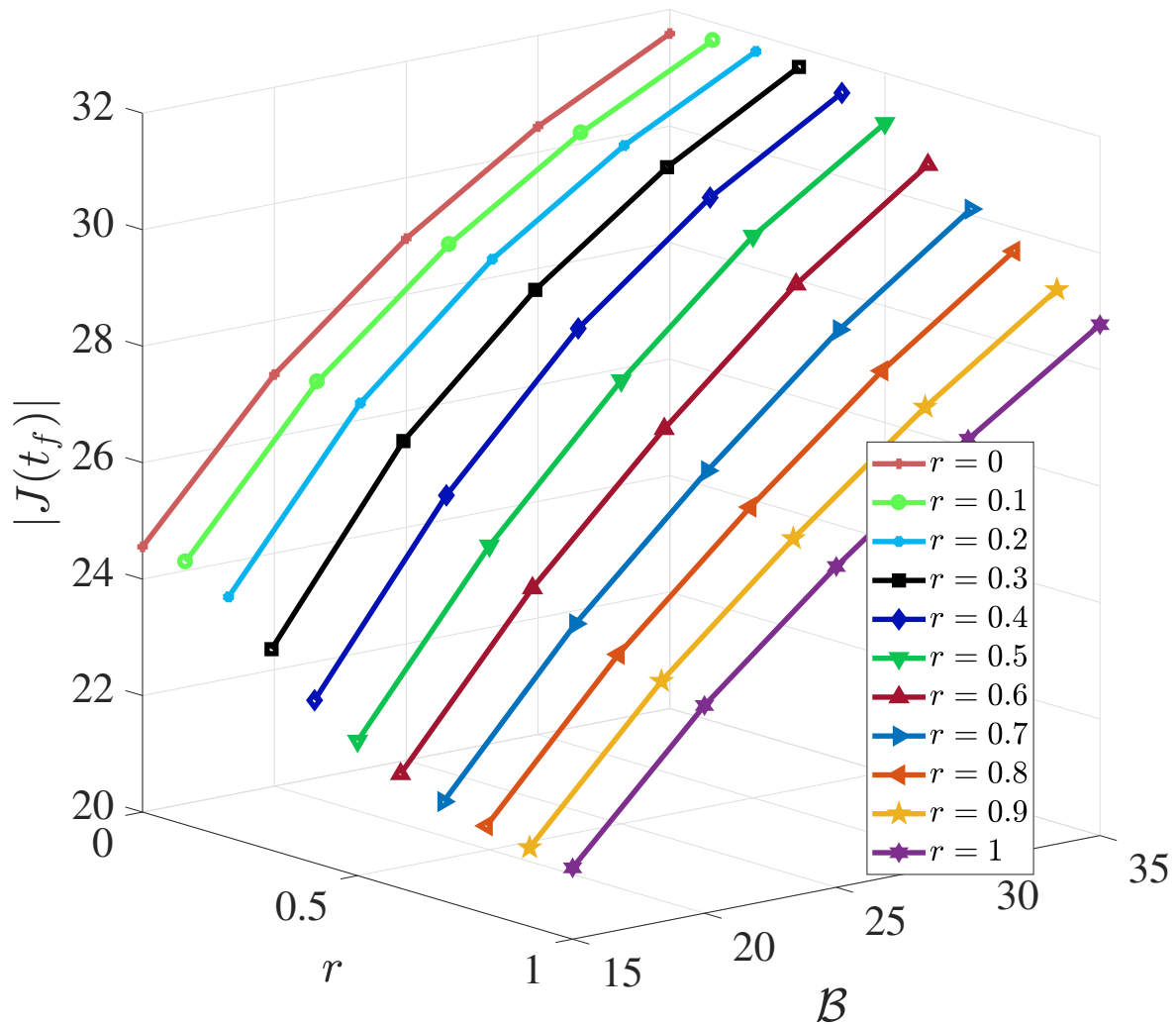


Figure 3.11.: $|J(t_f)|$ under different configuration of r and \mathcal{B} . The parameter r is chosen from 0 to 1 with step 0.1 and \mathcal{B} from 15 to 30 with step 5. The control input is computed by Algorithm 1 with each pair of the parameters. The initial condition $p_i(0)$ is chosen in $[0, 0.01)$ and is identical for every experiment. It reveals that more budget results in better spreading performance whereas the choice of r is nontrivial which may depends on the knowledge of noise.

rumor spreading as early as possible and ii) enough budget is the key factor to enhance the diffusion in a short period of time.

Furthermore, we address the robust optimal control problem for information epidemics in a heterogeneous network with noisy transition rates. Thus for the first time, the effects of natural uncertainties of the transition rates are considered to determine a robust optimal control strategy. A numerical solution is obtained based on distribution analysis. The diffusion is maximized in finite horizon with the proposed control strategy allowing for the constraint of limited budget. The proposed algorithm, which combines the forward backward

sweep method and the secant method, shows its effectiveness and efficiency in dealing with the diffusion processes over real networks. The numerical experiments on the influence of parameters confirm the common sense that the more budget the better dissemination performance. Apart from that, it is of great significance to properly weigh the impact of the noise while utilizing the proposed approach. The addressed formulation and the proposed optimal strategy not only solve the specific problem caused by the noisy transition rates but also provide a general solution to social networks with stochastic perturbations.

Although the control problems proposed in this chapter are successfully addressed, the following interesting topics for this young field remain to be solved.

- i) Distributed control algorithms for information diffusion processes. The proposed algorithms are actually centralized control but not in a distributed manner. These algorithms are valid when rich data sources are accessible. For general case when only limited access is possible, the fully distributed control algorithms should be considered, which is also naturally suitable for large scale social networks.
- ii) Effectiveness of the proposed algorithms in the Markov chain models. In this chapter, the control rules are directly designed for the node-based models. Although the node-based models can well approximate the performance of the Markov chain models, the error between them may affect the effectiveness of the proposed control law. However, the difficulty of conducting the comparisons lies in the simulation of the Markov chain model with huge amount of states. A potential approach to tackle this issue may be using the Monte Carlo simulation. The Monte Carlo simulation, however, takes long period of time as a trade-off to make the simulation possible for large scale networks. Apart from the comparison, to directly control the Markov chain model is of great interests since precisely the node-based models are the approximations of the Markov chain model.
- iii) Control design for the node-based models with stochastic noise. In Section 3.2, we deal with the deterministic disturbances and propose the robust optimal control. Whereas, taking into consideration the randomness in spreading processes, the impacts of the stochastic noise needs to be investigated.
- iv) Control design for multi-layer multiple information epidemics. In this chapter, we only focus on the control of single-layer single information epidemics. Bearing in mind the single dominant information equilibrium of the multi-layer multiple SIS model in Section 2.3, a promising extension is to design an optimal strategy for certain propagator such that his/her information can be dominant.

Opinion Dynamics on Coopetitive Social Networks

Although the well-known French-DeGroot model could result in the consensus opinion, public opinions do not always exhibit unanimous behavior but lead to persistent disagreement or clustering. Among others, the phenomenon “polarity” or “polarization” under a specific protocol that the opinions of the agents reach two opposite values is of considerable interest. The phenomenon of polar opinions appears broadly in multitudes of fields, e.g., political voting, segregation of residential communities, and cultural conflicts [105]–[107]. Apart from polarity and consensus, people may also keep neutral on topics in which they have no interest. Accordingly, the concept of “neutralization” is another central issue in opinion-dynamics engineering [105].

Although a notable size of the dedicated literature works on opinion clustering problems of DeGroot-type dynamics on signed graphs [46], [48], the primary focus is on the control protocol design and the associated convergence analysis. However, the manipulability of opinion dynamics, which concerns the existence of opinion protocols such that systems in question empower polarity, neutrality, and consensus, is a fundamental problem and of great significance in both theoretic synthesis and engineering implementation. Only very recently, researchers from the control theory field have started to investigate the consensusability [108] and synchronizability [109] of multi-agent systems on cooperative networks. These articles, nevertheless, focus only on addressing the existence question for linear time-invariant (LTI) systems with identical continuous dynamics and trustful interactions. Thus, studying polarizability, consensusability, and neutralizability of opinion dynamics in a more general setting becomes a prime desideratum in social network science.

The main contribution of this chapter is to address the fundamental question: Under what conditions, there exists certain kind of distributed protocols such that the opinion dynamics over coopetitive (cooperative-competitive) networks are polarized, consensus and neutralized, respectively. In specific, the formal definitions of these novel concepts, under the umbrella of “modulus consensusability”, are introduced as an appetizer. In view of the bipartite consensus at the heart of modulus consensus, we set out to study the bipartite consensusability that examines whether or not there exist admissible protocols such that the individual opinions asymptotically reach the same value but may differ in signs. Specifically, sufficient and/or necessary conditions for bipartite consensusability of opinion systems with identical dynamics are provided. The developed criterion emphasizes the functional role of interaction topological properties in conjunction with the dynamic structure of the

subsystems. Along with the examination of bipartite consensusability, neutralizability is taken into account as well and is characterized by sufficient and necessary conditions. With the emphasis on individual diversity, another significant contribution of is to extend the procured results to heterogeneous opinion dynamics. Criteria to examine the polarizability, consensusability, and neutralizability of non-identical opinion dynamics are explored. In particular, some common algebraic properties shared among individuals play an essential role in establishing polarization, consensus, and neutralization.

4.1 Modulus Consensusability

Consider $N \geq 2$ agents indexed 1 through N and the interaction among individuals characterized by a digraph $\mathcal{G} = (\mathcal{V}, \mathcal{E}, W)$ with $W = [w_{ij}] \in \mathbb{R}^{N \times N}$. In contrast to the conventional opinion models which usually consider scalar-valued opinions, we deal with simultaneous opinion discussion on multiple topics, thus necessitating the consideration of vector-valued opinions [11], [110], [111].

Each agent is associated with a vector $x_i \in \mathbb{R}^n$ that represents her attitudes on n issues (subtopics) and updates continuously her opinion in the following fashion

$$\dot{x}_i(t) = Ax_i(t) + Bu_i(t), \quad i \in \mathcal{V}, \quad (4.1)$$

where $u_i \in \mathbb{R}^m$ is the control input of individual i . The state matrix $A \in \mathbb{R}^{n \times n}$ characterizes the level of ‘‘anchorage’’ on their topic-specific opinions, which has been formed by some exogenous conditions, e.g., the past social experience, or endogenous factors, e.g., personal intelligence and character. The input matrix $B \in \mathbb{R}^{n \times m}$ stands for the susceptibility of agents to the interpersonal influence. We consider a distributed feedback control under coopetitive interaction as follows,

$$u_i(t) = -K \sum_{(j,i) \in \mathcal{E}} |w_{ij}| (x_i - \text{sgn}(w_{ij})x_j), \quad i \in \mathcal{V}, \quad (4.2)$$

where $K \in \mathbb{R}^{m \times n}$ is the feedback gain matrix. In the recent literature of opinion evolution on signed graphs [46], [48], the control protocol (4.2) can often be found.

Remark 3. This LTI system (4.1) has been widely adopted in analyzing the collective behavior of multi-agent systems on cooperative networks, including agreement- [109], [112] and disagreement-problems [113]. Only very recently in the context of coopetitive networks have researchers started to employ such a state-feedback LTI model to study bipartite consensus [110], [114]. In the special case $A = O$, $B = I$, the model (4.1) of opinion evolving on single topic degenerates to Altafini-type model [46]. Furthermore, a nonlinear counterpart of the model (4.1) with the controller (4.2) is proposed in [47].

After denoting $u(t) := [u_1^\top(t), \dots, u_n^\top(t)]^\top$, we consider the following admissible set,

$$\begin{aligned} \mathcal{U} = \{ & u(t) \in \mathbb{R}^{mN} \mid u_i(t) = -K \sum_{j=1}^N |w_{ij}| (x_i - \text{sgn}(w_{ij})x_j), \\ & \forall t > 0, K \in \mathbb{R}^{m \times n}, i = 1, \dots, N\}. \end{aligned} \quad (4.3)$$

The admissible control set (4.3) covers a relatively large number of distributed protocols with antagonistic interactions. The overarching question before entering into the stage of

protocol design is to determine under what conditions, the opinion dynamics of interest is polarizable, consensusable, and neutralizable w.r.t. such an admissible control set \mathcal{U} . To investigate such question, we first provide the formal definitions of the polarizability, consensusability, and neutralizability in the context of the so-called modulus consensusability of an opinion system w.r.t. \mathcal{U} .

Definition 3 (Modulus consensusability). The system (4.1) is *modulus consensusable* w.r.t. \mathcal{U} , if one can find a $u \in \mathcal{U}$ and scalars $\rho_i, \rho_j \in \{\pm 1\}$, $\forall i, j \in \mathcal{V}$ such that for any initial value $x_i(0)$, the solution of (4.1) on a graph $\mathcal{G} = (\mathcal{V}, \mathcal{E}, W)$ satisfies

$$\lim_{t \rightarrow \infty} \rho_i x_i(t) - \rho_j x_j(t) = 0, \lim_{t \rightarrow \infty} \|x_i(t)\| < \infty, \forall i, j \in \mathcal{V}. \quad (4.4)$$

Specifically, modulus consensusability can be classified into the following cases:

- a). if $\lim_{t \rightarrow \infty} x_i(t) = 0, \forall i \in \mathcal{V}$, we say the system (4.1) is *neutralizable* w.r.t. \mathcal{U} ;
- b). if $\rho_i = \rho_j, \forall i, j \in \mathcal{V}$ and a) is not satisfied, we say the system (4.1) is *consensusable* w.r.t. \mathcal{U} ;
- c). if $\rho_i = -\rho_j$ holds for at least a pair of nodes $i, j \in \mathcal{V}$ and a) is not satisfied, we say the system (4.1) is *polarizable* w.r.t. \mathcal{U} .
- d). the system (4.1) is *bipartite consensusable* if it is either consensusable or polarizable. Specially, the system (4.1) is *stationary bipartite consensusable*, if $\lim_{t \rightarrow \infty} \rho_i x_i(t) = v$ is further satisfied for all $i \in \mathcal{V}$, where $v \in \mathbb{R}^n \setminus \{0\}$ is a constant vector.

A Venn diagram is presented in Figure 4.1 to illustrate the relations of the concepts proposed in Definition 3. Note that modulus consensusability proposed in this technical note is equivalent to consensusability in [108] on unsigned graphs, where the trivial case of neutralization is not specialized. In the literature on opinion dynamics, neutralization is commonly referred to stabilization as an inheritance of the seminal work [46]. Since social actors preferably take a neutral stance on sensitive issues and uninteresting topics, we tend to use the sociological terminology, neutralization, instead in this technical note. Furthermore, agents constantly keep neutralized in the neutral configuration of initial opinions. In the following of this technical note, we are more interested in studying opinion dynamics when the initial conditions are non-neutral. The non-trivial case of modulus consensus, i.e., the opinions reach consensus or oppositely separate, is named as bipartite consensus. Polarizability is based on the phenomenon of polarity [46], [48], but the detailed content here is slightly different. First, the opinion variable is a vector rather than a scalar, thus the case when some (not all) of the entries of the opinion vector are 0 is also allowed for bipartite consensusability. Second, Definition 3 enables us to investigate the opinion formation process in a more general setting in which the opinion states may converge to trajectories but not to a set of fixed points. Convergence to trajectories mirrors the fact that the amplitudes of the steady-state opinions may fluctuate in some degree caused by exogenous influence or endogenous vibration, but an about-turn of individual attitudes seldom happens. We also point out that the opinion states should be bounded no matter how extreme they could be since infinite values of opinions make no sense from the perspective of sociology and psychology.

One may notice that there may exist two types of bipartition of the opinion dynamics over cooperative networks, i.e., the bipartition of the graph structure (the SB property defined

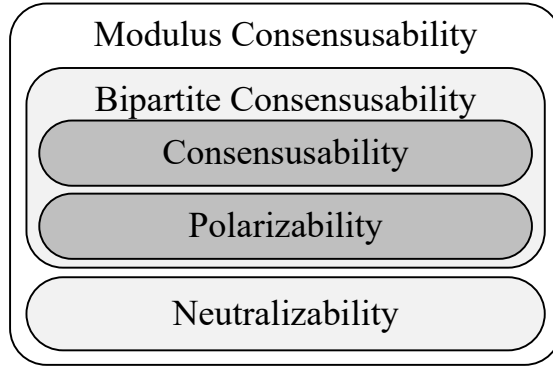


Figure 4.1.: Venn diagram on the relations between the concepts in Definition 3.

in Section A.2) and the bipartition of the public opinions. Modulus consensusability by definition only focuses on the opinion partition in the view of dynamic systems. A natural conjecture is that the SB property of the graph may serve as a condition for modulus consensusability, which will be further illustrated in the following sections. To make the concepts clear and precise, we fix some notations and terminology, before embarking on the main results. Throughout this chapter, symbols $\rho_i \in \{\pm 1\}$ characterize the signatures of individual opinions at steady-state, while the structural balance of a graph, if it has, is specified by $d_i \in \{\pm 1\}$.

4.2 Modulus Consensusability of Homogeneous Opinion Dynamics on Coopetive Networks

In this section, we elaborate on whether or not there exist a matrix $K \in \mathbb{R}^{m \times n}$ and a signed graph \mathcal{G} such that the system (4.1) with a controller (4.2) establishes polarization, consensus, and neutralization.

4.2.1 Bipartite Consensusability of Opinion Dynamics

In comparison to the trivial case in modulus consensus, the bipartite consensus is of great interest for sociological studies. Such bipartition of opinions is known to have a tight connection to the structural balance of the underlying interaction topology. Following this line of thought, the sufficient condition for bipartite consensusability of the system (4.1) can be derived.

For the convenience of presentation, we introduce the set of marginally stable matrices

$$\mathcal{M} = \left\{ M : \text{sp}\{M\} \subseteq \mathbb{C}_{\leq 0}, \text{sp}\{M\} \cap i\mathbb{R} \neq \emptyset, \right. \\ \left. \lambda \text{ is semi-simple, } \forall \lambda \in \text{sp}\{M\} \cap i\mathbb{R} \right\}, \quad (4.5)$$

where i is the imaginary unit, i.e., $i^2 = -1$, and a semi-simple eigenvalue possesses equal algebraic and geometric multiplicities. In the next theorem, we first provides a sufficient condition for bipartite consensusability of opinion dynamics.

Theorem 7. *Given a graph $\mathcal{G} = (\mathcal{V}, \mathcal{E}, W)$, the system (4.1) is bipartite consensusable for any non-zero initial conditions w.r.t. \mathcal{U} , if the following conditions are satisfied:*

- i) \mathcal{G} is structurally balanced and quasi-strongly connected.
- ii). $A \in \mathcal{M}$ and (A, B) is stabilizable.

Moreover, the system (4.1) is consensusable if \mathcal{G} is an unsigned graph, otherwise polarizable if \mathcal{G} is a signed graph.

Proof. The SB property of \mathcal{G} means that there exist N scalars $d_i \in \{\pm 1\}$ such that $d_i d_j w_{ij} = \bar{w}_{ij}$. By denoting $\bar{x}_i(t) := d_i x_i(t)$, one can obtain its time-derivative from (4.1) as follows

$$\dot{\bar{x}}_i(t) = A\bar{x}_i(t) - BK \sum_{j=1}^N \bar{w}_{ij}(\bar{x}_i(t) - \bar{x}_j(t)), i \in \mathcal{V}. \quad (4.6)$$

By adopting Kronecker product, the system (4.6) can be rewritten in a compact form as below.

$$\dot{\bar{x}}(t) = \left(I_N \otimes A - \bar{L} \otimes BK \right) \bar{x}(t), \quad (4.7)$$

where $\bar{x}(t) = [\bar{x}_1^\top(t), \dots, \bar{x}_N^\top(t)]^\top$ and \bar{L} is the Laplacian matrix of the associated unsigned graph $\bar{\mathcal{G}}$.

The bipartite consensusability problem of (4.1) can be transformed into the consensusability problem of (4.7). According to [108, Theorem 2], the system (4.7) is modulus consensusable if the unsigned graph $\bar{\mathcal{G}}$ associated to \mathcal{G} is QSC and (A, B) is stabilizable. After setting $\rho_i = d_i, \forall i \in \mathcal{V}$, the system (4.7) achieving consensus, i.e., $\lim_{t \rightarrow \infty} \bar{x}_i - \bar{x}_j = 0$, implies the establishment of bipartite consensus in the opinion dynamics (4.1), specifically, $\lim_{t \rightarrow \infty} \rho_i x_i - \rho_j x_j = 0$. Accordingly, it is illuminating to view that the original system (4.1) is bipartite consensusable if condition i) and ii) occur. It is worthy to note that for non-zero initial opinions, the constraint $A \in \mathcal{M}$ guarantees that $x_i(t)$ does not converge to 0, and is bounded when $t \rightarrow \infty, \forall i \in \mathcal{V}$.

Moreover, a signed graph \mathcal{G} associated with at least one negative weighted edge results in opinion polarization otherwise opinion consensus. \square

Remark 4. The feedback control gain K which guarantees the system to be bipartite consensus can be obtained by the following approach given in [115]:

Let $\sigma = \min_{\lambda_i \in \text{sp}\{A\} \setminus \{0\}} \{\text{Re}\lambda_i\}$. Bearing in mind that (A, B) is stabilizable, there holds that $A - BB^\top P$ is Hurwitz, where P is the unique positive semi-definite solution of the following Riccati equation

$$A^\top P + PA - PBB^\top P + I_n = 0. \quad (4.8)$$

It follows that the feedback control gain can be selected as

$$K = \max\{1, \sigma^{-1}\} B^\top P. \quad (4.9)$$

The conditions in Theorem 7 involve two aspects, i.e., the requirements for the network topology and for the subsystem dynamics. In condition i), quasi-strongly connectivity ensures that there exists at least one agent who can deliver directly or indirectly his/her willing

to the remaining members, while the structural balance of graphs paves the way for the bipartite consensus of opinions. Condition ii), on the other hand, emphasizes the importance of the dynamical properties of individuals. Specifically, it excludes the situation of neutralization and the meaningless case in which opinions are unbounded, $A \in \mathcal{M}$ is of significance. Besides, the stabilizability of (A, B) implies that the individual is open to interpersonal influence.

In Theorem 7, we only focus on the sufficient conditions for bipartite consensusability, wherein a graph being SB is indispensable in the sufficient criterion. Through the next analysis, however, we will address that this graph property is not necessary for an opinion dynamics to achieve stationary bipartite consensus, let alone for the generic case.

Theorem 8. *Given a graph $\mathcal{G} = (\mathcal{V}, \mathcal{E}, W)$, the system (4.1) is stationary bipartite consensusable w.r.t. \mathcal{U} , only if the following conditions are satisfied:*

- i). \mathcal{G} is quasi-strongly connected and there exists a non-negative scalar $\alpha \geq 0$ such that there holds

$$\alpha_i \equiv \alpha, \quad \forall i \in \mathcal{V} \quad (4.10)$$

where $\alpha_i := \sum_{j=1}^N (|\tilde{w}_{ij}| - \tilde{w}_{ij})$ and $\tilde{w}_{ij} := \rho_i \rho_j w_{ij}$.

- ii). (A, B) is stabilizable, $A - \alpha BK \in \mathcal{M}$ and the spectral subset $\text{sp}\{A - \alpha BK\} \cap i\mathbb{R}$ contains only 0.

Proof. We first prove \mathcal{G} is QSC by contradiction. If \mathcal{G} is not QSC, then it has either at least two nodes without inward edges or two separate subgraphs [116]. The first situation means that there exist at least two “isolated” actors (say agent p and agent q) whose opinions remain independent of the others’ thoughts. Accordingly, the dynamics of these two agents reduces to $\dot{x}_k = Ax_k$ with $k = p, q$. It is evident that such subsystems cannot reach bipartite consensus for arbitrary initial states. In the second case, even if a stationary bipartite consensus is achieved in each subgraph, it is unlikely to be established across the entire graph \mathcal{G} for all initial configuration. As a result, the contradictions arising in both two cases allow us to state that the QSC property of a graph is necessary for bipartite consensusability.

Next, we begin to demonstrate the relation (4.10). According to Definition 3, the system (4.1) being stationary bipartite consensusable means there exist a sequence of scalars $\rho_i, \rho_j \in \{\pm 1\}$ and a constant vector $v \in \mathbb{R}^n \setminus \{0\}$ such that $\lim_{t \rightarrow \infty} \rho_i x_i(t) = v$ is valid for all $i \in \mathcal{V}$. After denoting $\tilde{x}_i := \rho_i x_i$ for $i \in \mathcal{V}$, in analogy with the system dynamics (4.6), one can obtain

$$\dot{\tilde{x}}_i(t) = A\tilde{x}_i(t) - BK \sum_{j=1}^N (|\tilde{w}_{ij}| \tilde{x}_i(t) - \tilde{w}_{ij} \tilde{x}_j(t)), \quad i \in \mathcal{V}, \quad (4.11)$$

where $\tilde{w}_{ij} := \rho_i \rho_j w_{ij}$. With the notation $\tilde{x} = [\tilde{x}_1^\top, \dots, \tilde{x}_N^\top]^\top$, the compact form of (4.11) can be given by

$$\dot{\tilde{x}}(t) = (I_N \otimes A - \tilde{L} \otimes BK) \tilde{x}(t), \quad (4.12)$$

where

$$\tilde{L} := \text{diag}(\rho) L \text{diag}(\rho) = \begin{bmatrix} \sum_{j=1}^N |\tilde{w}_{1j}| & \tilde{L}_{12} \\ \tilde{L}_{21} & \tilde{L}_{22} \end{bmatrix}. \quad (4.13)$$

Arisen from the fact that the system (4.1) is stationary bipartite consensusable, the stationary consensusability of the dynamics (4.11) is unambiguous.

To promote the analysis, we introduce an auxiliary variable $\xi_i = \tilde{x}_1 - \tilde{x}_i$ ($i = 2, 3, \dots, N$) associated with the time evolution as follows

$$\begin{aligned} \dot{\xi}_i = & A\xi_i - BK \sum_{j=1}^N [(\tilde{w}_{1j} - \tilde{w}_{ij})\xi_j + |\tilde{w}_{ij}|\xi_i] \\ & - BK\tilde{x}_1 \sum_{j=1}^N [(|\tilde{w}_{1j}| - \tilde{w}_{1j}) - (|\tilde{w}_{ij}| - \tilde{w}_{ij})]. \end{aligned} \quad (4.14)$$

We can immediately infer that the auxiliary system (4.14) is asymptotically stable, i.e., $\lim_{t \rightarrow \infty} \xi_i(t) = 0$ as the system (4.11) is stationary consensusable. As a consequence, the third item in the right-hand side of (4.14) needs to approach to 0 as $t \rightarrow \infty$ for all $i = 2, \dots, N$, which is equivalent to the condition

$$\sum_{j=1}^N [(|\tilde{w}_{1j}| - \tilde{w}_{1j}) - (|\tilde{w}_{ij}| - \tilde{w}_{ij})] = 0, \text{ for } i = 2, \dots, N. \quad (4.15)$$

and/or $\lim_{t \rightarrow \infty} BK\tilde{x}_1 = 0$ succeeds.

In order to rule out the second situation, we first postulate, without loss of generality, that $\lim_{t \rightarrow \infty} BK\tilde{x}_i = BKv = 0$ holds for all $i \in \mathcal{V}$ due to the fact $\lim_{t \rightarrow \infty} \tilde{x}_i = v$ for $i \in \mathcal{V}$. In other words, we have $v \in \ker BK$. The limiting behavior of the dynamics (4.11) and its stationary consensusability manifest that $Av = 0$, i.e., $v \in \ker A$. Meanwhile, let $e(t) := \tilde{x}(t) - \mathbb{1}_N \otimes v$ be an error vector. By noticing the fact that

$$(I_N \otimes A - \tilde{L} \otimes BK)(\mathbb{1}_N \otimes v) = \mathbb{1}_N \otimes (Av) - (\tilde{L}\mathbb{1}_N) \otimes (BKv) = 0_{nN}, \quad (4.16)$$

the dynamics of the error vector obeys the evolution rule

$$\dot{e}(t) = (I_N \otimes A - \tilde{L} \otimes BK)e(t). \quad (4.17)$$

Thanks to $\lim_{t \rightarrow \infty} e = 0$, one can obtain $\text{sp}\{I_N \otimes A - \tilde{L} \otimes BK\} \subseteq \mathbb{C}_{<0}$. That is to say, the system (4.12) is asymptotically stable, i.e., $\lim_{t \rightarrow \infty} \tilde{x} = 0$, which is contradictory to the definition of stationary bipartite consensus. To this end, we illustrate that the equality (4.15) is necessary for bipartite consensusability of the opinion system (4.1), which is equivalent to

$$\sum_{j=1}^N (|\tilde{w}_{ij}| - \tilde{w}_{ij}) = \alpha, \quad \forall i \in \mathcal{V}, \quad (4.18)$$

where $\alpha \geq 0$ is a non-negative scalar. As a result, the dynamics (4.14) can be compactly written as

$$\dot{\xi}(t) = (I_{N-1} \otimes A - \tilde{\mathcal{L}} \otimes BK)\xi(t), \quad (4.19)$$

where $\xi(t) = [\xi_2^\top(t), \dots, \xi_N^\top(t)]^\top$ and $\tilde{\mathcal{L}} = \tilde{L}_{22} - \mathbb{1}_{N-1} \tilde{L}_{12}$.

Next, we illustrate (A, B) stabilizable in condition ii). The equality (4.18) can be rephrased to $\tilde{L}\mathbb{1} = \alpha\mathbb{1}$ which facilitates the matrix decomposition as follows

$$\begin{bmatrix} 1 & 0 \\ \mathbb{1}_{N-1} & I_{N-1} \end{bmatrix}^{-1} \tilde{L} \begin{bmatrix} 1 & 0 \\ \mathbb{1}_{N-1} & I_{N-1} \end{bmatrix} = \begin{bmatrix} \alpha & \tilde{L}_{12} \\ 0 & \tilde{\mathcal{L}} \end{bmatrix}. \quad (4.20)$$

Then, the fact that the transformation $L \rightarrow \text{diag}(\rho)L\text{diag}(\rho)$ is a similar transformation leads to $\text{sp}\{L\} = \text{sp}\{\tilde{L}\}$, which immediately implies $\text{sp}\{L\} = \text{sp}\{\tilde{\mathcal{L}}\} \cup \{\alpha\}$. As a result, one can compute

$$\text{sp}\{I_{N-1} \otimes A - \tilde{\mathcal{L}} \otimes BK\} = \cup_{\lambda \in \text{sp}\{L\} \setminus \{\alpha\}} \text{sp}\{A - \lambda BK\}. \quad (4.21)$$

Thereby, the asymptotic stability of the auxiliary system (4.19) accords to

$$\text{sp}\{A - \lambda BK\} \subseteq \mathbb{C}_{<0}, \quad \forall \lambda \in \text{sp}\{\tilde{\mathcal{L}}\}. \quad (4.22)$$

We then prove (A, B) is stabilizable by using (4.22).

On the one hand, for $\lambda = 0$, the negative definiteness of matrix $A - \lambda BK$ entails a Hurwitz matrix A . Thus, it is intuitively clear that (A, B) is stabilizable. On the other hand, for those non-zero eigenvalues, we discuss the necessity on two cases: real-valued and complex-valued eigenvalues. For any real-valued λ , $\text{sp}\{A - \lambda BK\} \in \mathbb{C}_{<0}$ means obviously that (A, B) is stabilizable.

In regard to the complex-valued case, without loss of generality, we suppose $\lambda_{1,2} = a \pm bi$ is a pair of conjugate eigenvalues of $\text{sp}\{\tilde{\mathcal{L}}\}$. By means of the properties of the determinant operator, one can have the reformulation of the characteristic polynomial to

$$\det \left(sI_{2n} - \begin{bmatrix} A - aBK & bBK \\ -bBK & A - aBK \end{bmatrix} \right) = \det(sI_n - (A - \lambda_1 BK)) \det(sI_n - (A - \lambda_2 BK)). \quad (4.23)$$

Namely, all eigenvalues of $\begin{bmatrix} A - aBK & bBK \\ -bBK & A - aBK \end{bmatrix}$ are in $\mathbb{C}_{<0}$ because of $\text{sp}\{A - \lambda_1 BK\} \subseteq \mathbb{C}_{<0}$ and $\text{sp}\{A - \lambda_2 BK\} \subseteq \mathbb{C}_{<0}$. In addition, the decomposition

$$\begin{bmatrix} A - aBK & bBK \\ -bBK & A - aBK \end{bmatrix} = \text{diag}(A, A) - \text{diag}(B, B) \begin{bmatrix} aK & -bK \\ bK & aK \end{bmatrix} \quad (4.24)$$

discloses that the pair $(\text{diag}(A, A), \text{diag}(B, B))$ must be stabilizable. According to Popov-Belevitch-Hautus (PBH) stabilizability criterion [117], the stabilizability of the linear system with state matrix $\text{diag}(A, A)$ and input matrix $\text{diag}(B, B)$ equals to

$$\text{rank} \begin{bmatrix} sI_n - A & \mathbb{0}_n & B & \mathbb{0}_n \\ \mathbb{0}_n & sI_n - A & \mathbb{0}_n & B \end{bmatrix} = 2n, \quad \forall s \in \mathbb{C}_{>0}, \quad (4.25)$$

from which one can straightforwardly derive $\text{rank}(sI_n - A \quad B) = n$, for all $s \in \mathbb{C}_{>0}$. Thus, we can conclude that (A, B) is stabilizable if system (4.1) is stationary bipartite consensusable.

We are now on our way to prove the last part of the statement ii). The system matrix in (4.11), in spirit similar to (4.21), has the spectrum

$$\text{sp}\{I_N \otimes A - \tilde{L} \otimes BK\} = \cup_{\lambda \in \text{sp}\{\tilde{\mathcal{L}}\} \cup \{\alpha\}} \text{sp}\{A - \lambda BK\}. \quad (4.26)$$

Based upon the fact that $\text{sp}\{A - \lambda BK\} \subseteq \mathbb{C}_{<0}$ for all $\lambda \in \text{sp}\{\tilde{\mathcal{L}}\}$, the spectral property of matrix $A - \alpha BK$ primarily characterizes the dynamical behavior of the system (4.12). Then, the statement that \tilde{x} converges to a bounded constant non-zero vector $\mathbb{1} \otimes v$ for any initial conditions, indicates that $A - \alpha BK \in \mathcal{M}$ and all the marginally stable eigenvalues of matrix $A - \alpha BK$ are 0. Therefore, we complete the proof. \square

The most noticeable point of Theorem 8 is no explicit requirement of SB graphs for stationary bipartite consensus of opinion dynamics. Nevertheless, one still can extract the SB condition from the equality relation (4.10) but far more than that. Structural balance theory [36] states that for an unweighted graph being not exactly SB, the least number of edges that must be changed of sign can be used to compute a distance to exact structural balance (i.e., a measure of the amount of structural unbalance in the network.). This statement has an immediate extension in weighted graphs [118]. In specific, we can argue that the quantity $\sum_i \alpha_i = \sum_{i,j} (|\tilde{w}_{ij}| - \tilde{w}_{ij})$ can be treated as an unbalance metric which measures the distance to a desired SB structure specified by $\rho = [\rho_1, \dots, \rho_N]^\top$. Since such a metric captures the collective effect of unbalance, the index α_i distinguishes the individual contribution of node i to disrupt the global structural balance w.r.t. ρ . Hence, the relation (4.10) reads that all agents contribute an equal impact on network unbalance. In the special case of $\alpha_i = 0$ for all $i \in \mathcal{V}$, all nodes exhibit a local structural balance, and the network entails a natural SB structure: the community splits into two hostile camps, individuals with the same sign of ρ_i come from the same camp, the social ties inside each fraction are cooperative, whereas the interrelations cross fractions are competitive. Hence, Theorem 8 reveals an appealing, and previously unexplored, relationship between SB bipartition of topology and state clustering of opinion dynamics. In particular, the scenario $\alpha > 0$ meaning the mismatch of the bipartition pattern between opinion organization and network structure, mirrors real-world phenomena, especially, in political and commercial voting. The U.S. House Vote [119] in the two-party congress serves as a typical example. Although the underlying interconnection topology of Republicans and Democrats exhibits a natural SB graph, representatives from the same party would not always vote for the same (pros or cons, usually) and the vote result is highly dependent on the specific content of the bills. For instance, in the House Vote #132 in 2018, it is clear that within both Republicans and Democrats, the representatives did not reach an agreement. This reveals that not only the graph but also the topic and even other exogenous reasons could lead to the bipartition of opinions. Moreover, in some act, the representatives in two parties may even achieve consensus, like H.R. 5447: Music Modernization Act.

Throughout this chapter, we call the polarization is *consistent* if the bipartition of the public opinions and the network topology is the same; and *inconsistent* while different. From mathematical point of view, the inconsistent case can be illustrated as the fact that there exists $\alpha > 0$ such that the limit performance of the dynamics is governed by $A - \alpha BK$. To fulfill this condition, one may raise the algebraic requirement for the communication topology that there exists $\bar{d} \in \mathbb{R}^N$ with each entry in $\{\pm 1\}$ such that $L\bar{d} = \alpha\bar{d}$, i.e., (α, \bar{d}) is an eigen-pair of L . Thus by proper choice of K , the inconsistent polarization can be achieved. For an SB and QSC graph, $\dim \ker L = 1$ holds by Lemma 17. It follows that, $\bar{d} \neq d$ in this situation. Further explanations are provided in Subsection 4.2.3 by numerical experiments.

Until now, the discussion is carried out in terms of sufficient and necessary conditions, respectively. In particular, the necessary conditions in a generic circumstance are missing. In the following theorem, we make a step towards filling this gap.

Theorem 9. *Let the system (4.1) with non-zero initial conditions be of a non-Hurwitz matrix A and satisfy*

$$\rho_i \rho_j = d_i d_j, \quad \forall i, j \in \mathcal{V}. \quad (4.27)$$

The opinion dynamics (4.1) evolving over a SB graph \mathcal{G} is bipartite consensusable w.r.t. \mathcal{U} , if and only if the following conditions hold:

i) \mathcal{G} is quasi-strongly connected.

ii). $A \in \mathcal{M}$ and (A, B) is stabilizable.

Proof. Sufficiency is an immediate result from Theorem 7. Here we need only to prove the necessity.

The assembly line of Theorem 8 exposes that a QSC graph is necessary. The relation (4.27) results in $\alpha_i = \sum_{j=1}^N (|\tilde{w}_{ij}| - \tilde{w}_{ij}) = 0$ for $i \in \mathcal{V}$, implying $\alpha = 0$. Meanwhile, the dynamics (4.11) becomes

$$\dot{\tilde{x}}_i(t) = A\tilde{x}_i(t) - BK \sum_{j=1}^N (|\bar{w}_{ij}|\tilde{x}_i(t) - \bar{w}_{ij}\tilde{x}_j(t)), \quad (4.28)$$

where $\bar{w}_{ij} = d_i d_j w_{ij} \geq 0$ due to the structural balance of the graph. Consequently, the auxiliary system (4.14) here reduces to

$$\dot{\xi}_i = A\xi_i - BK \sum_{j=1}^N [(\bar{w}_{1j} - \bar{w}_{ij})\xi_j + \bar{w}_{ij}\xi_i], \quad (4.29)$$

where $\xi_i = \tilde{x}_1 - \tilde{x}_i$ and $i = 2, \dots, N$. The compact form of (4.29) can be given by

$$\dot{\xi}(t) = (I_{N-1} \otimes A - \overline{\mathcal{L}} \otimes BK)\xi(t), \quad (4.30)$$

where $\overline{\mathcal{L}} := \overline{L}_{22} - \mathbf{1}_{N-1} \overline{L}_{12}$ upon the matrix partition

$$\overline{L} = DLD = \begin{bmatrix} \sum_{j=1}^N \bar{w}_{1j} & \overline{L}_{12} \\ \overline{L}_{21} & \overline{L}_{22} \end{bmatrix}. \quad (4.31)$$

The remainder of the proof mimics the procedure of Theorem 8 which entails the stabilizability of (A, B) and $A \in \mathcal{M}$ as a result. Noteworthy, by revisiting the similarity transformation (4.20) with the Laplacian matrix \overline{L} of the associated unsigned graph $\overline{\mathcal{G}}$ which is QSC, $\overline{\mathcal{L}}$ inherits all nonzero eigenvalues of \overline{L} . \square

4.2.2 Neutralizability of Opinion Dynamics

Besides bipartition of opinions, either unanimous or opposite behaviors, among individuals, sometimes people tend to hold neutral opinions for certain political or economic reasons in social activities. This phenomenon motivates us to discuss the neutralizability of opinion dynamics.

The answer to neutralizability of systems (4.1) with a Hurwitz matrix A , is affirmative, where $K = O$ is an intuitive option. In this scenario, individuals, who are totally closed to the social influence, persist neutral attitudes to all topics. Thus, we restrict ourselves to the case of non-Hurwitz A while dealing with neutralizability.

Theorem 10. *Given a graph $\mathcal{G} = (\mathcal{V}, \mathcal{E}, W)$, the system (4.1) with non-Hurwitz matrix A is neutralizable w.r.t. to \mathcal{U} , if and only if the following conditions are satisfied,*

i) (A, B) is stabilizable.

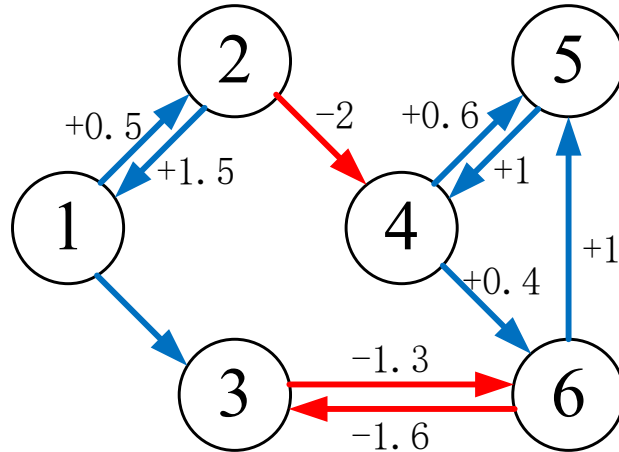


Figure 4.2.: An example of SB and QSC graph

ii) \mathcal{G} is neither structurally balanced nor contains an in-isolated structurally balanced subgraph.

Proof. Consider the compact form of the system (4.1) as below

$$\dot{x}(t) = (I_N \otimes A - L \otimes BK)x(t), \quad (4.32)$$

from which, one can easily obtain

$$\text{sp}\{I_N \otimes A - L \otimes BK\} = \cup_{\lambda \in \text{sp}\{L\}} \text{sp}\{A - \lambda BK\}. \quad (4.33)$$

Therefore, the neutralizability problem can be transformed to show $\text{sp}\{A - \lambda BK\} \subseteq \mathbb{C}_{<0}$ for all $\lambda \in \text{sp}\{L\}$.

Sufficiency: Since \mathcal{G} is not SB and contains no isolated SB subgraphs, it is already known that $0 \notin \text{sp}\{L\}$. In addition, the stabilizability of (A, B) always allows one to find a matrix K to such that the matrix $A - \lambda BK, \forall \lambda \in \text{sp}\{L\}$ is stable, thereby evidencing the neutralizability of the compact system (4.32) w.r.t. \mathcal{U} .

Necessity: The background that the system (4.32) is neutralizable w.r.t. \mathcal{U} amounts to $\text{sp}\{A - \lambda BK\} \subseteq \mathbb{C}_{<0}$ for all $\lambda \in \text{sp}\{L\}$. We posit that graph \mathcal{G} is SB or contains an in-isolated SB subgraph, which leads to $0 \in \text{sp}\{L\}$. The condition $\text{sp}\{A - \lambda BK\} \subseteq \mathbb{C}_{<0}$ for $\lambda = 0$ means A is a stable matrix which is contradictory to the fact that A is not Hurwitz. Therefore, we derive the necessity of condition ii). In reference to condition i), we can adopt the same method presented in Theorem 8 to display that (A, B) is stabilizable. \square

4.2.3 Numerical Experiments

In this subsection, several simulations serve to demonstrate the main results of the homogeneous opinion dynamics. As is shown in Figure 4.2, a paradigmatic network consisting of 6 individuals is introduced as an example. The weighted adjacency matrix is

$$W = \begin{bmatrix} 0 & 1.5 & 0 & 0 & 0 & 0 \\ 0.5 & 0 & 0 & 0 & 0 & 0 \\ 1 & 0 & 0 & 0 & 0 & -1.6 \\ 0 & -2 & 0 & 0 & 1 & 0 \\ 0 & 0 & 0 & 0.6 & 0 & 1 \\ 0 & 0 & -1.3 & 0.4 & 0 & 0 \end{bmatrix} \quad (4.34)$$

Evidently, the underlying weighted graph is QSC as any node can be regarded as a root. The graph in Figure 4.2 is selected to be SB: node 1, 2, and 3 are in the same camp while the rest nodes in the competitive camp.

Consider a homogeneous opinion dynamics in (4.1) with the state and input matrices

$$A = \begin{bmatrix} 0 & 0 & 0 \\ 0 & 0 & 1 \\ 0 & -1 & 0 \end{bmatrix}, \quad B = \begin{bmatrix} 1 \\ 1 \\ 1 \end{bmatrix}, \quad (4.35)$$

respectively. It is apparent that (A, B) is stabilizable by Kalman's criterion. By solving (4.8) and using (4.9), the feedback gain matrix can be attained as

$$K = [1, 1.41, 0]. \quad (4.36)$$

As is shown in Figure 4.3, individual opinions achieve asymptotically polarization wherein the steady-state opinions on the second and third issues are non-stationary, but they are stationary on the first issue. In this case, the bipartition of opinions and the network topology is consistent, i.e., nodes 1, 2, and 3 hold the same opinions towards three different subtopics and their opinions are opposite to the ones held by nodes 4, 5, and 6 towards each subtopics, respectively.

Theorem 8 implies that there could exist the case when the inconsistency happen, i.e., opinion polarization is achieved but the individuals in the same camp do not reach an agreement. The following simulation serves as an explanatory example. Consider the 4-node QSC and SB network in Figure 4.4. The weighted adjacency matrix reads

$$W = \begin{bmatrix} 0 & 0 & -0.7 & 0.3 \\ -0.1 & 0 & 0 & -1 \\ -1 & 0 & 0 & -0.1 \\ 0 & -1 & -0.09 & 0 \end{bmatrix}. \quad (4.37)$$

Let the homogeneous opinion dynamics described by the pair (A, B) as

$$A = \begin{bmatrix} -4 & 1 \\ -1 & -4 \end{bmatrix} \text{ and } B = 1. \quad (4.38)$$

By selecting the feedback gain matrix as

$$K = \begin{bmatrix} -2 & 0 \\ 0 & -2 \end{bmatrix}, \quad (4.39)$$

we can attain the opinion dynamics shown in Figure 4.5. It manifests that node 1 and 3 reaches an agreement and their opinions towards two subtopics are opposite to the ones of node 2 and 4. However, as is shown in Figure 4.4, node 1 and 4 are in the same camp while node 2 and 3 are in the other. Notice that the Lagrangian of the network in Figure 4.4 possesses two eigenvector with entries all in $\{\pm 1\}$. To be specific, these two eigen-pairs are $(0, [1, -1, -1, 1]^T)$ and $(2, [1, -1, 1, -1]^T)$. It yields that α in this case can be chosen as 0 or 2. If $\alpha = 0$, neutralization will be achieved since A is Hurwitz. By choosing K in (4.39), the limit behavior of the dynamics is governed by $(A - 2BK)$, whose eigenvalues are $\pm i$. To this end, oscillation occurs in Figure 4.5. Furthermore, the opinion polarization is characterized

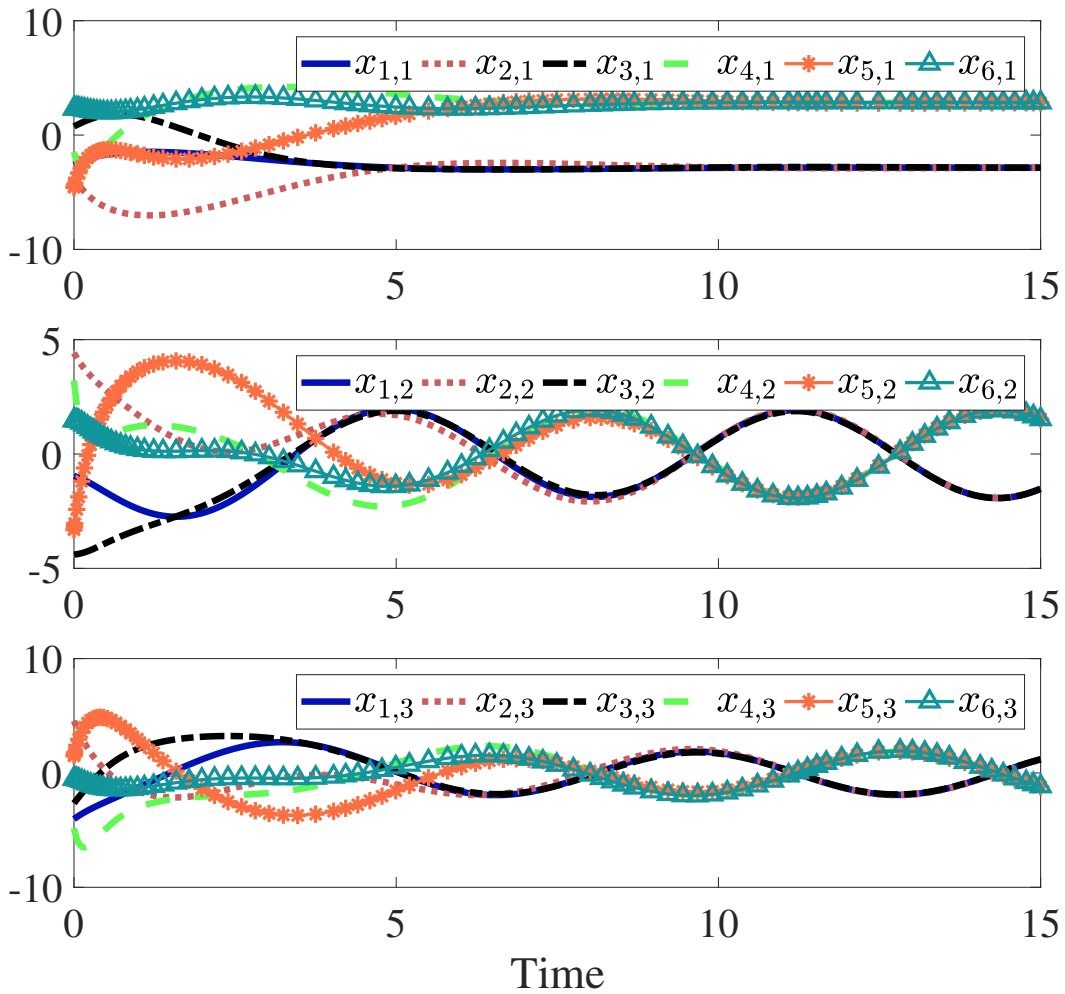


Figure 4.3.: Polarization of homogeneous opinion dynamics

by the signs of the entries of the eigenvector $[1, -1, 1, -1]^T$, i.e., node 1 and 3 shares the same opinion as well as node 2 and 4.

As is mentioned in the discussion of Theorem 8, structural balance is not a necessary condition for bipartite consensus. Here an example is provided. As is presented in Figure 4.6, this communication network is QSC but not SB. Hence, the adjacency matrix reads

$$W = \begin{bmatrix} 0 & 0 & 0.1 & 0.25 \\ -1 & 0 & -0.03 & 0.07 \\ 0.1 & 0 & 0 & -1 \\ 0 & 0.1 & -1 & 0 \end{bmatrix}. \quad (4.40)$$

Let the homogeneous opinion dynamics described by the pair (A, B) as

$$A = \begin{bmatrix} 0.2 & -1 \\ 1 & 0.2 \end{bmatrix} \text{ and } B = \begin{bmatrix} 1 & 0 \\ 0 & 1 \end{bmatrix}. \quad (4.41)$$

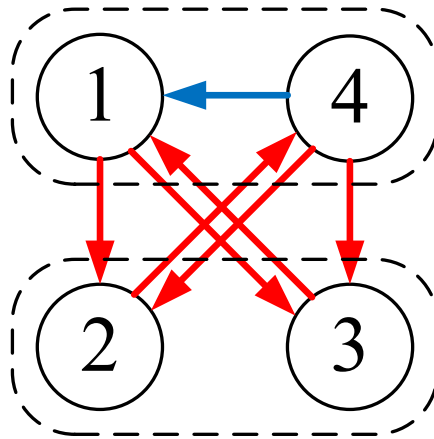


Figure 4.4.: A network topology on which the opinion dynamics can achieve inconsistent polarization

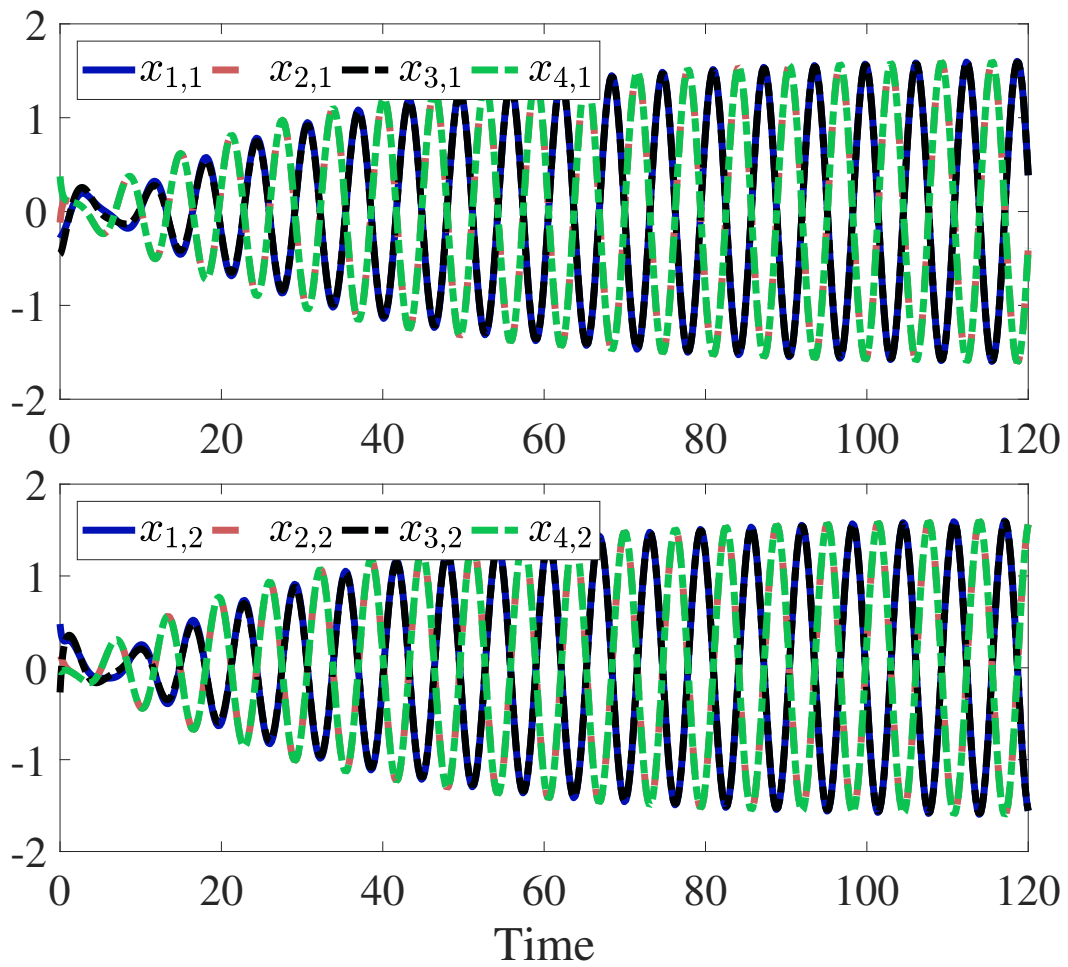


Figure 4.5.: Polarization can be inconsistent with structural bipartition in homogeneous opinion dynamics

By selecting the feedback gain matrix as

$$K = \begin{bmatrix} 1 & 0 \\ 0 & 1 \end{bmatrix}, \quad (4.42)$$

the opinions over time is shown in Figure 4.7. Apparently, polarization is achieved and nodes 1 and 4 are in a camp while node 2 and 3 in the other, although the communication topology is not SB. In this case, $\alpha = 0.2$ and the corresponding eigenvector of L at α is $[1, -1, -1, 1]^T$.

Both of the simulations on inconsistent polarization and polarization on structurally unbalanced graph infers that the eigen-pair (α, \bar{d}) where $\text{diag}(\bar{d}) \in \mathcal{D}$, but not structural balance, plays the key role in the bipartite consensus phenomenon. Hence, further inspections on the eigenvalues and eigenvectors of $I \otimes A - BK \otimes L$ is needed to provide precise results on the analysis of the closed-loop system.

Finally, by adding an edge of weight +1 from node 4 to node 1 in Figure 4.2, a structurally unbalanced graph with no in-isolated SB subgraphs is obtained. For a homogeneous opinion dynamics described by the pair (A, B) given in (4.35) and the same feedback gain matrix K in (4.36), the public opinions become neutral asymptotically in Figure 4.8.

4.3 Modulus Consensusability of Heterogeneous Opinion Dynamics on Coopetive Networks

In the real world, individuals even living in the same house may be tremendously different in educational background, life history, personal preference, etc., and all these discrepancies, in turn, influence the decision-making of each agent. Therefore, heterogeneity is of great significance and necessity in practice.

4.3.1 Problem Formulation

With the illustration of individual heterogeneity in mind, we consider the following dynamics for the opinion-forming process,

$$\dot{x}_i(t) = A_i x_i(t) + B_i u_i(t), \quad i \in \mathcal{V}, \quad (4.43)$$

where $A_i \in \mathbb{R}^{n \times n}$ and $B_i \in \mathbb{R}^{n \times m}$ are system and input matrices, respectively. Correspondingly, the feedback control is chosen as

$$u_i(t) = -K_i \sum_{(j,i) \in \mathcal{E}} |w_{ij}| (x_i(t) - \text{sgn}(w_{ij}) x_j), \quad \forall i \in \mathcal{V}, \quad (4.44)$$

and the admissible protocol set in the heterogeneous case becomes

$$\begin{aligned} \widehat{\mathcal{U}} = \{u(t) \in \mathbb{R}^{mN} \mid u_i(t) = -K_i \sum_{j=1}^N |w_{ij}| (x_i - \text{sgn}(w_{ij}) x_j), \\ \forall t > 0, K_i \in \mathbb{R}^{m \times n}, i = 1, \dots, N\}. \end{aligned} \quad (4.45)$$

Aside from the same social interpretations as in the homogeneous setting, the subscripts associated to the matrices A_i , B_i and K_i emphasize individual diversity. The compact form of the closed-loop system (4.43) reads

$$\dot{x}(t) = [\mathbf{A} - \mathbf{B}(L \otimes I_n)]x(t), \quad (4.46)$$

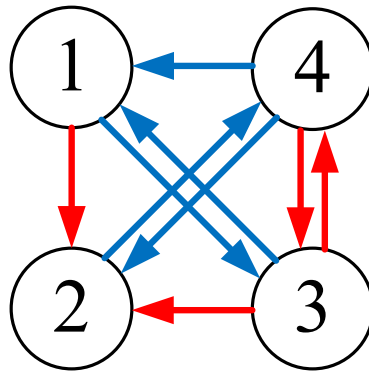


Figure 4.6.: A structurally unbalanced graph on which the opinion dynamics is polarizable

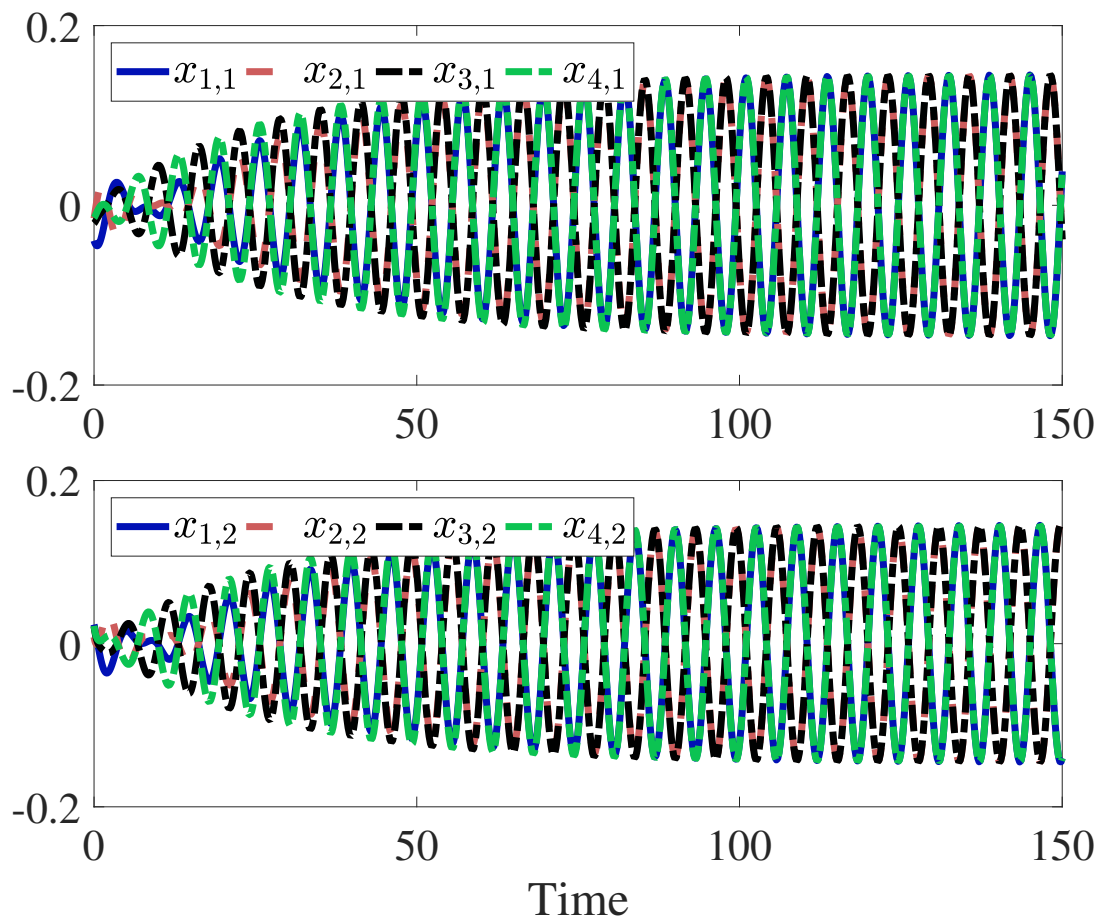


Figure 4.7.: Polarization of homogeneous opinion dynamics on a structurally unbalanced graph

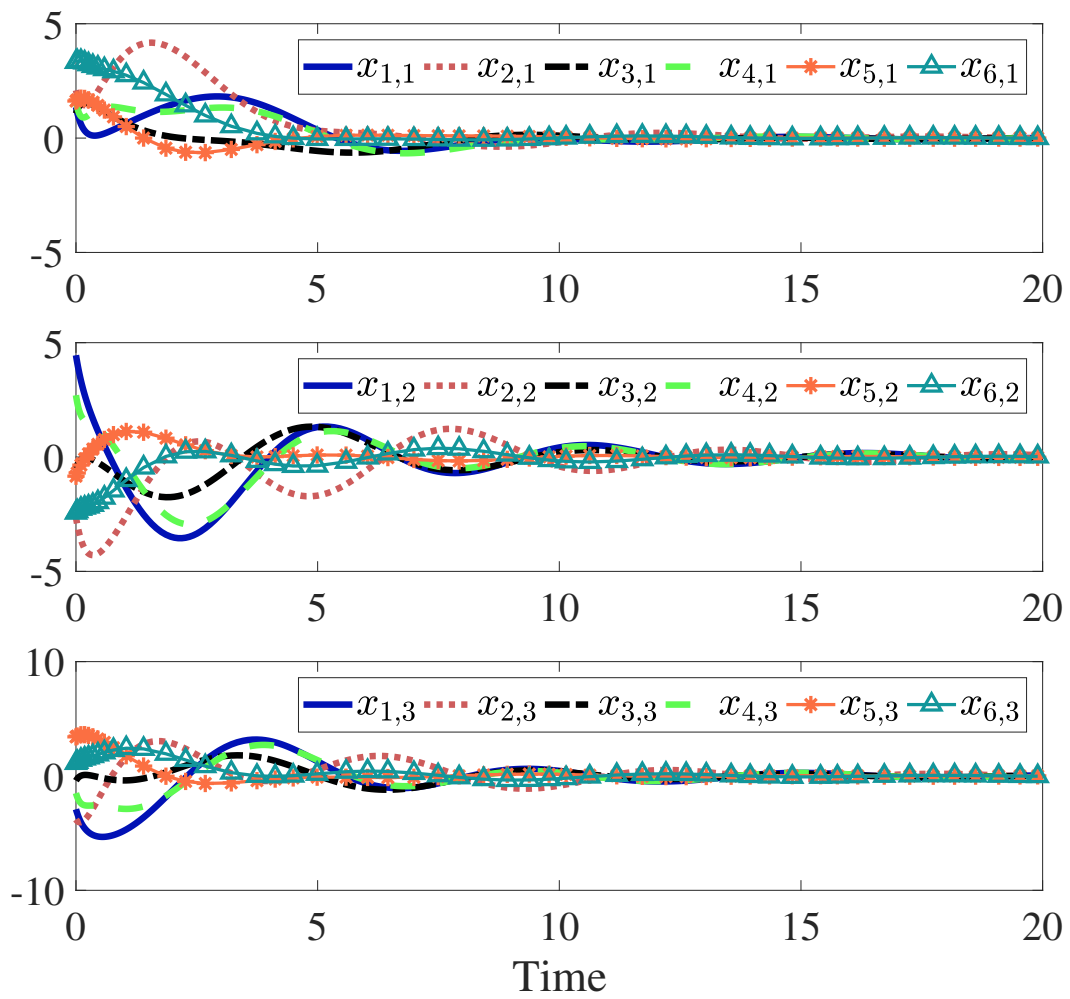


Figure 4.8.: Neutralization of homogeneous opinion dynamics

where $\mathbf{A} = \text{diag}(A_1, \dots, A_N)$ and $\mathbf{B} = \text{diag}(B_1K_1, \dots, B_NK_N)$. We then address the problem: Under which conditions there exist a series of K_i such that the heterogeneous opinion dynamics (4.43) is polarizable, consensusable and neutralizable with the opinion protocol in $\tilde{\mathcal{U}}$.

4.3.2 Bipartite Consensusability of Opinion Dynamics

Although the involvement of system heterogeneity in opinion formation opens up the possibility of richer social psychological findings, considerable challenges arise naturally in their theoretical and empirical exploration. As a starting point, we study the necessary conditions for bipartite consensusability of heterogeneous dynamics. To save cliché, we assume that (A_i, B_i) of the individual systems is stabilizable for $i = 1, \dots, N$.

Theorem 11. *Let the relation (4.27) hold. The stabilizable systems (4.43) evolving on a SB graph \mathcal{G} is bipartite consensusable w.r.t. $\tilde{\mathcal{U}}$, only if both of the following conditions are satisfied:*

- i). \mathcal{G} is quasi-strongly connected.
- ii). There exist a positive integer $q \leq n$, a sequence of matrices $\mathcal{Q}_i \in \mathbb{R}^{n \times q}$ of full column rank and a diagonalizable matrix $\mathcal{S} \in \mathbb{R}^{q \times q}$ satisfying $\text{sp}\{\mathcal{S}\} \in \imath\mathbb{R}$ such that

$$A_i \mathcal{Q}_i = \mathcal{Q}_i \mathcal{S}, \quad \forall i \in \mathcal{V}. \quad (4.47)$$

Proof. The proof of condition i) is an immediate result of Theorem 8.

As for condition ii), the bipartite consensusability of systems (4.43) amounts to the accessibility of the following systems to consensus,

$$\dot{\tilde{x}}(t) = [\mathbf{A} - \mathbf{B}(\bar{L} \otimes I_n)]\tilde{x}(t), \quad (4.48)$$

where $\tilde{x} = [\tilde{x}_1^\top, \dots, \tilde{x}_N^\top]^\top$ with $\tilde{x}_i = \rho_i x_i$. The matrix \bar{L} is defined in (4.31) and is, thanks to the implication $\rho_i \rho_j w_{ij} = d_i d_j w_{ij}$ in (4.27), the Laplacian matrix of the unsigned graph associated to \mathcal{G} . Therefore, the dynamics (4.48) achieving consensus $\lim_{t \rightarrow \infty} \tilde{x}_i - \tilde{x}_j = 0$ for all $i, j \in \mathcal{V}$ infers the existence of an asymptotically attractive invariant subspace $\tilde{\mathbb{X}}$ on which $\tilde{x}_i = \tilde{x}_j$. By noticing $\mathbb{1} \subseteq \ker \bar{L}$, the dynamical behavior of the closed-loop system (4.48) on $\tilde{\mathbb{X}}$ is governed by the dynamics $\dot{\tilde{x}}(t) = \mathbf{A}\tilde{x}(t)$. The requirement that the uniformly bounded \tilde{x}_i has no asymptotically stable equilibrium set, allows $\tilde{\mathbb{X}}$ to contain marginally stable modes with dimension $q \in \mathbb{N}_{>0}$ and $q \leq n$. Especially, one can construct a diagonalizable matrix $\mathcal{S} \in \mathbb{R}^{q \times q}$ which possesses q marginally stable eigenvalues and a block matrix $\mathbf{Q} := [\mathcal{Q}_1^\top, \dots, \mathcal{Q}_N^\top]^\top \in \mathbb{R}^{nN \times q}$ whose columns span the subspace $\tilde{\mathbb{X}}$, such that $\mathbf{A}\mathbf{Q} = \mathbf{Q}\mathcal{S}$ from which the equalities (4.47) emerge and $\text{sp}\{\mathcal{S}\} \subset \imath\mathbb{R}$ can be inferred. \square

It should be emphasized that $\text{sp}\{\mathcal{S}\} \subseteq \bigcap_{i \in \mathcal{V}} \{ \text{sp}\{A_i\} \cap \imath\mathbb{R} \}$, which implies matrix \mathcal{S} lumps together some (or all) of those marginally stable modes that individual system matrices commonly share. In other words, the existence of one or more common pure imaginary eigenvalues in the spectrum of matrix A_i is essentially important to bipartite consensusability of opinion dynamics. This finding is reminiscent of the real-life situation that certain basic social norms serve a baseline to reach an opinion consensus among diverse social actors.

Note that the statements shown in Theorem 11 are a necessary but not sufficient condition. This is because, for example, when A_i for all $i \in \mathcal{V}$ share a common eigenvalue λ_c which associates with an identical eigenspace, i.e., there exists $\mu \in \mathbb{R}^n \setminus \{0\}$ such that $A_i\mu = \lambda_c\mu$, then one can obtain

$$(\mathbf{A} - \mathbf{B}(\bar{L} \otimes I_n))\boldsymbol{\mu} = \mathbf{A}\boldsymbol{\mu} - \mathbf{B}(\bar{L} \otimes I_n)(\mathbf{1}_N \otimes \mu) = \lambda_c\boldsymbol{\mu}, \quad (4.49)$$

where $\boldsymbol{\mu} = [\mu^\top, \dots, \mu^\top]^\top \in \mathbb{R}^{nN}$. Thus, λ_c is an eigenvalue of the system matrix of the dynamics (4.48) with corresponding eigenvector $\boldsymbol{\mu}$. That is to say, the mode associated with λ_c would appear in the solution of equation (4.48). If λ_c is a defective pure imaginary eigenvalue or $\lambda_c \in \mathbb{C}_{>0}$, individual opinions may not converge to bipartite consensus, even go to infinity.

To avoid the occurrence of these undesired scenarios, we impose some specifications on the system matrix A_i and then provide sufficient conditions for bipartite consensusability of heterogeneous opinion dynamics.

Theorem 12. *Consider the stabilizable system (4.43) with non-zero initial conditions forming opinions on a graph $\mathcal{G} = (\mathcal{V}, \mathcal{E}, W)$. Suppose A_i satisfies the similarity transformation*

$$T_i^{-1}A_iT_i = \text{diag}(S, \hat{S}, J_i), \quad \forall i \in \mathcal{V}, \quad (4.50)$$

where $S \in \mathbb{R}^{k \times k}$ and $\hat{S} \in \mathbb{R}^{(q-k) \times (q-k)}$ with positive integers k and q satisfying $k \leq q \leq n$ and $\mathcal{S} := \text{diag}(S, \hat{S}) \in \mathbb{R}^{q \times q}$ is a diagonalizable matrix in real Jordan normal form satisfying $\text{sp}\{\mathcal{S}\} \subseteq i\mathbb{R}$; $J_i \in \mathbb{R}^{(n-q) \times (n-q)}$ is a stable matrix. Moreover, $T_i := [Q, Q_i, P_i] \in \mathbb{R}^{n \times n}$ is a nonsingular matrix wherein $Q_i := [Q, Q_i] \in \mathbb{R}^{n \times q}$ of full column rank with $Q \in \mathbb{R}^{n \times k}$ and $Q_i \in \mathbb{R}^{n \times (q-k)}$ and $P_i \in \mathbb{R}^{n \times (n-q)}$.

If the following conditions hold,

i). \mathcal{G} is structurally balanced and quasi-strongly connected.

ii). Matrix Ξ is Hurwitz, where

$$\begin{aligned} \Xi = \text{diag}(J_1, A_2, \dots, A_N) - & \begin{bmatrix} [O \ I_{n-q}]T_1^{-1} & O & \dots & O \\ -[Q_2 \ O]T_1^{-1} & I_n & \dots & O \\ \vdots & & \ddots & \\ -[Q_N \ O]T_1^{-1} & O & \dots & I_n \end{bmatrix} \\ & \times \mathbf{B}(\bar{L} \otimes I_n) \text{diag}(P_1, I_n, \dots, I_n), \end{aligned} \quad (4.51)$$

then the system (4.43) is bipartite consensusable w.r.t. \hat{U} . Moreover, the system (4.43) is consensusable if \mathcal{G} is an unsigned graph while polarizable if \mathcal{G} is a signed graph.

Proof. Since \mathcal{G} is SB, one can denote $\bar{x}_i(t) = d_i x_i(t)$ for all $i \in \mathcal{V}$, and obtain a closed-loop system as below

$$\dot{\bar{x}}_i(t) = A_i \bar{x}_i(t) - B_i K_i \sum_{j=1}^N \bar{w}_{ij} (\bar{x}_i(t) - \bar{x}_j(t)), \quad \forall i \in \mathcal{V}. \quad (4.52)$$

With the help of the notation $z_i := T_i^{-1} \bar{x}_i$ and the matrix transformation (4.50), it is not difficult to attain

$$\dot{z}_i = \text{diag}(S, J_i) z_i - T_i^{-1} B_i K_i \sum_{j=1}^N \bar{w}_{ij} (T_i z_i - T_j z_j), \quad \forall i \in \mathcal{V}. \quad (4.53)$$

For the convenience of further derivation, the following decompositions are needed

$$z_1(t) = \begin{bmatrix} z_{1q} \\ z_{1p} \end{bmatrix}, \quad T_i^{-1}B_iK_i = \begin{bmatrix} F_{iq} \\ F_{ip} \end{bmatrix}, \quad \forall i \in \mathcal{V}, \quad (4.54)$$

where $z_{1q}(t)$ and $z_{1p}(t)$ are the first q rows and the last $(n - q)$ rows of $z_1(t)$, respectively. F_{iq} and F_{ip} are analogously defined. After denoting $\hat{z}_i(t) := z_i(t) - [z_{1q}^\top(t), 0_p^\top]^\top$ and $e_i(t) = \sum_{j=1}^N \bar{w}_{ij}(\bar{x}_i(t) - \bar{x}_j(t))$, $\forall i \in \mathcal{V}$, the opinion dynamics (4.52) for $i = 2, 3, \dots, N$ can be rewritten as

$$\begin{aligned} \dot{z}_{1p}(t) &= J_1 z_{1p}(t) - F_{1p} e_1(t) \\ \dot{\hat{z}}_i(t) &= \text{diag}(\mathcal{S}, J_i) \hat{z}_i - \begin{bmatrix} F_{iq} \\ F_{ip} \end{bmatrix} e_i(t) + \begin{bmatrix} F_{1q} \\ O \end{bmatrix} e_1(t). \end{aligned} \quad (4.55)$$

Let $\zeta(t) := [z_{1p}^\top(t), \hat{z}_2^\top(t), \dots, \hat{z}_N^\top(t)]^\top$ to be the aggregation of variables. The compact form of (4.55) can be written as

$$\dot{\zeta}(t) = \hat{\Xi} \zeta(t), \quad (4.56)$$

where

$$\begin{aligned} \hat{\Xi} &= \text{diag}(J_1, \mathcal{S}, J_2, \dots, \mathcal{S}, J_N) \\ &- \begin{bmatrix} F_{1p} & O & \dots & O \\ -[F_{1q}^\top \ O]^\top & [F_{2q}^\top \ F_{2p}^\top]^\top & \dots & O \\ \vdots & \ddots & \ddots & \\ -[F_{1q}^\top \ O]^\top & O & \dots & [F_{Nq}^\top \ F_{Np}^\top]^\top \end{bmatrix} \\ &\times (\bar{L} \otimes I_n) \text{diag}(P_1, T_2, \dots, T_N). \end{aligned} \quad (4.57)$$

The observation that $\hat{\Xi}$ is similar to the Hurwitz matrix Ξ in condition ii) can be obtained from the transformation below

$$\Xi = \text{diag}(I_{n-q}, T_2, \dots, T_N) \hat{\Xi} \text{diag}(I_{n-q}, T_2^{-1}, \dots, T_N^{-1}), \quad (4.58)$$

which guarantees that $\hat{\Xi}$ is also Hurwitz and $\lim_{t \rightarrow \infty} \zeta(t) = \mathbf{0}$. Then the difference between \bar{x}_1 and \bar{x}_i , $i = 2, 3, \dots, N$ needs to be inspected and thus, we denote $\delta(t) = [\bar{x}_1^\top - \bar{x}_2^\top, \dots, \bar{x}_1^\top - \bar{x}_N^\top]^\top$ and one can obtain

$$\delta(t) = \Gamma \zeta(t), \quad (4.59)$$

where

$$\Gamma = \begin{bmatrix} P_1 & -T_2 & \dots & O \\ \vdots & & \ddots & \\ P_1 & O & \dots & -T_N \end{bmatrix}. \quad (4.60)$$

The asymptotic stability of (4.56) yields that $\lim_{t \rightarrow \infty} \delta(t) = \mathbf{0}$ in (4.59), which implies that (4.52) reaches consensus. Since the eigenvalues in $\text{sp}\{S\}$ have the same eigenspace Q , in reference to (4.49), one can explore $\text{sp}\{S\} \subseteq \text{sp}\{\mathbf{A} - \mathbf{B}(\bar{L} \otimes I_n)\}$. That is to say, the matrix $\mathbf{A} - \mathbf{B}(\bar{L} \otimes I_n)$ contains at least one eigenvalue on imaginary axis, which is commonly shared by all A_i with $i \in \mathcal{V}$. As the equation (4.50) stated that \mathcal{S} is a diagonalizable matrix with all eigenvalues on the imaginary axis and J_i is stable, we can further display that the matrix \mathbf{A} is marginally stable. Namely, for any non-zero initial conditions, the limit behavior of $\bar{x}_i(t)$ is bounded and does not converge to $\mathbf{0}$, $\forall i \in \mathcal{V}$. Finally, if $d_i = 1$, $\forall i \in \mathcal{V}$, which implies $\bar{L} = L$, the sufficient conditions for consensusability can be also derived. \square

4.3.3 Neutralizability of Opinion Dynamics

In the homogeneous case, we conclude that structural balance is an obstacle for public opinions to achieve neutralization. However, according to the compact form (4.46), the impact of L is extraordinarily weakened because of the diversity of A_i , B_i , and K_i . It implies that neutralization is much easier to establish in heterogeneous case. Here only a necessary condition is provided as an insight of the relation between neutralizability and network topology. Note that the assumption in the homogeneous case is then naturally extended as A_i is not Hurwitz for all $i \in \mathcal{V}$.

Theorem 13. *Consider a strongly connected signed graph $\mathcal{G} = (\mathcal{V}, \mathcal{E}, W)$ and the matrix transformation (4.50) holds. The stabilizable dynamics (4.43) is neutralizable w.r.t. \hat{U} only if \mathcal{G} is not structurally balanced.*

Proof. Taking the compact form of the heterogeneous opinion dynamics in (4.46) into consideration, one can obtain $\text{sp}\{\mathbf{A} - \mathbf{B}(L \otimes I_n)\} \in \mathbb{C}_{<0}$, if (4.43) is neutralized. Then we prove Theorem 13 by contradiction. If \mathcal{G} is SB, according to (4.49) and in conjugation with (4.50), the modes associated with the eigenvalues in \mathcal{S} appear in the solution of (4.46) which yields that neutralization is negated. Thus the opposite is true and we complete the proof. \square

Based on the above results and analysis, one may notice that the heterogeneity of the opinion dynamics and the weak reliability of neutralizability on network topology are the major reasons for incapability of forming valuable sufficient and necessary conditions. Intuitively, it is a primary requirement that the dynamics share some common eigenvalues to achieve modulus consensus, which is also true for bipartite consensus. However, neutralization is peculiar because the target is the origin which means that the common eigenvalues of all the agent dynamics are not necessary. Moreover, the diversity of parameter matrices in the dynamics leads to multitudes of ways to reach neutralization. As a consequence of the aforementioned facts, sufficient and necessary condition for modulus consensusability cannot be expected.

4.3.4 Numerical Experiments

In this subsection, several simulations serve to demonstrate the main results of the heterogeneous opinion dynamics over the same Figure 4.2. We consider the non-identical subsystems dynamics (4.43) whose state and input matrices are given respectively by

$$\begin{aligned}
 A_1 &= \begin{bmatrix} -0.5 & 0.25 & -0.5 \\ 0 & -1 & 0 \\ 0 & -0.5 & 0 \end{bmatrix}, & A_2 &= \begin{bmatrix} 0 & 0 & 0 \\ -2 & -1 & -2 \\ -2 & 0 & -2 \end{bmatrix}, \\
 A_3 &= \begin{bmatrix} 0 & 0 & 0 \\ 0 & -3 & 0 \\ -3.5 & -0.25 & -3.5 \end{bmatrix}, & A_4 &= \begin{bmatrix} -2 & 1 & -2 \\ 0 & -5 & 0 \\ 0 & -2.5 & 0 \end{bmatrix}, \\
 A_5 &= \begin{bmatrix} 0 & 0 & 0 \\ -13 & -1.5 & -13 \\ -8 & 0 & -8 \end{bmatrix}, & A_6 &= \begin{bmatrix} 0 & 0 & 0 \\ 0 & -1 & 0 \\ -3 & 1 & -3 \end{bmatrix}, \\
 B_1 &= [1, 2, 3]^T, & B_2 &= [-1, 3, 1]^T, & B_3 &= [1, 1, -7]^T, \\
 B_4 &= [1, -3, 1]^T, & B_5 &= [-2, 1, 1]^T, & B_6 &= [1, 1, -1]^T.
 \end{aligned} \tag{4.61}$$

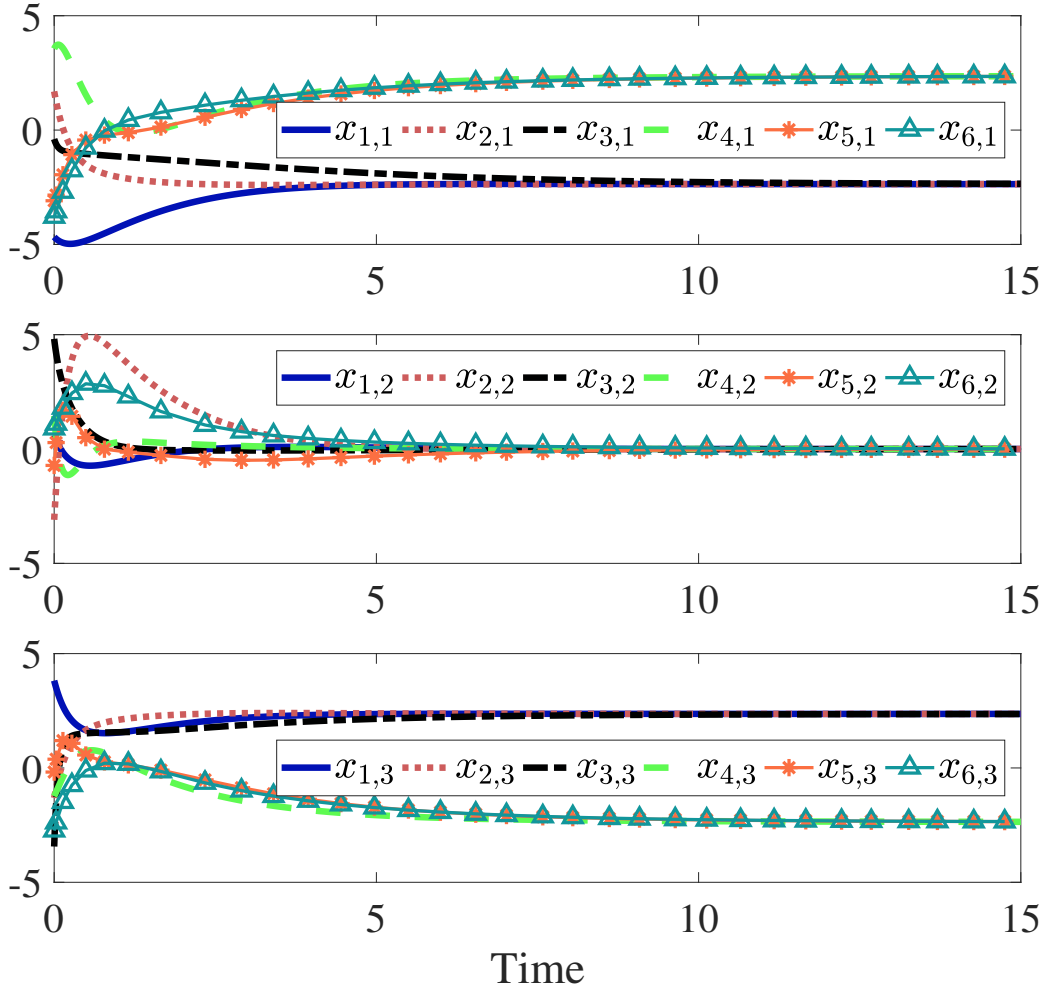


Figure 4.9.: Polarization of heterogeneous opinion dynamics

Note that A_i for $i = 1, \dots, 6$ shares the same marginally stable eigenvalue 0 w.r.t. the same eigenvector $[1, 0, -1]^T$ but possesses different stable eigenvalues. By choosing

$$\begin{aligned}
 K_1 &= [-0.1437, -0.0853, 1.2705], & K_2 &= [-1.2283, 0.4789, 0.1860], \\
 K_3 &= [0.8217, 0.0701, -0.5925], & K_4 &= [-0.1401, -0.7124, 1.2742], \\
 K_5 &= [-1.5199, 0.2548, -0.1057], & \text{and } K_6 &= [1.2190, 0.1231, -0.1952],
 \end{aligned} \tag{4.62}$$

the bipartite consensusability conditions of Theorem 12 are satisfied. It can be observed from Figure 4.9 that the opinions of individuals reach polarity on the first and third topics, while neutrality on the second topic, which is allowable from Definition 3.

Finally, after adding an edge of weight +1 from node 4 to node 1 in Figure 4.2, we obtain a structurally unbalanced graph which has no in-isolated SB subgraph and test the heterogeneous dynamics (4.61) on this modified network by choosing the same series of the feedback control gain matrices in (4.62). Figure 4.10 shows the opinion formation process of heterogeneous dynamics over such network achieves asymptotically neutralization.

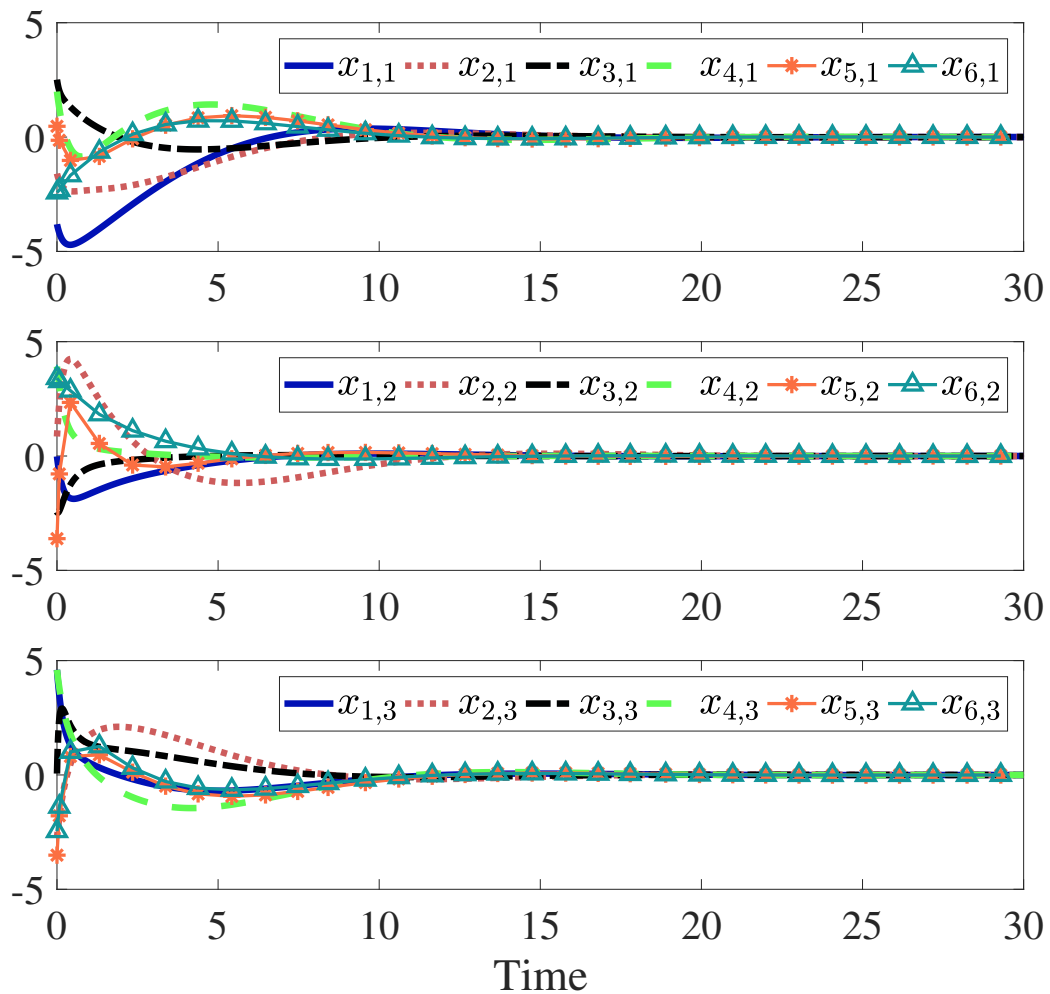


Figure 4.10.: Neutralization of heterogeneous opinion dynamics

4.4 Discussion

Opinion dynamics on social networks with cooperative (cooperative-competitive) interactions may result in polarity, consensus or neutrality under different opinion protocols. The antecedent of protocol design is to study the accessibility problem: whether or not there exist admissible control rules to polarize, consensus, or neutralize individual opinions in a large population. From an operational perspective, this chapter is aimed at the investigation of polarizability, consensusability, and neutralizability of opinion dynamics in question. Particular emphasis is on the joint impact of the dynamical properties of individuals and the interaction topology among them on polarizability, consensusability, and neutralizability, respectively. Sufficient and/or necessary conditions for those accessibility problems are provided by using powerful tools from spectral analysis and algebraic graph theory. To characterize the individual diversity in real life, we further investigate the solvability of opinion formation problems in heterogeneous systems with non-identical dynamics. Accordingly, sufficient and/or necessary criteria for heterogeneous network polarizability, consensusability,

and neutralizability are derived.

In Section 4.2, we provide the necessary conditions for stationary bipartite consensusability. The conditions for non-stationary bipartite consensusability, however, cannot be included in this result. If the non-stationary bipartite consensusability is achieved, there may exist no limit of individual opinion. Intuitively, the conditions given in Theorem 8 seem to be correct for this case, if the last part in condition ii) is replaced by “ $\text{sp}\{A - \alpha BK\} \cap \nu\mathbb{R}$ contains $\sigma\nu$, $\sigma \in \mathbb{R}$ ”. Although no simulation till now can serve as a counterexample for this result, rigorously prove is required to confirm this necessity condition.

We have to admit that the sufficient condition in Theorem 12 is not generally applicable due to the strict requirements on individual opinion dynamics and the network topology. However, bipartite consensusability w.r.t. the static protocol shows an interesting insight into the difficulty of individuals to (separately) reach an agreement. The heterogeneity rooted in different aspects, e.g., languages, ages, genders, political beliefs, is the major obstacle. Alternatively, dynamic protocols based on self-learning are more promising for bipartite consensusability of heterogeneous opinion dynamics, which will be our future work. It is worth pointing out that consistent polarization and structural balance are listed as prior conditions in Theorem 11 and Theorem 12, respectively. As is discussed in Section 4.2, these two conditions do not play dominant role for homogeneous opinion dynamics, let alone for heterogeneous. Whereas, they are adopted because they are commonly accepted and existed in the real life.

Besides, the opinion dynamics considered in this chapter is a linear system. In [47], the nonlinear dynamics is considered. However, the neutralization case, which is of significant social meaning, is not separately analyzed. It is still open problem on how to distinguish the neutralization situation from general consensus in the nonlinear opinion dynamics on coopetitive networks.

Furthermore, in this chapter, we only consider the opinion dynamics on fixed social networks. A naturally extension is to take into account non-fixed networks. This is inspired by [48] and [120], where the Altafini’s model has been considered on time-varying networks and switching networks, respectively. As another trend in the field of opinion dynamics, the opinions between individuals are considered to influence the social ties. Related works can be referred to in [121]. Thus the opinion dynamics is changed from the dynamics on networks to the dynamics of networks and their interactions.

Conclusions and Outlook

5.1 Conclusions

In this dissertation, we inspect the dynamical processes on social networks focusing on the modeling, analysis, and control problems. Here we conclude this dissertation by chapters.

In Chapter 2, the information diffusion processes are well modeled as epidemics spreading on social networks by using the mean-field approximation for the Markov chain. Focusing on information diffusion processes in heterogeneous networks, the node-based susceptible-infected-recovered/removed-susceptible (SIRS) model is introduced. Under different conditions, the node-based SIRS model could possess different equilibria, i.e., the disease-free equilibrium and the endemic equilibrium. Specifically, the existence and stability of both the equilibria are analyzed. The procured results emphasize the importance of both the transition rates of the information diffusion process and network connection. We then extend the information epidemics into multi-layer networks and propose the heterogeneous discrete-time susceptible-infected-susceptible (SIS) model for multiple information spreading. The existence, uniqueness, and stability of the equilibria are highly dependent with the transition rates, communication topology, and the sampling period.

In Chapter 3, an optimal control framework by interacting with the infection rate is proposed, following which two scenarios, i.e., to impede rumor spreading and to enhance the diffusion in marketing or campaign, are separately described. The solutions to the optimal control problems are proved to be existed and obtained by Pontryagin Maximum Principle. Forward-backward sweep algorithm and `fmincon` are used to get the solution numerically. Furthermore, for the first time, the effects of natural uncertainties of the transition rates are considered to determine a robust optimal control strategy. A numerical solution is obtained based on distribution analysis. The diffusion is maximized in finite horizon with the proposed control strategy allowing for the constraint of limited budget. The proposed algorithm, which combines the forward backward sweep method and the secant method, shows its effectiveness and efficiency in dealing with the diffusion processes over real networks. The numerical experiments on the influence of parameters confirm the common sense that the more budget the better dissemination performance. Apart from that, it is of great significance to properly weigh the impact of the noise while utilizing the proposed approach. The addressed formulation and the proposed optimal strategy not only solve the specific problem caused by the noisy transition rates but also provide a general solution to social networks with stochastic perturbations.

In Chapter 4, we investigate modulus consensusability (polarizability, consensusability, and neutralizability) of opinion-forming protocols in cooperative networks. Criteria to test those accessibility-like issues in terms of sufficient and/or necessary conditions are our major contributions. Specifically, the joint effect of the algebraic constraints of the system dynamics and topological properties of the interaction structure is underlined in the examination of modulus consensusability. Different from sufficient conditions, we demonstrate that the structural balance of quasi-strongly connected social networks is not necessary for polarizability. With the emphasis on the individual heterogeneity, the investigation of modulus consensusability of systems with non-identical dynamics displays that the existence of commonality in eigenvalues and eigenvectors of system dynamics is of central importance to develop consensus and polarization protocol.

5.2 Outlook

The topic inspected in this dissertation is giant, highly interdisciplinary, and of broad extensions. There remain variant future works and open problems to be investigated. Thus we list several potential interesting fields for the dynamical processes on social networks.

Modeling and Analysis of Information Epidemics

- i) General epidemics model. Although there exist many different kinds of epidemics models, no general one has been reported in literature. Very recently the generalized susceptible-exposed-infected-vigilant (G-SEIV) model paves the way to this target. However, to develop a generic model that covers all the possible compartments, as well as the time-varying network topology, and the potential noise, is still an open problem.
- ii) The stability of the endemic equilibrium of the node-based SIRS model and the discrete-time SIS model. In Chapter 2, we provide two conjectures on these two problems and support them by simulation, respectively. The precise and rigorous proofs are left for the future work.
- iii) Computationally cheap algorithms to check the existence, uniqueness, and stability of the DFE and endemic equilibrium. In the conditions obtained in In Chapter 2, the eigenvalues of an N -dimensional matrix need to be calculated. For large scale networks, this result cannot be expected due to high computation cost. An attractive idea is to develop fast algorithms taking into consideration the network structure. The sparseness and connectivity properties may be of great significance.

Control Design for Information Epidemics

- i) Distributed control algorithms for information diffusion processes. In Chapter 3, we proposed the optimal control and the robust optimal control algorithms for the information epidemics. It is actually centralized control but not in a distributed manner. For general case when only limited access is possible, the distributed control algorithms should be considered, which is also naturally suitable for large scale social networks. The algorithms for the consensus problem of multi-agent systems may provide a hint for the control of information diffusion processes.

- ii) Effectiveness of the proposed algorithms in the Markov chain models. In this chapter, the control rules are directly designed for the node-based models. Although the node-based models can well approximate the performance of the Markov chain models, the error between them may be the effectiveness of the proposed control law. However, the difficulty of conducting the comparisons lies in the simulation of the Markov chain model with huge amount of states. Alternatively, this issue may be tackled by using the Monte Carlo simulation. The Monte Carlo simulation, however, takes long period of time as a trade-off to make the simulation possible for large scale networks. Apart from the comparison, to directly control the Markov chain model is of great interests since precisely the node-based models are the approximations of the Markov chain model. The challenges arising from designing such control law are the massive computation burden due to large scale social networks, the rigorous proof to guarantee the optimality, and the method to conduct (numerical) experiments implementing the control.
- iii) Control design for the node-based models with stochastic noise. In Section 3.2, we deal with the deterministic disturbances and propose the robust optimal control. Whereas, taking into consideration the randomness in spreading processes, the impacts of the stochastic noise needs to be investigated.
- iv) Control design for multi-layer multiple information epidemics. In this chapter, we only focus on the control of single-layer single information epidemics. Bearing in mind the single dominant information equilibrium of the multi-layer multiple SIS model in Section 2.3, a promising extension is to design an optimal strategy for certain propagator such that his/her information can be dominant.

Opinion Dynamics

- i) General opinion dynamic model and validating experiments. As is discussed in Chapter 1, opinion dynamic models are mainly in three categories. General model of social influence is needed to understand the fundamental mechanisms of the change of opinions. Furthermore, most existing opinion dynamic models have not been tested by real experiments. The validation of these models is essential and may also lead to new theory to build more general models.
- ii) Evolution of social ties. Instead of the prior given social networks, individuals may form their own social ties in a group. The appraisals between each pair of individuals thus play an important role in this process. Compared with opinion dynamics, which is the dynamics of nodes in graphs, the dynamics of appraisals is the dynamics of edges. Furthermore, the appraisals, in turn, can influence the individual's opinion. To this end, there exists an interplay between dynamics on networks and the dynamic of networks. They are still open problems to model, analyze, and control this interplay model.
- iii) Extracting opinion values from accessible information. In the study of the opinion dynamic models, the opinions are considered as exact numbers. However, in real word, to obtain the accurate opinion values seems to be impossible. Common ways to collect public opinions, e.g., questionnaires and customer reviews, may only need

to an approximation of the true opinion. Sentiment analysis should be introduced in combination of opinion dynamics to better understanding the opinion forming and updating process.

- iv) Local rule-global emergent properties (LrGep). On social networks, an interesting phenomenon is that a certain local rule or protocol may result in global emergence, e.g., the opinion consensus or polarization. Why this kind of emergence is possible and how to design the local rule to achieve desired global emergence are attractive topics to be solved. Possible frameworks may be the social influence theory and the evolutionary game theory.

Graph Theory

The major focus of this dissertation is on the dynamical processes on social networks. Thus how to model the social networks is a fundamental problem. Mathematically, graphs are commonly used to describe the structure of the networks where the agents and their relation are abstracted as vertices and edges. The elementary graph theory that is used in this dissertation is introduced.

A.1 Unsigned Graphs

A graph \mathcal{G} is made up of *vertices (nodes)* and *edges (links, arcs)*. We denote the set of labeled vertices as $\mathcal{V} = \{1, 2, \dots, N\}$ and the set of edges as $\mathcal{E} \subseteq \mathcal{V} \times \mathcal{V}$. $\mathcal{G}_s(\mathcal{V}_s, \mathcal{E}_s)$ is a subgraph of \mathcal{G} if $\mathcal{V}_s \subseteq \mathcal{V}$ and $\mathcal{E}_s \subseteq (\mathcal{V}_s \times \mathcal{V}_s) \cap \mathcal{E}$. To avoid ambiguity, the terms *vertex*, *node*, *individual*, and *agent* are interchangeably used in this dissertation. The graph \mathcal{G} is an *undirected* graph if for any edge $(v_i, v_j) \in \mathcal{E}$ there exist an edge $(v_j, v_i) \in \mathcal{E}$, $i, j \in \mathcal{V}$; otherwise, a *directed* graph (*digraph*).

Weights can be assigned to each edge to form a *weighted graph*. Thus an adjacency matrix $W = [w_{ij}] \in \mathbb{R}^{N \times N}$ is obtained. $w_{ij} \neq 0$ if and only if $(v_j, v_i) \in \mathcal{E}$. The graph \mathcal{G} is called an unsigned graph if and only if $w_{ij} \geq 0$ for all $i, j \in \mathcal{V}$. The *Lagrangian* of an unsigned graph is defined as follows

$$\bar{L} = [l_{ij}]_{N \times N}, \quad l_{ij} = \begin{cases} \sum_{k=1}^N w_{ik}, & i = j, \\ -w_{ij}, & i \neq j. \end{cases} \quad (\text{A.1})$$

The spectrum of \bar{L} satisfied the following lemma. There holds $\text{sp}\{\bar{L}\} \in \mathbb{C}_{\geq 0}$ [116].

A weighted graph is said to be directed if there exist some $i, j \in \mathcal{V}$ such that $w_{ij} \neq w_{ji}$. Weighted digraphs are commonly adopted in social network models because of the fact that it characterizes a significant feature: asymmetry. On one hand, the connection between people are not always bidirectional, especially in online social networks. This phenomenon is named as asymmetric follow referring to the fact that many people follow an individual or account without having to follow them back. On the other hand, the influence between a pair of social neighbors is generally different, which may lead to the study of social power.

Apart from the direction and weight of the links, the connectivity of the graph is of great importance. The basic concept, *path*, e.g. from vertex i_0 to i_n , is defined as a series of vertices $i_0, i_1, i_2, \dots, i_n$, $n \in \mathbb{N}^+$ such that $(i_j, i_{j+1}) \in \mathcal{E}$, $j = 0, 1, \dots, n-1$. A digraph is said to be *quasi-strongly connected* (QSC) if there exists one node (*root*) which possesses paths to all

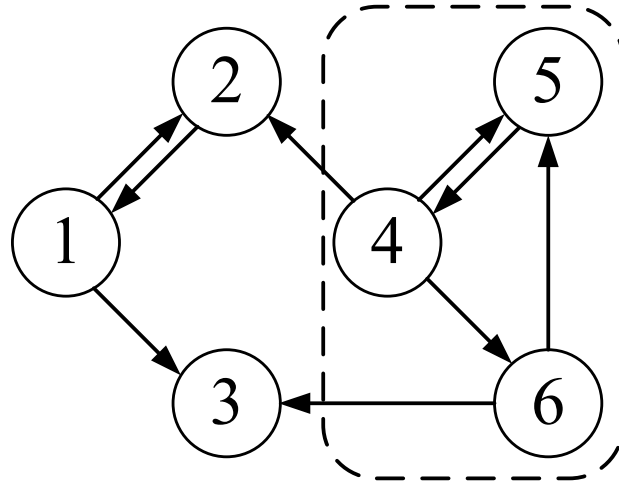


Figure A.1.: A graph with in-isolated subgraphs

other nodes in this graph. Moreover, if each node is a root, the digraph is *strongly connected* (SC). Any SC graph is QSC and a graph is QSC if and only if it contains a spanning tree. As is shown in Figure A.2, it is evident that every node is a root in Figure A.2a while only node 1 is a root in Figure A.2b. From the algebraic point of view, we have the following lemmas.

Lemma 13. *A graph \mathcal{G} with adjacency matrix W is SC if and only if W is irreducible.*

Lemma 14. [116] *Given an unsigned graph \mathcal{G} with Lagrangian \bar{L} , the zero eigenvalue of \bar{L} is simple and $\text{Re}\lambda > 0$ for all $\lambda \in \text{sp}\{\bar{L}\} \setminus \{0\}$ if and only if \mathcal{G} is QSC.*

The proofs are saved for triviality. The structure of the Lagrangian of a QSC graph is characterized by the following lemma.

Lemma 15. [122], [123] *Given a QSC graph \mathcal{G} with Lagrangian \bar{L} , there exists a vertex permutation such that \bar{L} is transformed to the Frobenius normal form*

$$\bar{L} = \begin{bmatrix} \bar{L}_{11} & O & \cdots & O \\ \bar{L}_{21} & \bar{L}_{22} & \cdots & O \\ \vdots & \vdots & \ddots & \vdots \\ \bar{L}_{m1} & \bar{L}_{m2} & \cdots & \bar{L}_{mm} \end{bmatrix}, \quad (\text{A.2})$$

where $\bar{L}_{ii}, i = 1, \dots, m - 1, m \leq N$ are irreducible square matrices, each \bar{L}_{ii} has at least one row with positive row sum, and \bar{L}_{mm} is irreducible or a scalar zero.

A subgraph is *in-isolated* if there exist no edges from outside of itself.

In Chapter 2, we confine ourselves to consider only unsigned graphs.

A.2 Signed Graphs

In social relations, there exist not only cooperation but also competition. Taking into this phenomenon into consideration, the signed graphs are introduced.

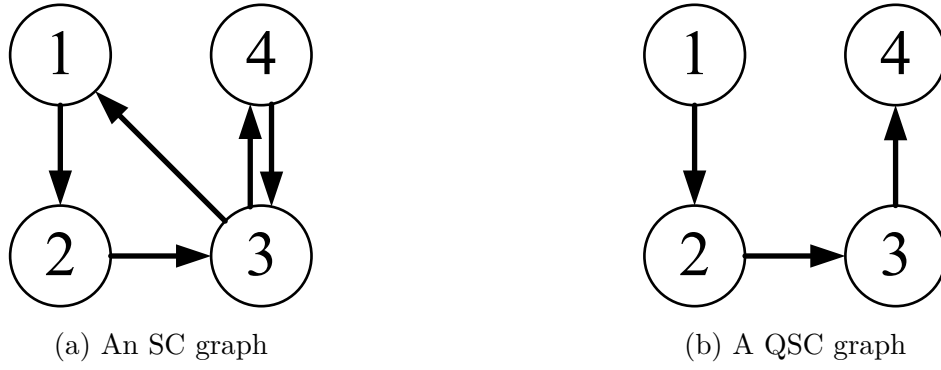


Figure A.2.: Examples of SC and QSC graphs

A weighted signed digraph \mathcal{G} is described as a triple $(\mathcal{V}, \mathcal{E}, W)$, where $\mathcal{V} = \{1, 2, \dots, N\}$, $\mathcal{E} \subseteq \mathcal{V} \times \mathcal{V}$ and $W = [w_{ij}] \in \mathbb{R}^{N \times N}$ are the set of vertices, the set of edges and the weighted adjacency matrix, respectively. For any entry of W , $w_{ij} \neq 0$ if and only if there exists a link from j to i . Furthermore, $w_{ij} > 0$ indicates that j is cooperative with i , while $w_{ij} < 0$ means that j is competitive towards i . We call \mathcal{G} a signed graph if at least one of the entries of W is negative; otherwise, \mathcal{G} is unsigned. The associated unsigned graph of signed graph $\mathcal{G} = (\mathcal{V}, \mathcal{E}, W)$ is denoted as $\bar{\mathcal{G}} = (\mathcal{V}, \mathcal{E}, \bar{W})$. They possess the same sets of nodes and links, respectively, while $\bar{W} = [\bar{w}_{ij}] \in \mathbb{R}^{N \times N}$ is formed by $|w_{ij}|, \forall i, j \in \mathcal{V}$ at each entry. Two fundamental assumptions about the signed graphs in this dissertation are as follows.

Assumption 4. *There exist no self-loops, i.e., $w_{ii} = 0, \forall i \in \mathcal{V}$.*

Assumption 5. *The graphs are digon sign-symmetric, i.e., $w_{ij}w_{ji} \geq 0, \forall i, j \in \mathcal{V}$.*

Assumption 1 implies that there is no self influence in the communication graph. Assumption 2 is based on the common sense that in most circumstances it may not happen that agent i treats j as a friend while j treats i as a foe.

The connectivity of a digraph \mathcal{G} is of great significance in the analysis of network-based dynamics. A subgraph of $\mathcal{G} = (\mathcal{V}, \mathcal{E}, W)$ is a graph formed from subsets of \mathcal{V} , \mathcal{E} and the associated weights in W .

For the subsequent analysis, the *Laplacian matrix* of $\mathcal{G} = (\mathcal{V}, \mathcal{E}, W)$ is introduced as

$$L = [l_{ij}]_{N \times N}, \quad l_{ij} = \begin{cases} \sum_{k=1}^N |w_{ik}|, & i = j, \\ -w_{ij}, & i \neq j. \end{cases} \quad (\text{A.3})$$

Analogously, \bar{L} is denoted as the Laplacian of the associated unsigned graph $\bar{\mathcal{G}} = (\mathcal{V}, \mathcal{E}, \bar{W})$. To cluster the nodes and analysis the performance of dynamics, *structurally balanced* (SB) signed graph is introduced following the definition

Definition 4 (Structural Balance). [48] A graph $\mathcal{G} = (\mathcal{V}, \mathcal{E}, W)$ is structurally balanced, if there exist two disjoint subsets \mathcal{V}_1 and \mathcal{V}_2 , i.e., $\mathcal{V}_1 \cap \mathcal{V}_2 = \emptyset$ and $\mathcal{V}_1 \cup \mathcal{V}_2 = \mathcal{V}$, such that $w_{ij} \geq 0$ if $i, j \in \mathcal{V}_q, q \in \{1, 2\}$ and $w_{ij} \leq 0$ if $i \in \mathcal{V}_q, j \in \mathcal{V}_r, q \neq r, q, r \in \{1, 2\}$.

An illustrative figure on structural balance is given in Figure A.3. It is notable that the definition of structural balance is independent of connectivity of graphs, i.e., SB is established no matter the graph is SC, QSC, etc., which is ignored by most of the previous works.

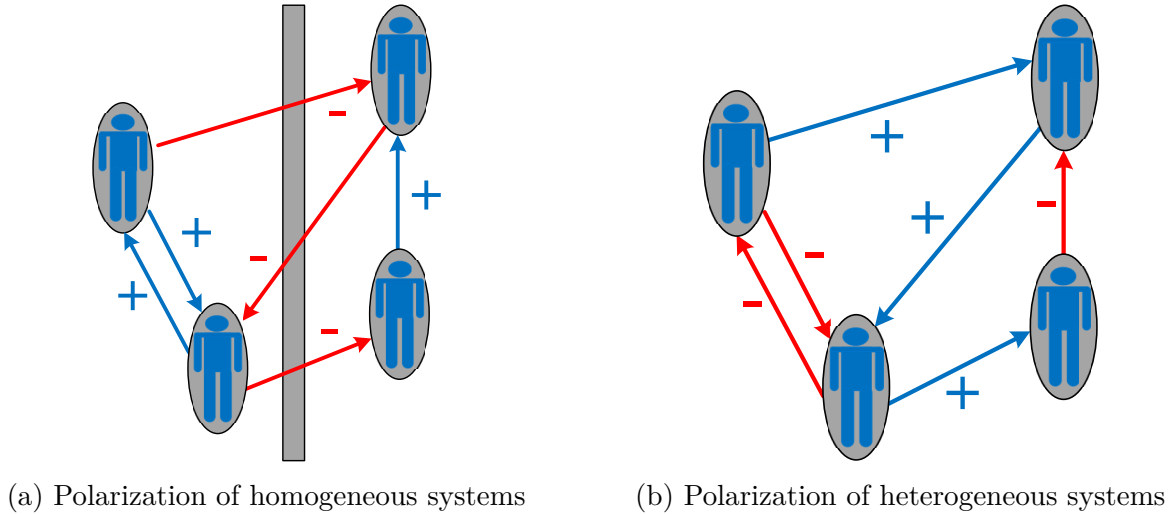


Figure A.3.: Structural balance and unbalance of cooperative networks

Structural balance plays an important role in the convergence analysis of systems on networks with antagonistic interaction (negative weighted edges on graphs). For illustration, we can consider in the context of the election campaign. The SB graph picturesquely implies votaries of two political parties splitting into two hostile camps, where the relations inside each faction are supportive and between them are repellent. In contrast to general graphs with negative weighted edges, SB graph organizes only a subset but is critical to forming opinion polarity or polarization. In addition, despite of minority, SB topological structure appears widely in real-world society, such as the system of governance, political voting, commercial investigation, etc. Especially, an unsigned graph is always SB where one of the subsets is \emptyset . Moreover, we have the following criterion to describe the algebraic characterization of an SB graph.

Lemma 16. *A graph $\mathcal{G} = (\mathcal{V}, \mathcal{E}, W)$ is structurally balanced, if and only if there exists a diagonal matrix $D = \text{diag}(d_1, d_2, \dots, d_N), d_i \in \{\pm 1\}, i = 1, 2, \dots, N$ such that all entries of DWD are nonnegative.*

Proof. Sufficiency: From the condition, we have $d_i w_{ij} d_j \geq 0, i, j \in \mathcal{V}$. Construct the following two sets of nodes.

$$\mathcal{V}_1 = \{i \in \mathcal{V} : d_i = 1\}, \quad \mathcal{V}_2 = \{i \in \mathcal{V} : d_i = -1\}. \quad (\text{A.4})$$

Then we examine the edges to show that graph \mathcal{G} is SB.

Without loss of generality, for two nodes $p, q \in \mathcal{V}_1$, we have $d_p = d_q = 1$. If there exists an edge from q to p , it follows that

$$w_{pq} = d_p w_{pq} d_q > 0. \quad (\text{A.5})$$

The result in (A.5) is also true when $p, q \in \mathcal{V}_2$. Thus we conclude that all weights of edges (if the edges exist), which link the nodes in the same set, are positive. In case two nodes in the same set are not connected, the weight is 0, which also fulfill Definition 4.

When p and q are in different sets, say, $p \in \mathcal{V}_1$ and $q \in \mathcal{V}_2$, we obtain $d_p = 1$ and $d_q = -1$. If there exists an edge from q to p , it follows that

$$w_{pq} = -d_p w_{pq} d_q < 0. \quad (\text{A.6})$$

The result in (A.6) is also true when the edge is from p to q . Thus we conclude that all weights of edges (if the edges exist), which link nodes in different sets, are negative. In case two nodes in different sets are not connected, the weight is 0, which also fulfills Definition 4.

Necessity: Assume that graph $\mathcal{G} = (\mathcal{V}, \mathcal{E}, W)$ is SB. Choose $d_i = 1$ if $i \in \mathcal{V}_1$ and $d_i = -1$ otherwise, to construct the matrix $D = \text{diag}(d_1, d_2, \dots, d_N)$. It is evident that D has the property described in Lemma 16. \square

To characterize the property of D , the set

$$\mathcal{D} = \{\text{diag}(d_1, d_2, \dots, d_n) : d_i \in \{\pm 1\}, i = 1, 2, \dots, n\} \quad (\text{A.7})$$

is introduced. The transformation with $D \in \mathcal{D}$ to make DWD a nonnegative matrix is named as *gauge transformation* [105], [124]. Obviously, there exists a gauge transformation for graph $\mathcal{G} = (\mathcal{V}, \mathcal{E}, W)$ if and only if it is SB. Lemma 16 is a general extension of the results in [110], [125], i.e., both unsigned and signed weighted digraphs are considered.

Further properties of an SB graph are characterized by the following lemma.

Lemma 17. [48] *Given an SB graph $\mathcal{G}(\mathcal{V}, \mathcal{E}, W)$, there holds that L has eigenvalue at 0. Furthermore, the graph \mathcal{G} is QSC if and only if $\dim \ker L = 1$.*

Lemma 17 implies that for an SB and QSC graph, d is the eigenvector of L at 0, where $\text{diag}(d) \in \mathcal{D}$.

Note that to avoid ambiguity, the signed graphs are only considered here and in Chapter 4. In other parts of this dissertation, we generally take into account only unsigned graphs.

Consensus Theory

With the increasing interest in distributed control and coordination of networks consisting of multi-agents, the consensus problem becomes canonical in the field of networked dynamic systems, e.g., ad hoc wireless communication networks, sensor networks, power networks, and social networks. Specially, in sociology, the consensus theory, as an opposite to the conflict theory, means a fair system to hold particular political or economic entities, in which the social changes should take place within the social institutions provided by it [126], [127]. In this section, we introduce the consensus theory in view of both control theory and social theory.

Distinct to the conventional control systems, the networked systems usually possess the features of large scale, big data, diverse information flow, and time-varying connectivity. These characteristics lead to the impractical implement of centralized control strategy due to the expensive computation and the fully access to information. To this end, the distributed protocols are more preferable in which only the local information is required. In addition, the distributed control laws are more robust with respect to the network topology and can be implemented more easily compared with centralized control. Taking this reason into consideration, the interesting topic is to design a distributed control such that consensus of states or outputs of the agents in networks can be reached.

Among all the consensus algorithms, the linear consensus algorithm plays an important role in multitudes of networked systems. The pioneering works [128], [129] in multi-agent system theory have thoroughly studied the collective group behaviors such as consensus, synchronization, flocking, swarming [130]–[134]. The consensus phenomena occur not only in the above typical multi-agent systems but also social systems, e.g., the opinion formation processes. The focus on the consensus of opinion traced back to the study by French and DeGroot [37], [38]. The proposed *iterative opinion pooling* process is now known as the DeGroot model or the French-DeGroot model.

Mathematically, the French-DeGroot model is described as the following discrete-time difference equation.

$$x(k+1) = Wx(k), \quad (\text{B.1})$$

where $x(k) = [x_1(k), \dots, x_N(k)]^T \in \mathbb{R}^N$ is vector encapsulating the respective opinions of each individual in a N -node network; $W = [w_{ij}] \in \mathbb{R}^{N \times N}$ is the adjacency matrix of the communication topology representing the influence weights among each pair of nodes. Without loss of generality, w_{ij} is normalized such that W is *row stochastic*, i.e., for any $i \in \mathcal{V}$, there holds $\sum_{j=1}^N w_{ij} = 1$. In detail, $w_{ij} > 0$ stands for node j can influence node i .

$0 < w_{ii} < 1$ represents that individual i is open-minded so that the opinions of her social neighbors and herself are all considered; $w_{ii} = 0$ implies that individual i only rely on others' opinions; whereas $w_{ii} = 1$ indicates that i is a stubborn person who only consider her own opinion. Entry-wise, the individual opinion dynamics reads

$$x_i(k+1) = \sum_{j=1}^N w_{ij} x_j(k). \quad (\text{B.2})$$

It implies that the individual i updates her opinion by taking weighted average of all her social neighbors (including herself if $w_{ii} > 0$). In this case, consensus is defined as follows.

Definition 5 (Consensus). Consider the opinion dynamic in (B.1) on a graph $\mathcal{G} = (\mathcal{V}, \mathcal{E}, W)$. The opinions are said to be consensus if there holds

$$\lim_{k \rightarrow \infty} x_i(k) - x_j(k) = 0, \forall i, j \in \mathcal{V}. \quad (\text{B.3})$$

Besides consensus, a weaker phenomenon is convergence described as follows

Definition 6 (Convergence). Consider the opinion dynamic in (B.1) on a graph $\mathcal{G} = (\mathcal{V}, \mathcal{E}, W)$. The opinions are said to be convergent if there exists

$$x(\infty) = \lim_{k \rightarrow \infty} x(k) = \lim_{k \rightarrow \infty} W^k x(0), \forall x(0). \quad (\text{B.4})$$

Clearly, the opinions reaches consensus if $x_1(\infty) = \dots = x_N(\infty)$. Although the French-DeGroot model is developed to illustrate the *social power* but not aiming at the consensus or convergent study, it serves as a perfect instance to combine the social-network-based model with control theory. Mathematically, the convergence and consensus of this model is confirmed by the following lemma under certain condition on the communication topology.

Lemma 18. [135] *The French-DeGroot model (B.1) is convergent if and only if $\lambda = 1$ is the only eigenvalue of W on the unit circle. Moreover, the opinions reach consensus if and only if this eigenvalue 1 is simple.*

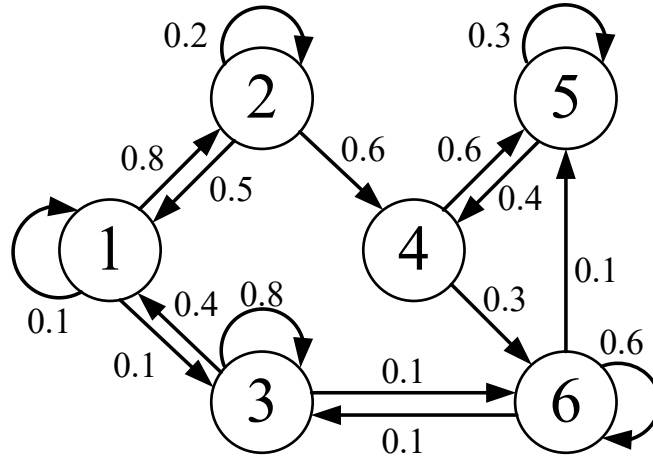
Lemma 18 infers that it is equivalent for the French-DeGroot model to be convergent and consensus if W is irreducible, i.e., the underneath graph is strongly connected. Figure B.1 depicts an example of the French-DeGroot model where the public opinion reaches consensus. By writing down the adjacency matrix of the graph in the left subgraph, it is straightforward to check that the conditions in Lemma 18 are satisfied. Thus the consensus is established.

In the French-DeGroot model, the opinion pooling is based on the average of the social neighbors and in the discrete time. As a counterpart of the French-DeGroot model, the Abelson's model [39] is proposed in a continuous-time manner.

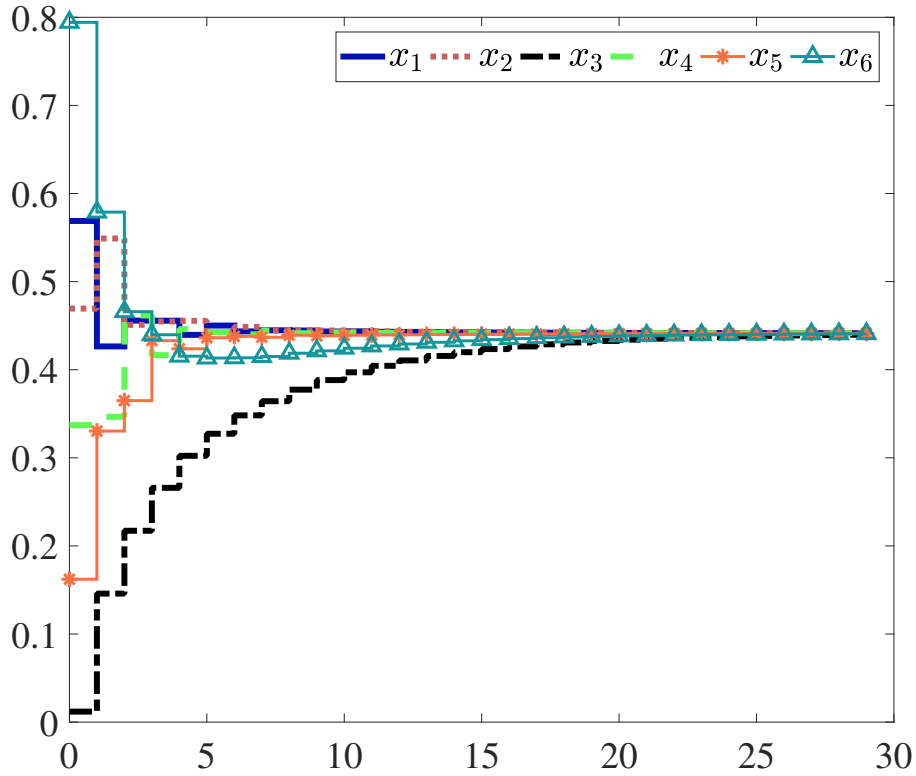
Bearing in mind the model (B.2) and the relation $w_{ii} = 1 - \sum_{j \neq i} w_{ij}$, we can attain for each node i , there holds

$$x_i(k+1) - x_i(k) = \sum_{j \neq i} w_{ij} (x_j(k) - x_i(k)). \quad (\text{B.5})$$

It implies that the increment of node i th opinion is the weighted sum of the opinion difference between each of her neighbors and herself. Moreover, the equation (B.5) also infers that node



(a) An example graph which runs the French-DeGroot model



(b) Public opinion reaches consensus in the French-DeGroot model

Figure B.1.: Opinion dynamics described as the French-DeGroot model reaches consensus

i shifts her opinion towards node j with certain weights. For sufficiently small amount of time between two steps, the dynamics (B.5) is rewritten in continuous-time as

$$\dot{x}_i = \sum_{j \neq i} w_{ij}(x_j(k) - x_i(k)), \forall i \in \mathcal{V}. \quad (\text{B.6})$$

Recalling the Laplacian for unsigned graph in (A.1), the compact form of the Abelson's

model reads

$$\dot{x}(t) = -\bar{L}x(t). \quad (\text{B.7})$$

The differential equation (B.7) is not only valid to explain the opinion dynamics in social networks but also plays an important role in the recent works in the field of multi-agent systems [116], [130].

Since all the eigenvalues of \bar{L} are not in the right half complex plain, the limit $\lim_{t \rightarrow \infty} e^{-\bar{L}t}$ always exists. It implies that the opinions in the Abelson's model always converges. By using Lemma 14, one can obtain the following lemma regarding the consensus condition.

Lemma 19. *The Abelson's model (B.7) reaches consensus if and only if the graph \mathcal{G} is quasi-strongly connected. Moreover, the consensus opinion satisfies*

$$\lim_{t \rightarrow \infty} x_i(t) = p^\top x(0), \quad (\text{B.8})$$

where p is the left eigenvector of \bar{L} associated with the simple eigenvalue 0, i.e., $p^\top \bar{L} = 0$, such that $p^\top \mathbf{1} = 1$.

This result which is fully proved in [116] is now fundamental in the study of multi-agent systems. What is interesting is that Abelson is the first one to point out that the quasi-strongly connectivity is sufficient and necessary for achieving consensus. The remarkable connection between opinion dynamics and multi-agent system continues and is extended to generic cases where the vector opinions, nonlinear consensus algorithms and time-varying networks are taken into consideration. Here we show several examples of the performance of the Abelson's model. This model is first implemented on the same network which is used in Figure B.1. Since $\text{sp}\{-L\} \subseteq \mathbb{C}_{<0}$, the public opinion becomes neutral as is presented in Figure B.2. By slightly modification of the underneath communication topology, we use the graph in the left subgraph in Figure B.3. On this graph, the public opinion establishes consensus.

Very recently, the Abelson's model is extended to the signed graph by the seminal work of C. Altafini [46], which leads the trend of research on opinion dynamics on the cooperative-competitive networks. The Altafini's model on a time invariant network is described as the following differential equation

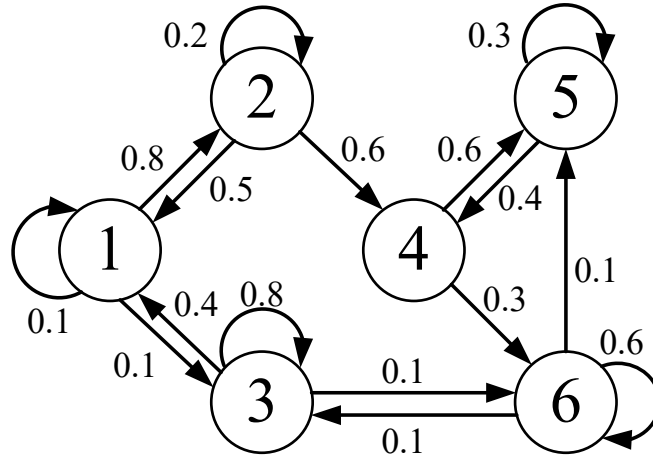
$$\dot{x}(t) = -Lx(t), \quad (\text{B.9})$$

where $x \in \mathbb{R}^N$ encapsulates the opinion values of the N nodes in a signed graph $\mathcal{G} = \{\mathcal{V}, \mathcal{E}, W\}$. Compared with the Abelson's model, the Laplacian L is specifically for signed graphs, which is defined in (A.3).

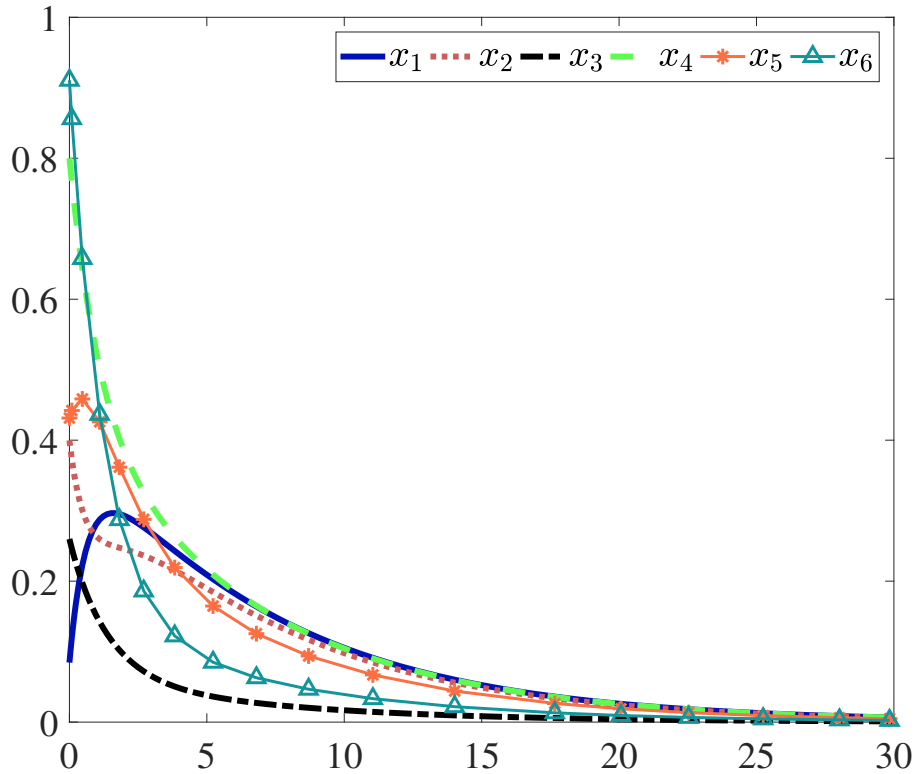
Due to the properties of signed graphs, the Altafini's model may result in modulus consensus, i.e., there exist a scalar $a \geq 0$ such that

$$\lim_{t \rightarrow \infty} |x_i(t)| = a, \forall i \in \mathcal{V}. \quad (\text{B.10})$$

Specially, if $a = 0$, we name it *neutralization*, which is a trivial case. Whereas, the non-trivial case of modulus consensus, *bipartite consensus*, contains two situations: i) consensus, i.e., the opinion of each node converge to a same value and ii) polarization, i.e., the absolute value of the converged opinion is the same but there exists at least one node with the opposite opinion. The conditions on modulus consensus of the Altafini's model has been thoroughly studied. We conclude the associated results in the following lemma.



(a) An example network on which runs the Abelson's model

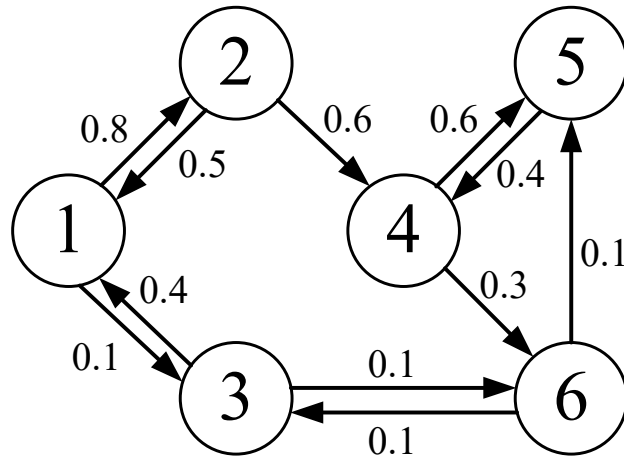


(b) Public opinion becomes neutral in the Abelson's model

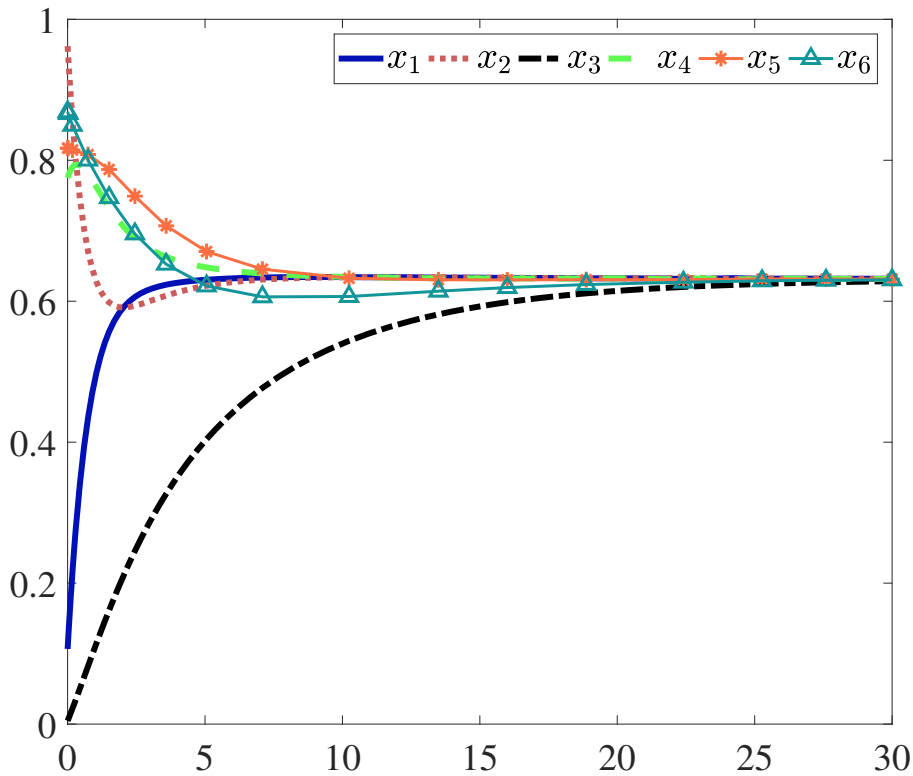
Figure B.2.: Opinion dynamics described as the Abelson's model reaches neutralization

Lemma 20. *Given the Altafini's model (B.9) on a signed graph \mathcal{G} with Laplacian L , the opinion reaches bipartite consensus if and only if \mathcal{G} is quasi-strongly connected and structural balanced. Moreover, if $w_{ij} \geq 0, \forall i, j$, consensus is established; polarization is achieved otherwise. The opinion approaches neutralization if and only if neither \mathcal{G} is structurally balanced nor \mathcal{G} contains in-isolated structurally balanced subgraphs.*

The proof of Lemma 20 can be referred to in [48] and is saved here for triviality. Two



(a) An example network on which runs the Abelson's model

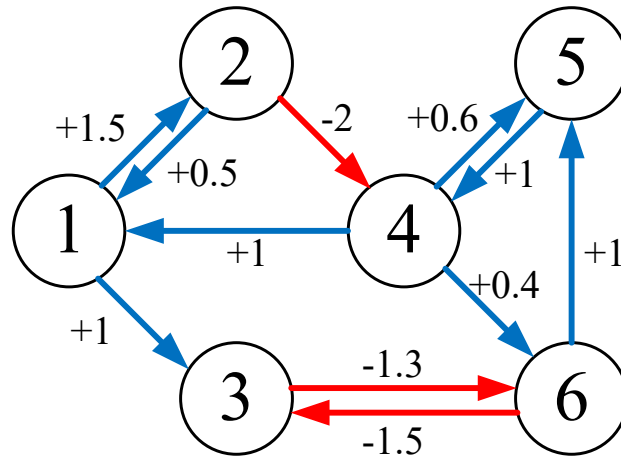


(b) Public opinion reaches consensus in the Abelson's model

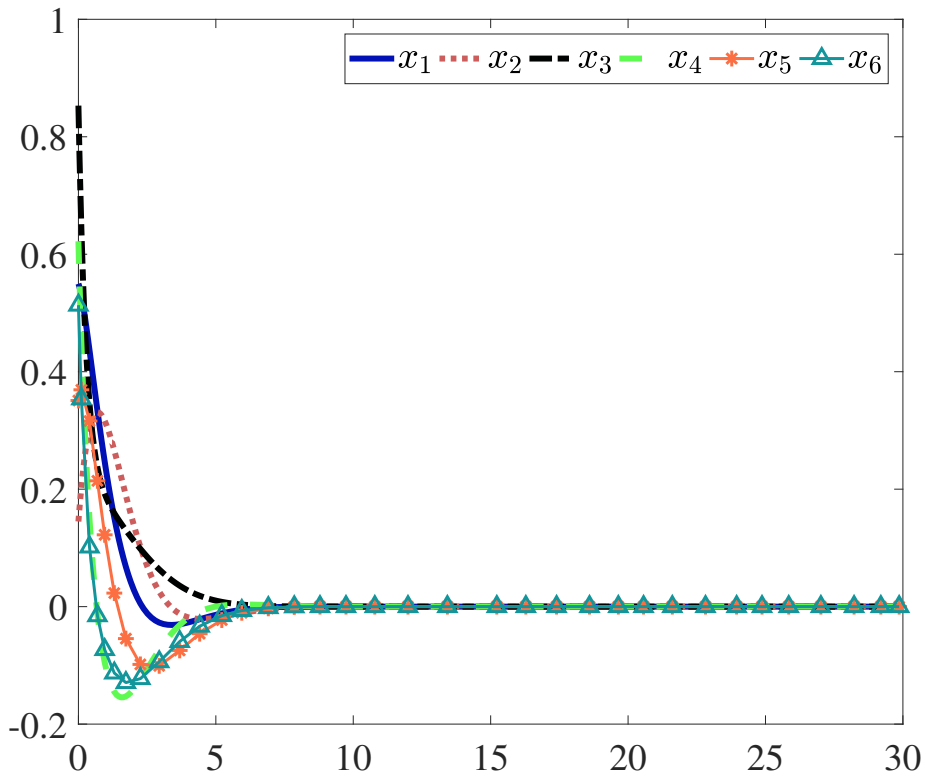
Figure B.3.: Opinion dynamics described as the Abelson's model reaches consensus

numerical experiments are conducted to illustrate the modulus consensus defined in (B.10). In Figure B.4, the signed graph is not SB, which leads to the neutralization of the public opinion. While on an SB signed graph, polarization is established as is shown in Figure B.5.

The polarization phenomenon reflects Heider's theory on social balance [136], which can be vividly described as "my friend's friends are my friends; my friend's enemies are my enemies; my enemy's friends are my enemies; my enemy's enemies are my friends.". Based on this



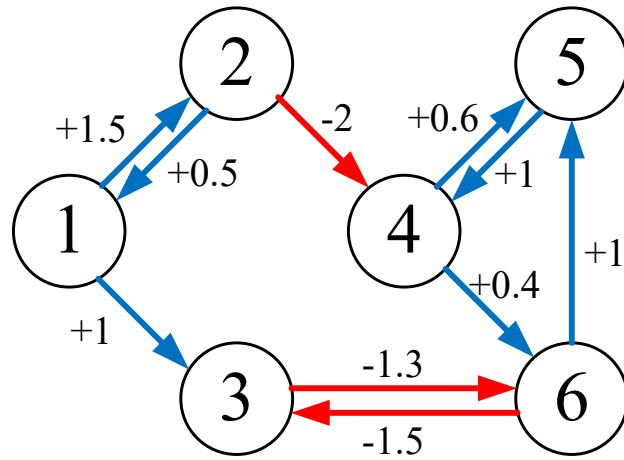
(a) Public opinion becomes neutral in the Altafini's model



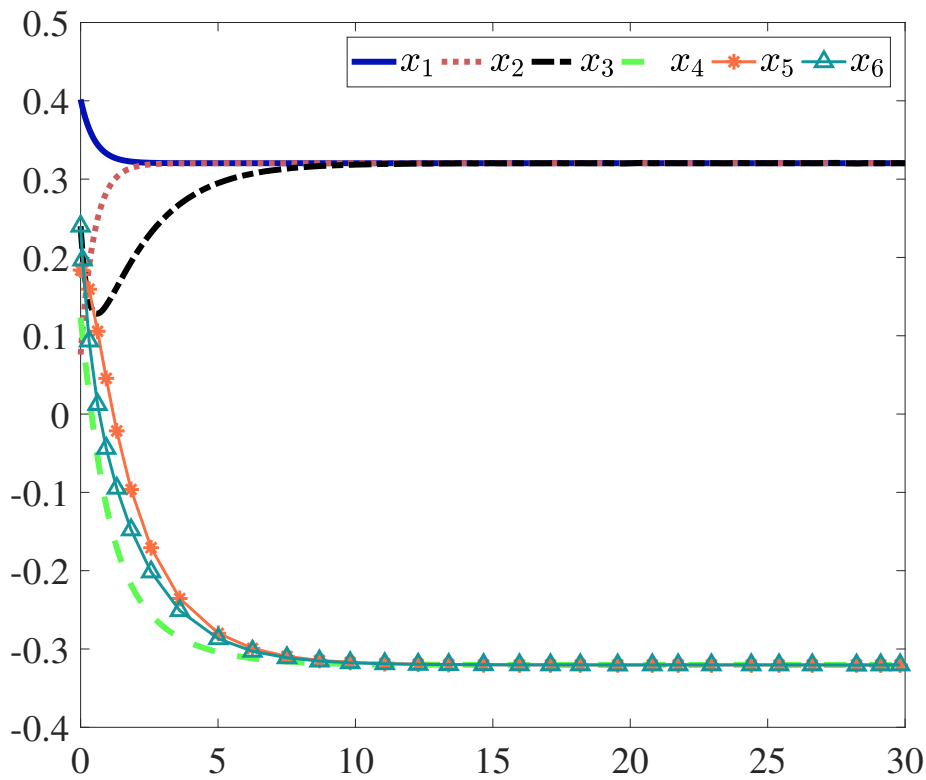
(b) Public opinion reaches polarization in the Altafini's model

Figure B.4.: Opinion dynamics described as the Altafini's model reaches neutralization on structural unbalanced graphs

setting, the modulus consensus problem has been extended to time-varying networks in [48] and the accessibility problem in [49].



(a) Public opinion becomes neutral in the Altafini's model



(b) Public opinion reaches polarization in the Altafini's model

Figure B.5.: Opinion dynamics described as the Altafini's model reaches polarization on SB graphs.

Bibliography

- [1] T. W. Valente, L. A. Palinkas, S. Czaja, K.-H. Chu, and C. H. Brown, “Social network analysis for program implementation”, *PLOS ONE*, vol. 10, no. 6, e0131712, 2016.
- [2] S. Luo, F. Morone, C. Sarraute, M. Travizano, and H. A. Makse, “Inferring personal economic status from social network location”, *Nature Communications*, vol. 8, e15227, 2017.
- [3] G. Simmel, *Soziologie*. Leipzig: Duncker & Humblot, 1908.
- [4] J. Scott, *Social Network Analysis: A Handbook*. Sage Publications, 2000.
- [5] J. L. Moreno, *Who Shall Survive: A New Approach to the Problem of Human Interrelations*. Nervous and Mental Disease Publishing Co., 1934.
- [6] ———, *Sociometry, experimental method and the science of society; an approach to a new political orientation*. Beacon House, 1951.
- [7] L. Freeman, *The Development of Social Network Analysis: A Study in the Sociology of Science*. Empirical Press, 2004.
- [8] M. Diani, *Social Movements and Networks*. Oxford University Press, 2003.
- [9] C. Chamley, A. Scaglione, and L. Li, “Models for the diffusion of beliefs in social networks: An overview”, *IEEE Signal Processing Magazine*, vol. 30, no. 3, pp. 16–29, 2013.
- [10] K. Kandhway and J. Kuri, “Using node centrality and optimal control to maximize information diffusion in social networks”, *IEEE Transactions on Systems, Man, and Cybernetics: Systems*, vol. 47, no. 7, pp. 1099–1110, 2017.
- [11] N. Friedkin, A. Proskurnikov, R. Tempo, and S. Parsegov, “Network science on belief system dynamics under logic constraints”, *Science*, vol. 354, no. 6310, pp. 321–326, 2016.
- [12] A. V. Proskurnikov and R. Tempo, “A tutorial on modeling and analysis of dynamic social networks. part i”, *Annual Reviews in Control*, vol. 43, pp. 65–79, 2017.
- [13] N. Friedkin, “The problem of social control and coordination of complex systems in sociology: A look at the community cleavage problem”, *IEEE Control System Magazine*, vol. 35, no. 3, pp. 40–51, 2015.
- [14] R. Crane and D. Sornette, “Robust dynamic classes revealed by measuring the response function of a social system”, *Proceedings of the National Academy of Sciences*, vol. 105, no. 41, pp. 15 649–15 653, 2008.

- [15] Y. Matsubara, Y. Sakurai, B. A. Prakash, L. Li, and C. Faloutsos, “Rise and fall patterns of information diffusion: Model and implications”, in *the 18th ACM SIGKDD international conference on Knowledge discovery and data mining*, 2012, pp. 6–14.
- [16] J. Yang and J. Leskovec, “Modeling information diffusion in implicit networks”, in *the 2010 IEEE International Conference on Data Mining*, 2010, pp. 599–608.
- [17] R. Pastor-Satorras, C. Castellano, P. V. Mieghem, and A. Vespignani, “Epidemic processes in complex networks”, *Review of Modern Physics*, vol. 87, no. 3, pp. 1–61, 2014.
- [18] W. O. Kermack and A. G. McKendrick, “A contribution to the mathematical theory of epidemics”, *Proc. Roy. Soc. A*, vol. 115, no. 772, pp. 700–721, 1927.
- [19] R. Pastor-Satorras and A. Vespignani, “Epidemic spreading in scale-free networks”, *Physical Review Letters*, vol. 86, no. 14, pp. 3200–3203, Apr. 2001.
- [20] M. E. J. Newman, “Threshold effects for two pathogens spreading on a network”, *Physical Review Letters*, vol. 95, no. 10, p. 108 701, 2005.
- [21] Y. Jin, W. Wang, and S. Xiao, “An sirs model with a nonlinear incidence rate”, *Chaos, Solitons & Fractals*, vol. 34, no. 5, pp. 1482–1497, 2007.
- [22] M. Li, X. Wang, K. Gao, and S. Zhang, “A survey on information diffusion in online social networks: Models and methods”, *Information*, vol. 8, no. 118, pp. 1–21, 2017.
- [23] M. Granovetter, “Threshold models of collective behaviors”, *The American Journal of Sociology*, vol. 83, no. 6, pp. 1420–1433, 1978.
- [24] T. Schelling, *Micromotives and Macrobehavior*. W. W. Norton & Company, 1978.
- [25] D. J. Watts, “A simple model of global cascades on random networks”, *Proceedings of the National Academy of Sciences*, vol. 99, no. 9, pp. 5766–5771, 2002.
- [26] P. V. Mieghem, J. Omic, and R. Kooij, “Virus spread in networks”, *IEEE/ACM Transactions on Networking*, vol. 17, no. 1, pp. 1–14, 2009.
- [27] C. Castellano and R. Pastor-Satorras, “Thresholds for epidemic spreading in networks”, *Phys. Rev. Lett*, vol. 105, no. 21, pp. 87–101, 2010.
- [28] A. Khanafer, T. Basar, and B. Gharesifard, “Stability properties of infected networks with low curing rates”, in *American Control Conference*, Portland, OR, American, 2014, pp. 3579–3584.
- [29] J. E. Hunter, J. E. Danes, and S. H. Cohen, *Mathematical Models of Attitude Change*. Academic Press, 1984.
- [30] Y. J. Halpern, “The relationship between knowledge, belief, and certainty”, *Annals of Mathematics and Artificial Intelligence*, vol. 4, no. 3, pp. 301–322, 1991.
- [31] A. Flache, M. Mäs, T. Feliciani, E. Chattoe-Brown, G. Deffuant, S. Huet, and J. Lorenz, “Models of social influence: Towards the next frontiers”, *Journal of Artificial Societies and Social Simulation*, vol. 20, no. 4, p. 2, 2017.
- [32] R. L. Akers, M. D. Krohn, L. Lanza-Kaduce, and M. Radosevich, “Social learning and deviant behavior: A specific test of a general theory”, *American Sociological Review*, vol. 44, no. 4, pp. 636–655, 1979.

-
- [33] S. Bikhchandani, D. Hirshleifer, and I. Welch, “A theory of fads, fashion, custom, and cultural change as informational cascades”, *Journal of Political Economy*, vol. 100, no. 5, pp. 992–1026, 1992.
- [34] W. Wood, “Attitude change: Persuasion and social influence”, *Annual Review of Psychology*, vol. 51, no. 1, pp. 539–570, 2000.
- [35] L. Festinger, *A Theory of Cognitive Dissonance*. Stanford University Press, 1957.
- [36] F. Heider, “Attitudes and cognitive organization”, *The Journal of Psychology*, vol. 21, pp. 107–122, 1946.
- [37] J. R. P. French, “A formal theory of social power”, *Psychological Review*, vol. 63, pp. 181–194, 1956.
- [38] M. H. DeGroot, “Reaching a consensus”, *Journal of American Statistical Association*, vol. 69, pp. 118–121, 1974.
- [39] R. P. Abelson, “Mathematical models of the distribution of attitudes under controversy”, in *Contributions to Mathematical Psychology*, N. Frederiksen and H. Gulliksen, Eds., Holt, Rinehart & Winston, Inc, 1964, pp. 142–160.
- [40] R. Hegselmann and U. Krause, “Opinion dynamics and bounded confidence models, analysis, and simulation”, *Journal of Artificial Societies and Social Simulation*, vol. 5, no. 3, p. 2, 2002.
- [41] G. Deffuant, D. Neau, F. Amblard, and G. Weisbuch, “Mixing beliefs among interacting agents”, *Advances in Complex Systems*, vol. 3, no. 01n04, pp. 87–98, 2000.
- [42] W. Jager and F. Amblard, “Uniformity, bipolarization and pluriformity captured as generic stylized behavior with an agent-based simulation model of attitude change”, *Computational & Mathematical Organization Theory*, vol. 10, no. 4, pp. 295–303, 2005.
- [43] N. Mark, “Culture and competition: Homophily and distancing explanations for cultural niches”, *American Sociological Review*, vol. 68, no. 3, pp. 319–345, 2003.
- [44] A. Flache and M. W. Macy, “Small worlds and cultural polarization”, *Journal of Mathematical Sociology*, vol. 35, no. 1-3, pp. 146–176, 2011.
- [45] T. Feliciani, A. Flache, and J. Tolsma, “How, when and where can spatial segregation induce opinion polarization? two competing models”, *Journal of Mathematical Sociology*, vol. 20, no. 2, p. 6, 2017.
- [46] C. Altafini, “Consensus problems on networks with antagonistic interactions”, *IEEE Transactions on Automatic Control*, vol. 58, no. 4, pp. 935–946, 2013.
- [47] A. V. Proskurnikov and M. Cao, “Polarization in cooperative networks of heterogeneous nonlinear agents”, in *Decision and Control (CDC), 2016 IEEE 55th Conference on*, Las Vegas, US, 2016, pp. 6915–6920.
- [48] A. Proskurnikov, A. Matveev, and M. Cao, “Opinion dynamics in social networks with hostile camps: Consensus vs. polarization”, *IEEE Transactions on Automatic Control*, vol. 61, no. 6, pp. 1524–1536, 2016.
- [49] “Polarizability, consensusability and neutralizability of opinion dynamics on cooperative networks”, *IEEE Transactions on Automatic Control*, 2018.

- [50] J. M. Hendrickx, V. D. Blondel, and J. N. Tsitsiklis, “On krause’s multi-agent consensus model with state-dependent connectivity”, *IEEE Transactions on Automatic Control*, vol. 54, no. 11, pp. 2586–2597, 2009.
- [51] W. Su, G. Chen, and Y. Hong, “Noise leads to quasi-consensus of hegselmann–krause opinion dynamics”, *Automatica*, vol. 65, pp. 448–454, 2017.
- [52] F. Liu and M. Buss, “Node-based sirs model on heterogeneous networks: Analysis and control”, in *American Control Conference (ACC)*, 2016, pp. 2852–2857.
- [53] ———, “Optimal control for information diffusion over heterogeneous networks”, in *55th IEEE Conference on Decision and Control (CDC)*, 2016, pp. 141–146.
- [54] “Robust optimal control of deterministic information epidemics with noisy transition rates”, *Physica A: Statistical Mechanics and its Applications*, vol. 517, pp. 577–587, 2019.
- [55] C. Chamley, A. Scaglione, and L. Li, “Models for the diffusion of beliefs in social networks: An overview”, *IEEE Singal Processing Magazine*, vol. 30, no. 3, pp. 16–29, 2013.
- [56] Y. Lin, J. C. Lui, K. Jung, and S. Lim, “Modeling multi-state diffusion process in complex networks: Theory and applications”, in *21st European Conference on Artificial Intelligence*, Prague, Czech, 2014.
- [57] C. Wang, Z. Tan, Y. Ye, L. Wang, K. H. Cheong, and N.-g. Xie, “A rumor spreading model based on information entropy”, *Scientific Report*, vol. 7, no. 9615, 2017.
- [58] Y. Matsubara, Y. Sakurai, B. A. Prakash, L. Li, and C. Faloutsos, “Rise and fall patterns of information diffusion: Model and implications”, in *the 18th ACM SIGKDD international conference on Knowledge Discovery and Data Mining*, Beijing, China, 2012, pp. 6–14.
- [59] J. Goldenberg, “Talk of the network: A complex systems look at the underlying process of word-of-mouth”, *Marketing Letters*, vol. 12, no. 3, pp. 211–223, 2001.
- [60] W. Goffman and V. Newill, “Generalization of epidemic theory”, *Nature*, vol. 204, no. 4955, pp. 225–228, 1964.
- [61] W. O. Kermack and A. G. McKendrick, “A contribution to the mathematical theory of epidemics”, *Proc. Roy. Soc. A*, vol. 115, no. 772, pp. 700–721, 1927.
- [62] B. Qu and H. Wang, “Sis epidemic spreading with heterogeneous infection rates”, *IEEE Transactions on Network Science and Engineering*, vol. 4, no. 3, pp. 177–186, 2017.
- [63] E. Lukacs, *Probability and Mathematical Statistics*. Academic Press, 1957.
- [64] E. Cator and P. V. Mieghem, “Nodal infection in markovian sis and sir epidemics on networks are non-negatively correlated”, *Physical Review E*, vol. 89, p. 052 802, 2014.
- [65] P. V. Mieghem and R. van de Bovenkamp, “Accuracy criterion for the mean-field approximation in susceptible-infected-susceptible epidemics on networks”, *Physical Review E*, vol. 91, p. 032 812, 2015.
- [66] L. Chen and J. Sun, “Global stability and optimal control of an sirs epidemic model on heterogeneous networks”, *Physica A:Statistical Mechanics and its Applications*, vol. 410, pp. 196–204, 2015.

-
- [67] N. Bailey, *The Mathematical Theory of Infectious Diseases and Its Applications*. London: Griffin, 1975.
- [68] D. Gruhl, R. Guha, D. Liven-Nowell, and A. Tomkins, “Information diffusion through blogspace”, in *the 13th International Conference on World Wide Web(WWW’04)*, New York, 2004.
- [69] W. Jiyoung and C. Hsinchun, “Epidemic model for information diffusion in web forums: Experiments in marketing exchange and political dialog”, *SpringerPlus*, vol. 5, no. 1, p. 66, 2016.
- [70] R. Wang, Y. Jin, and F. Li, “A review of microblogging marketing based on the complex network theory”, in *International Conference in Electrics, Communication and Automatic Control Proceedings*, New York, 2011.
- [71] A. Khanafer and T. Basar, “Information spread in networks: Control, games, and equilibria”, in *Information Theory and Applications Workshop (ITA)*, San Diego, USA, 2014.
- [72] P. E. Paré, C. L. Beck, and A. Nedić, “Epidemic processes over time-varying networks”, *IEEE Transactions on Control of Networked Systems*, 2017, . In press.
- [73] F. D. Sahneh, C. Scoglio, and P. V. Miegheem, “Generalized epidemic mean-field model for spreading processes over multilayer complex networks”, *IEEE/ACM Transactions on Networking*, vol. 21, no. 5, pp. 1609–1619, 2013.
- [74] K. S. Narendra and R. Shorten, “Hurwitz stability of metzler matrices”, *IEEE Transactions on Automatic Control*, vol. 55, no. 6, pp. 1484–1487, 2010.
- [75] R. Varga, *Matrix Iterative Analysis*. Princeton University Press, 2000.
- [76] H. K. Khalil, *Nonlinear Systems*. Prentice Hall Upper Saddle River, 2002.
- [77] A. Fall, A. Iggidr, G. Sallet, and J. J. Tewa, “Epidemiological models and lyapunov functions”, *Mathematical Modelling of Natural Phenomena*, vol. 2, no. 1, pp. 55–73, 2007.
- [78] M. Ibragimov, “Conditions for positive definiteness of m-matrices”, *Linear and Multilinear Algebra*, vol. 48, no. 2, pp. 93–106, 2000.
- [79] G.-r. Duan and R. O. N. J. Patton, “A Note on Hurwitz Stability of Matrices”, vol. 34, no. 4, pp. 509–511, 1998.
- [80] P. E. Paré, J. Liu, C. L. Beck, B. E. Kirwan, and T. Basar, “Analysis, identification, and validation of discrete-time epidemic processes”, *arXiv:1710.11149v1*, 2017.
- [81] M. Ogura and V. M. Preciado, “Efficient containment of exact sir markovian processes on networks”, in *55th IEEE Conference on Decision and Control*, 2016, pp. 967–972.
- [82] C. Nowzari, V. M. Preciado, and G. J. Pappas, “Optimal resource allocation for control of networked epidemic models”, *IEEE Transactions on Control of Network Systems*, vol. 4, no. 2, pp. 159–169, 2017.
- [83] N. J. Watkins, C. Nowzari, and G. J. Pappas, “Robust economic model predictive control of continuous-time epidemic processes”, *arXiv:1707.00742*, 2017.

- [84] A. Karnik and P. Dayama, “Optimal control of information epidemics”, in *Fourth International Conference on Communication Systems and Networks (COMSNETS)*, Bangalore, 2012, pp. 1–7.
- [85] M. Farda, X. Zhang, F. Lin, and M. R. Jovanović, “On the optimal dissemination of information in social networks”, in *51st IEEE Conference on Decision and Control*, Maui, Hawaii, USA, 2012, pp. 2539–2544.
- [86] C. Nowzari, V. M. Preciado, and G. J. Pappas, “Analysis and control of epidemics: A survey of spreading processes on complex networks”, *IEEE Control Systems*, vol. 36, no. 1, pp. 26–46, 2016.
- [87] A. Khanafer and T. Basar, “An optimal control problem over infected networks”, in *Int. Conf. Control, Dynamic Systems, Robotics*, Ottawa, ON, Canada, 2014, pp. 1–6.
- [88] X. Chen and V. M. Preciado, “Optimal coinfection control of competitive epidemics in multi-layer networks”, in *53rd IEEE Conference on Decision and Control (CDC)*, 2014, pp. 6209–6214.
- [89] K. Kandhway and J. Kuri, “How to run a campaign: Optimal control of sis and sir information epidemics”, *Applied Mathematics and Computation*, vol. 231, pp. 79–92, 2014.
- [90] R. M. Neilan and S. Lenhart, “Dimacs series in discrete mathematics and theoretical computer science”, *International Journal of Computer Applications*, vol. 75, pp. 67–81, 2010.
- [91] W. H. Fleming and R. W. Rishel, *Deterministic and Stochastic Optimal Control*. New York: Springer-Verlag, 1975.
- [92] W. Rudin, *Principles of Mathematical Analysis*. McGraw-Hill, Inc., 1976.
- [93] M. McAsey, L. Mou, and W. Han, “Convergence of the forward-backward sweep method in optimal control”, *Computational Optimization and Applications*, vol. 53, no. 1, pp. 207–226, 2012.
- [94] A. Hamdache, I. Elmouki, and S. Saadi, “Optimal control with an isoperimetric constraint applied to cancer immunotherapy”, *International Journal of Computer Applications*, vol. 94, no. 15, pp. 31–37, 2014.
- [95] *Highschool network dataset – KONECT*, Apr. 2017. [Online]. Available: http://konect.uni-koblenz.de/networks/moreno_highschool.
- [96] M. T. Gastner, N. Markou, G. Pruessner, and M. Draief, “Opinion formation models on a gradient”, *PLoS ONE*, vol. 23, no. 12, e114088, 2014.
- [97] N. Askitas, “Explaining opinion polarisation with opinion copulas”, *PLoS ONE*, vol. 12, no. 8, e0183277, 2017.
- [98] F. Lewis, D. Vrabie, and V. Syrmos, *Optimal Control*. John Wiley & Sons, Inc., 2012.
- [99] S. Peng, “A general stochastic maximum principle for optimal control problems”, *SIAM Journal of Control and Optimization*, vol. 28, no. 4, pp. 966–979, 1990.
- [100] Z. K. Nagy and R. D. Braatz, “Open-loop and closed-loop robust optimal control of batch processes using distributional and worst-case analysis”, *Journal of Process Control*, vol. 14, no. 4, pp. 411–422, 2004.

-
- [101] R. P. Dickinson and R. J. Gelinas, “Sensitivity analysis of ordinary differential equation systems—a direct method”, *Journal of Computational Physics*, vol. 21, no. 2, pp. 123–143, 1976.
- [102] W. F. Feehery, J. E. Tolsma, and P. I. Barton, “Efficient sensitivity analysis of large-scale differential-algebraic systems”, *Appl. Numer. Math.*, vol. 25, no. 1, pp. 41–54, 1997.
- [103] J. S. Coleman, “Introduction to mathematical sociology”, *London Free Press Glencoe*, 1964.
- [104] L. C. Freeman, C. M. Webster, and D. M. Kirke, “Exploring social structure using dynamic three-dimensional color images”, *Social Networks*, vol. 20, no. 2, pp. 109–118, 1998.
- [105] C. Altafini, “Dynamics of opinion forming in structurally balanced social networks”, *PLOS ONE*, vol. 7, no. 6, e38135, 2012.
- [106] P. Dandekar, A. Goel, and D. Lee, “Biased assimilation, homophily, and the dynamics of polarization”, *Proc. Natl. Acad. Sci.*, vol. 110, no. 15, pp. 5791–5796, 2013.
- [107] V. Amelkin, F. Bullo, and A. Singh, “Polar opinion dynamics in social networks”, *IEEE Transactions on Automatic Control*, vol. 62, no. 11, pp. 5652–5665, 2017.
- [108] C.-Q. Ma and J.-F. Zhang, “Necessary and sufficient conditions for consensusability of linear multi-agent systems”, *IEEE Transactions on Automatic Control*, vol. 55, no. 5, pp. 1263–1268, 2010.
- [109] T. Xia and L. Scardovi, “Output-feedback synchronizability of linear time-invariant systems”, *Systems & Control Letters*, vol. 94, pp. 152–158, 2016.
- [110] M. E. Valcher and P. Misra, “On the consensus and bipartite consensus in high-order multi-agent dynamical systems with antagonistic interactions”, *System & Control Letters*, vol. 66, pp. 94–103, 2014.
- [111] S. E. Parsegov, A. V. Proskurnikov, R. Tempo, and N. E. Friedkin, “Novel multi-dimensional models of opinion dynamics in social networks”, *IEEE Transactions on Automatic Control*, vol. 62, no. 5, pp. 2270–2285, 2017.
- [112] X. Li, Y. C. Soh, and L. Xie, “Output-feedback protocols without controller interaction for consensus of homogeneous multi-agent systems: A unified robust control view”, *Automatica*, vol. 81, pp. 37–45, 2017.
- [113] W.-G. Xia and M. Cao, “Clustering in diffusively coupled networks”, *Automatica*, vol. 47, pp. 2395–2405, 2011.
- [114] H. Zhang and J. Chen, “Bipartite consensus of multi-agent systems over signed graphs: State feedback and output feedback control approaches”, *Int. J. Robust Non-linear Control*, vol. 27, no. 1, pp. 3–14, 2017.
- [115] C. Q. Ma, *System Analysis and Control Synthesis of Linear Multi-agent Systems*. Ph.D. dissertation, Academy of Mathematics and Systems Science, Chinese Academy of Sciences, Beijing, China, 2009.
- [116] W. Ren and R. W. Beard, “Consensus seeking in multiagent systems under dynamically changing interaction topologies”, *IEEE Transactions on Automatic Control*, vol. 50, no. 5, pp. 655–661, 2005.

- [117] E. Hendricks, O. Jannerup, and P. Sørensen, *Linear Systems Control - Deterministic and Stochastic Methods*. Springer, 2010.
- [118] D. Easley and J. Kleinberg, *Networks, Crowds, and Markets. Reasoning about a Highly Connected World*. Cambridge, U.K.: Cambridge Univ. Press, 2010.
- [119] <https://www.govtrack.us/congress/votes>. [Online]. Available: <https://www.govtrack.us/congress/votes>.
- [120] Z. Meng, G. Shi, K. Johansson, M. Cao, and Y. Hong, “Behaviors of networks with antagonistic interactions and switching topologies”, *Automatica*, vol. 73, pp. 110–116, 2016.
- [121] M. Ye, J. Liu, B. D. O. Anderson, C. Yu, and T. Basar, “Evolution of social power in social networks with dynamic topology”, *IEEE Transactions on Automatic Control*, vol. 63, no. 11, pp. 3793–3808, 2018.
- [122] G. S. Seyboth, D. V. Dimarogonas, K. H. Johansson, and F. Allgöwer, “Static diffusive couplings in heterogeneous linear networks”, *IFAC Proceedings Volumes*, vol. 45, no. 26, pp. 258–263, 2012.
- [123] R. A. Brualdi and H. J. Ryser, *Combinatorial Matrix Theory*. Cambridge University Press, 1991.
- [124] S. Galam, “Fragmentation versus stability in bimodal coalitions”, *Physica A: Statistical Mechanics and its Applications*, vol. 230, no. 1-2, pp. 174–188, 1996.
- [125] D. Meng, W. Du, and Y. Jia, “Data-driven consensus control for networked agents: An iterative learning control-motivated approach”, *IET Control Theory & Applications*, vol. 9, no. 14, pp. 2084–2096, 2015.
- [126] I. L. Horowitz, “Consensus, conflict and cooperation: A sociological inventory”, *Social Forces*, vol. 41, no. 2, pp. 177–188, 1962.
- [127] H. Bakvis, “Consensus and conflict: Essays in political sociology”, *Canadian Journal of Political Science*, vol. 19, no. 3, pp. 634–635, 1985.
- [128] M. Mesbahi and M. Egerstedt, *Graph Theoretic Methods in Multiagent Networks*. Princeton and Oxford: Princeton University Press, 2010.
- [129] W. Ren and Y. Cao, *Distributed Coordination of Multi-agent Networks*. Springer, 2011.
- [130] R. Olfati-Saber and R. Murray, “Consensus problems in networks of agents with switching topology and time-delays”, *IEEE Transactions on Automatic Control*, vol. 49, no. 9, pp. 1520–1533, 2004.
- [131] Q. Hui, W. M. Haddad, and S. P. Bhat, “Finite-time semistability and consensus for nonlinear dynamical networks”, *IEEE Transactions on Automatic Control*, vol. 53, no. 8, pp. 1887–1900, 2008.
- [132] L. Scardovi and R. Sepulchre, “Synchronization in networks of identical linear systems”, *Automatica*, vol. 44, no. 11, pp. 2557–2562, 2009.
- [133] D. Sakai, H. Fukushima, and F. Matsuno, “Flocking for multirobots without distinguishing robots and obstacles”, *IEEE Transactions on Control of Network Systems*, vol. 25, no. 3, pp. 1019–1027, 2017.

- [134] W. Yu, G. Chen, M. Cao, J. Lü, and H. Zhang, “Swarming behaviors in multi-agent systems with nonlinear dynamics”, *Chaos*, p. 043 118, 2013.
- [135] F. Gantmacher, *The Theory of Matrices*. AMS Chelsea Publishing, 2000.
- [136] D. Cartwright and F. Harary, “Structural balance: A generalization of Heider’s theory”, *Psychological Review*, vol. 63, no. 5, pp. 277–293, 1956.